NTNU – Trondheim
Norwegian University of
Science and Technology

Simulation of Pilot Data with Aspen Plus

Trine Witzøe

Chemical Engineering and Biotechnology
Submission date: June 2015
Supervisor: Hanna Knuutila, IKP

Norwegian University of Science and Technology
Department of Chemical Engineering

Declaration of compliance

I declare that this is an independent work according to the exam regulations of the Norwegian University of Science and Technology (NTNU).

Trondheim, June 5. 2015

Signature:

Trine Witzøe

Preface

This thesis was written during the spring of 2015 as the final part of my master's degree at the Department of Chemical Engineering at the Norwegian University of Science and Technology (NTNU).

I would like to express my gratitude to my supervisor, Associate Professor Hanna Knuutila, for her valuable guidance and support during the work on this thesis. It has been an inspiring experience to work with the Environmental Engineering and Reactor Technology group.

I would also like to thank my friends in Trondheim for making these last five years so memorable. Last, but not least, I would like to thank my family for their invaluable support and everlasting encouragement.

Abstract

Over the last few decades there has been an increasing interest in climate change and global warming. It is believed that one of the major causes of the enhanced greenhouse effect, that causes global warming, is anthropogenic CO_2 emissions. In the work that has been done on reducing anthropogenic CO_2 emissions, research into carbon capture and storage is now of considerable importance. Today, one of the most promising near-term mitigating strategies is post-combustion capture and chemical absorption with amine solvents.

The objective of the research described in this thesis has been to develop a robust and reliable simulation model of the chemical absorption capture process with 30wt% MEA. The simulations were performed in Aspen Plus version 8.6, and an inbuilt template, "ENRTL-RK_Rate_based_MEA_Model", was used as a basis for the simulation model. The absorber and stripper columns were simulated separately using a rate-based model. Five different pilot campaigns were used in the absorber simulations, and four different pilot campaigns were used in the stripper simulations. The inbuilt template from Aspen Plus was used without any changes in the physicochemical package. However, during the absorber simulations, a kinetic constant from the literature was used to optimize the model performance. Flow rates, composition, temperatures and pressures of the inlet streams were used as inputs in the model, in addition to the reboiler duty in the stripper simulations. Analogous, flow rates, compositions and temperatures of the outlet streams from the simulations were compared with experimental data to verify the model's performance. In the evaluation of the simulation model, the absorption/desorption rate from the simulations was compared with the experimental values.

In total, 103 experimental runs were simulated in the absorber part, and 78 experimental runs were simulated in the desorber part. When the absorber simulation model was modified using the kinetic constant from the literature, the overall average deviation, including all runs, was found to be 9.8% and the absolute average deviation was found to be 8.5%. In addition, the predictions of the temperature profiles were found to be accurate, within a 2 °C deviation from experimental measurements for almost all runs, except in one of the campaigns. The performance of the simulation model was therefore deemed satisfactory in the absorber part. In addition, all campaigns showed similar results, thus indicating consistency.

In the desorber simulations, the performance of the simulation model was somewhat more variable, and several possible causes were examined in order to understand the

predictions. The Aspen Plus template without any changes performed better than the modified model using a kinetic constant from the literature, and thus the template was used directly. The performance in three out of the four campaigns was satisfactory. When one outlier was disregarded, the average deviation was found to be below 7.9% and the absolute average deviation was found to be below 7.6% for all three campaigns individually. The overall average deviation and absolute average deviation including all 78 runs was found to be 16.1% and 14.5%. Also for the desorber part, the deviation in the temperature profiles was below 2 °C for almost all runs. There were not found a reason why the predictions in one of the campaigns were poorer than the others.

Sammendrag

I løpet av de siste tiårene har interessen for klimaendringer og global oppvarming vært økende. Menneskelige utslipp av CO_2 er antatt å være en av de viktigste årsakene til den forsterkede drivhuseffekten som fører til global oppvarming. Forskning på CO_2 fangst og lagring har blitt svært viktig for å redusere de menneskeskapte CO_2-utslippene. En av de mest lovende strategiene på kort sikt er å skille ut CO_2 fra avgassen etter forbrenning (*eng. post-combustion*) og ved kjemisk absorpsjon med aminer.

Formålet med forskningen som er utført i arbeidet med denne hovedoppgaven var å utvikle en robust og pålitelig simuleringsmodell for kjemisk absorpsjon med 30vekt% MEA-løsning. Simuleringene er utført i Aspen Plus versjon 8.6, og en innebygd modell, "ENRTL-RK_Rate_based_MEA_Model", er brukt som utgangspunkt for simuleringsmodellen. Absorpsjonskolonnen og desorpsjonskolonnen er simulert hver for seg ved hjelp av en hastighetsbestemmende modell. Fem ulike kampanjer er simulert i absorpsjonsdelen og fire ulike kampanjer er simulert i desorpsjonsdelen. Den innebygde modellen fra Aspen Plus er uten fysisk-kjemiske endringer, men en kinetisk konstant fra litteraturen er brukt til å optimalisere ytelsen til modellen i absorpsjonsdelen av simuleringen. Strømningshastigheter, sammensetning, trykk og temperaturer til inngangsstrømmene er brukt som input i modellen, i tillegg til kokeeffekten i desorpsjonskolonnen. Tilsvarende er strømningshastigheter, sammensetning og temperaturer fra utgangsstrømmene gitt av simuleringsmodellen sammenliknet med eksperimentelle data. I evalueringen av simuleringsmodellen ble absorpsjonsraten/desorpsjonsraten funnet i simuleringene sammenlignet med den som ble målt eksperimentelt.

I alt har 103 eksperimentelle kjøringer blitt simulert for absorpsjonsdelen og 78 eksperimentelle kjøringer blitt simulert i desorpsjonsdelen. Simuleringsresultatene fra absorpsjonsdelen hvor den kinetiske konstanten fra litteraturen er brukt, var tilfredsstillende. Når alle kjøringer fra denne delen er inkludert, er det gjennomsnittlige avviket mellom simuleringene og de eksperimentelle målingene 9,8%, og det absolutte gjennomsnittlige avviket 8,5%. I tillegg er også predikeringene av temperaturprofilene bra. Med unntak av den ene kampanjen, er avvikene under 2 °C fra de eksperimentelle målingene for nesten alle kjøringer. Alle kampanjene gir også liknende simuleringsresultater, noe som indikerer samsvar mellom de ulike kampanjene.

For desorpsjonsdelen er ytelsen til simuleringsmodellen noe mer varierende, og flere mulige årsaker er undersøkt med hensikt å forstå prediksjonene. Det viste seg at modellen med den kinetiske konstant fra litteraturen gir dårligere resultater enn den innebygde Aspen Plus modellen uten endringer. Den innebygde Aspen Plus modellen uten endringer er derfor benyttet i simuleringene i desorpsjonsdelen. Ytelsen til denne modellen er tilfredsstillende for tre av fire kampanjer. Når ett punkt er utelatt, er gjennomsnittlig avvik under 7,9% og absolutt gjennomsnittlig avvik under 7,6% i hver av disse tre kampanjene. Når alle kjøringer er inkludert, er gjennomsnittlig avvik og absolutt gjennomsnittlig avvik funnet til å være henholdsvis 16,1% og 14,5%. Også for desorpsjonsdelen er avviket i temperaturprofilene under 2 °C for nesten alle kjøringer. Det ble ikke funnet noen grunn til at prediksjonene for den siste kampanjen er dårligere enn for de andre.

Table of Contents

List of Symbols

Symbol	Unit	Description
E	kJ/mole MBtu/lbmol	Activation energy (kinetic model)
F	kmol/h	Molar flow rate
k	-	Constant (kinetic model)
$N_{CO_2,abs}$	kmol/h	Absorption rate of CO_2
$N_{CO_2,des}$	kmol/h	Desorption rate of CO_2
n	-	Temperature exponent (kinetic model)
P	kPa	Pressure
T	K	Temperature
R	J K/kmole	Universal gas constant
v	kg/h	Absorption/Desorption rate
x	-	Mole fraction
x_i	%	Deviation absorption/desorption rate between simulated and experimental values

Abbreviations

AAD	Absolute average deviation
AD	Absolute deviation
CCS	Carbon capture and storage
CO_2	Carbon dioxide
COS	Carbon sulfide
CS_2	Carbon disulfide
DTU	Technological University of Denmark
IPCC	Intergovernmental Panel on Climate Change
MEA	Monoethanolamine
NTNU	Norwegian University of Science and Technology
VLE	Vapor liquid equilibrium

1 Introduction

1.1 Objective

Chemical absorption is a widely used technology for the removal of undesired components from gas streams, and it is one of the most promising technologies for capturing carbon dioxide (CO_2) from flue gases. Pilot testing is important in order to obtain reliable data on the kinetics of absorption and on energy consumption. However, pilot plants are relatively small compared to an industrial plant. Thus process simulation is needed for the design, development, analysis and optimization of chemical plants and processes.

It is important to establish and achieve high-quality process simulators in order to arrive at a reliable modeling framework. Due to lack of experience with large-scale CO_2 capture, however, the most reasonable means of evaluation the process is simulation and precise modeling using rate-based process simulations. Good process simulators can aid in the evaluation and optimization of operating conditions, and are important for the planning and design of full-scale plants (liquid flow rate, lean solvent loading, gas temperature, packing height, packing type, etc.)

The first objective of this thesis is to establish a simulation model for CO_2 absorption with 30wt% monoethanolamine (MEA) using Aspen Plus version 8.6. An inbuilt template is used as a basis for the simulation model, and it is desired to see how well this model predicts experimental data from different pilot campaigns. However, the main objective of the work is to achieve an insight in the robustness of the simulation model, and compare the different pilot campaigns to each other as well as to study the consistency of the different pilot campaigns.

During the simulations, the absorber and desorber column are simulated separately. Five different pilot campaigns are simulated in the absorber part and four different pilot campaigns are simulated in the desorber part. The campaigns are performed in different pilots, and thus have different absorber and desorber column diameters and different packing materials.

In the absorber simulations, the first campaign is used to adjust the rate-based model, and thereafter the other four campaigns are used for model validation. The simulated and experimental capture rates and temperature profiles in the columns are compared and

discussed. Additionally the influence of the column diameter and packing material on the model predictions are presented.

In the desorber simulations, all four campaigns are used for model validation and consistency studies. The reactions in the desorber column occur rapidly, thus the conditions are almost in equilibrium. The simulated and experimental capture rates and temperature profiles in the column are also compared and discussed in this case.

1.2 Outline of Thesis

The background and motivation for studying CO_2 capture are given in Chapter1. In addition, the status for CO_2 capture and storage projects in the World, and in Norway in particular, is given in the same chapter. In Chapter 2, a process description of the capture process using 30wt% MEA is presented, as well as a closer look onto the solvent and the chemical reactions involved. Chapter 3 includes several papers that are published regarding CO_2 capture with 30wt% MEA, and also several possible simulation packages. A short introduction to Aspen Plus and the template for the simulation model used in this thesis, is given in Chapter 4. Additionally, this chapter gives the procedure for evaluating the performance of the simulation model. In Chapter 5, the modifications made on the simulation model performed on one of the absorber campaigns are shown. Chapter 6 presents the simulation results from the four other absorber campaigns used to validate the simulation model. Chapter 7 gives the simulation results from the four desorber campaigns. In Chapter 8 and 9, the absorber and desorber campaigns are summarized in two separate tables, and the simulation results are discussed. At last, the performance of the simulation model is evaluated in Chapter 10. This chapter also includes suggestions to future work. Supplementary information can be found in Appendix A and B. Aspen Plus simulation files and additional simulation results in Excel files are available by request to hanna.knuutila@chemeng.ntnu.no.

1.3 Motivation

1.3.1 Carbon Dioxide and Global Warming

The Earth's surface absorbs some of the energy which comes from the sun in the form of sunlight, and reflects some of this energy as infrared radiation. Gases in the atmosphere absorb some of this radiation, thereby heating the Earth. This is called *the greenhouse effect*. Common, naturally-occurring greenhouse gases include water vapor, CO_2, methane, nitrous oxide and ozone [1]. However, since the industrial revolution, which started around 1750, greenhouse gas emissions have increased significantly with the result that the concentration of CO_2 has never been this high for at least 800,000 years [2]. This increase has been caused by anthropogenic emissions and enhances the greenhouse effect, resulting in global warming. The largest contributor to this enhanced greenhouse effect is CO_2.
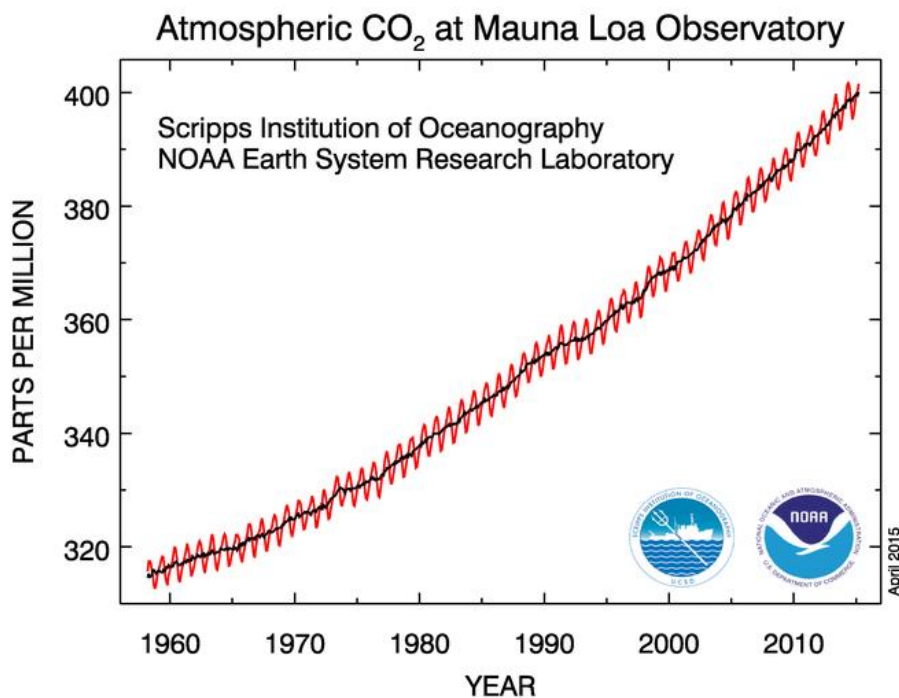
Figure 1-1 Figure illustrating the increased concentration of CO_2 in the atmosphere given by measurements from Mauna Loa Observatory in Hawaii, [3]

Figure 1-1shows measurements of the CO_2 concentration in the atmosphere from 1958 until today, as recorded by the Mauna Loa Observatory in Hawaii. The red line shows the natural yearly variations caused by seasonal changes. From the black line, showing the yearly average CO_2 concentration, it can be seen that the concentration of CO_2 has increased from

about 280 ppm in 1958 to over 400 ppm today. The rate of accumulation of CO_2 has been steep, and the world shows no signs of slowing this down.

The Earth's climate is becoming warmer, and the signs are everywhere. The temperature is rising, rain patterns are changing, sea levels are rising, the oceans are warming, glaciers are melting and sea ice coverage is shrinking. There are also more droughts and more turbulent weather. The Intergovernmental Panel on Climate Change (IPCC) stated in their fifth assessment report in 2014 that "*It is extremely likely that human influence has been the dominant cause of the observed warming since the mid-20th century*"[2].

The sources of anthropogenic carbon dioxide emissions are:

- Burning fossil fuels to produce electricity
- Burning gasoline and other fossil fuels to run vehicles
- Cutting down and burning trees or vegetation
- Some industrial and manufacturing processes, such as steel and cement production, and the production of certain chemicals

If one look at the CO_2 emissions from the consumption of energy since 1990, it can easily be seen that the emissions are growing.

Table 1-1 Table showing the world's CO_2 emissions from combustion of energy since 1990 and the percentage contribution from the United States, China and Norway[4]

Year	1990	2000	2010	2012
World's total emissions [Million Metric Tons]	21610.38	24041.05	31059.46	32723.21
The United States [%]	23.33	24.39	18.13	16.11
China [%]	10.49	13.17	23.98	26.12
Norway [%]	0.16	0.17	0.14	0.13

As can be seen from Table 1-1, the United States has been a large contributor to the world's CO_2 emissions since 1990. However, their percentage of total emissions has decreased since the year 2000. However, China has now overtaken the US as the major producer of CO_2 emissions as a result of its surging economic growth and increased industrialization. In Norway, on the other hand, 97% of all power production comes from hydropower, which is both environmentally friendly and a renewable energy source. At the

same time, Norway is also Europe's largest oil producer, the world's third largest natural gas exporter, and an important supplier of both oil and gas to other European countries [4].

To combat climate change and global warming, substantial and sustained reductions of greenhouse gas emissions, especially in CO_2 emissions, are required. A decrease in the use of coal and oil, and an increased use of renewable sources will become increasingly imperative. Nevertheless, the world's population is increasing, together with the standard of living, rapid economic growth and industrialization. These changes will continue to result in a higher demand for electricity, and therefore coal, oil and will probably remain important energy sources for years to come.

1.3.2 Mitigating CO_2 Emissions

Many organizations, including the International Energy Agency, IPCC and UK Committee on Climate change recommend that a range of clean energy solutions is the best way to tackle the climate change challenge. Their proposals include:

- Increased energy efficiency, either by conserving energy or through new technical solutions.

- A switch from CO_2 emitting to non-CO_2 emitting electricity sources like solar power, wind power, geothermal technology, hydropower and some forms of biomass.

- Carbon capture and storage (CCS). CCS can capture around 90% of the CO_2 from power stations and industrial facilities.

- Fuel-switching. Industries such as transport, manufacturing and building are energy-intensive and can benefit from using fuel sources that have low emissions.

Of these four mitigation strategies, CCS is probably the most promising in near-term, and can play a major role in reducing the world's greenhouse gas emissions. There are three basic types of CO_2 capture:

1. Pre-combustion – capture processes that convert fuel into a gaseous mixture of hydrogen and CO_2. The hydrogen is separated and can be burnt without producing CO_2, while the CO_2 can be compressed for transport and storage.

2. Post-combustion – processes that separate CO_2 from combustion exhaust gases. CO_2 is captured using liquid solvent or other separation methods.

3. Oxyfuel combustion – processes that use oxygen rather than air for the combustion of fuel which produces exhaust gas that is mainly water vapor and CO_2. The CO_2 can then easily be separated out to produce a high purity CO_2 stream.

Fossil fuel-fired power plants generate a larger percentage of CO_2 emissions than any other industry. Applying carbon capture technology to that sector has therefore the potential for the greatest reduction of CO_2 emissions compared to other sectors. The technology exists and works, but more research is required to reduce the cost and energy penalties [5].

1.3.3 Status for Post-combustion CO_2 Capture

The focus of this thesis will be on post-combustion capture and chemical absorption using 30wt% MEA solvent. Post-combustion can be retrofitted to existing coal-fired plants without requiring substantial modifications, and is the leading alternative for gas-fired power plants since neither oxyfuel combustion nor pre-combustion is suitable.

Several technologies are available for post-combustion capture of CO_2 from power plants. These include chemical absorption with amine solvents, cryogenics, and membrane separation either with or without absorption solvent. Of these, the most widely applied technology is absorption of CO_2 by amine solvents. This is because this process does not require modification to the existing power plant and the technology is commercially available. Cryogenics and membrane separation, on the other hand, require additional materials research and development before they can become viable [6].

The world's first large-scale CCS project in the power sector commenced operation in October 2014 at the Boundary Dam power station in Canada. This is the first commercial-scale post-combustion carbon capture system at a coal-fired power plant in the world, and it captures about 90% of its emissions. Aqueous amine solutions are used to capture the CO_2 which is used for enhanced oil recovery projects or injected into deep saline formations. Two additional large-scale CCS projects in the electric power sector – at the Kemper County Energy Facility in Mississippi and the Petra Nova Carbon Capture Project in Texas – are planned to come into operation in 2016. Also in Asia the interest in CCS is advancing, e.g. with several projects in China [7].

Carbon dioxide is also currently being captured in the industrial sector. For instance, the Sleipner CO_2 Storage project in Norway has been operating since 1996, and captures around one million tons of CO_2 a year [5].

1.3.4 CCS in Norway

In 2006, the minister for oil and energy in the Stoltenberg II Government, Odd Roger Enoksen, stated that Norway should be the leader in CO_2 capture and storage [8]. That same year, the Norwegian government and Statoil agreed to establish the world's largest full-scale CO_2 capture and storage project. This was done in conjunction with the projected combined heat and power plant at Mongstad. The test center is today the world's largest facility for testing and improving CO_2 capture.

After a long planning process, the tests at Mongstad started in 2012. In the initial phase two different technologies were tested, one amine based technology from Aker and one chilled ammonia technology from Alstorm. After the completion of the initial test operations, which ended in August 2014, Shell Cansolv started a new test campaign with amines in November of the same year. The test period is planned to last until 2017, but it has not yet been decided what will happen when this is finished. The planning of the full-scale plant was ended during the autumn in 2013 because the Norwegian government rated the uncertainty of the project as too great [9].

Nevertheless, carbon capture and storage techniques have also made great strides in Norwegian industry. Norcem in Breivik have reported results that exceed all expectations from its test facility for CCS in cement production [10]. At this site, amine technology from Aker is being used, and the tests are scheduled to continue until autumn 2015.

The CO_2 concentration in flue gas at cement factories is much higher than the concentration in flue gas from coal and gas fired power plants[1]. This high concentration makes the capture less energy intensive and cheaper compared to capture from coal and gas power plants.

---

[1] CO_2 concentration from standard flue gas from coal and gas fired power plants is 12 and 3.5% respectively, while the CO_2 concentration in flue gas from cement factories is 18% at Breivik, but can amount to as much as 22%.

10

2 CO$_2$ Absorption Using MEA Solvent

2.1 Process Description

Chemical absorption using MEA solvents was developed over 70 years ago as a general, non-selective solvent to remove acid gases, such as CO$_2$ and hydrogen sulfide, from natural gas streams. Concerns about degradation and corrosion kept the solvent strength relatively low (typically 20-30% amines by weight in water), resulting in relatively large equipment sizes and solvent regeneration costs [6].

Figure 2-1 is a diagram depicting a general process flow. The underlying principle is the exothermic, reversible reaction between CO$_2$ and MEA forming carbamate. The process consists of four stages. First, the inlet flue gas is brought into contact counter-currently with the lean solvent containing MEA in a packed absorber column, where the CO$_2$ is preferentially absorbed by the solution. The CO$_2$ enriched solution is then preheated in a cross heat exchanger before entering the stripper/desorber column, where the reaction is reversed by the addition of heat. Next, high-purity CO$_2$ is produced from the top of the stripper, where it is further compressed and transported to a geological storage site, or injected into an oil and gas reservoir. Finally, the regenerated lean solvent is recycled to the absorber column.

The supply of heat for solvent regeneration is by far the most expensive aspect of this process. The cost of solvents, electricity, and energy for pumps and cooling is also high, but to a lesser extent [11]. The lowest reboiler duty found from experimental work with 30wt% MEA solvent performed by Tobiesen et al., was 3.7 MJ/kg CO$_2$ removed [12].
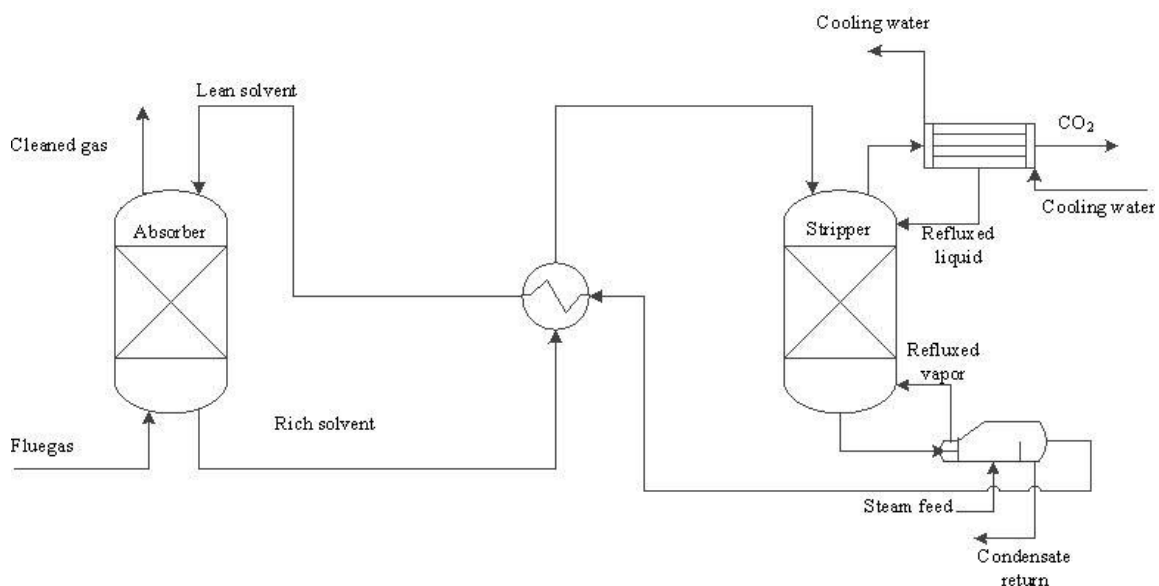
Figure 2-1 A general flow diagram of the CO$_2$-MEA absorption process

2.2 Monoethanolamine

A good solvent is generally characterized by the following properties [13]:

i.   High selectivity for CO_2

ii.   Low propensity to degrade over time and low volatility

iii.   High maximum solvent loading

iv.   Low lifetime cost

v.   Wide envelope of possible operating conditions (pressure, temperature, etc.)

vi.   Low enthalpy of absorption. The importance of this is often directly linked to the energy penalty that the solvent regeneration process imposes on the power plant.

MEA is the most widely used amine for CO_2 capture, and it is preferred for its capacity to achieve maximum removal in systems with low partial pressures of CO_2 and with no contaminations of COS and CS_2[2]. The advantages of MEA are that it reacts rapidly with CO_2 and has a high capacity due to its low molecular weight. It is also less volatile than many other amines and is relatively inexpensive. Disadvantages include limited loading, with a maximum loading of 0.5 mole CO_2/mole MEA, and higher corrosivity than most other amines, requiring more expensive construction materials. MEA also has a high heat of reactions, leading to high energy requirements in the reboiler. Additionally, since MEA gradually volatilizes and degrades, especially in the presence of oxygen and/or sulfur dioxide, it necessitates the timely injection of fresh solution [6].

$$H_2N \diagup \diagup OH$$

Figure 2-2 An illustration of the MEA molecule structure

Figure 2.2 represents the MEA molecule structure. As can be seen, MEA has two hydrogen atoms directly attached to a nitrogen atom, and is therefore called a primary amine.

---

[2] MEA forms irreversible products with COS and CS_2 resulting in vast chemical losses, 14. Sanggie, F.W., *Process modeling and comparison study of acid gas removal unit by using different aqueous amines* in *Chemical Engineering*. 2011, Universiti Malaysia Pahang.

2.3 Chemical reactions

The process whereby CO_2 is absorbed into the MEA solvent is called chemisorption. This is because the solvent chemically reacts with CO_2 and forms a bond. The reactions for CO_2 absorption as present in Aspen Plus, are shown in Table 2-1.

Table 2-1 The equilibrium and kinetic reactions defined in Aspen Plus for the CO_2-MEA system

Reaction Number	Reaction Type	Stoichiometry
1	Equilibrium	$MEAH^+ + H_2O \leftrightarrow MEA + H_3O^+$
2	Equilibrium	$2H_2O \leftrightarrow H_3O^+ + OH^-$
3	Equilibrium	$HCO_3^- + H_2O \leftrightarrow CO_3^{2-} + H_3O^+$
4	Kinetic	$OH^- + CO_2 \rightarrow HCO_3^-$
5	Kinetic	$HCO_3^- \rightarrow OH^- + CO_2$
6	Kinetic	$MEA + CO_2 + H_2O \rightarrow MEACOO^- + H_3O^+$
7	Kinetic	$MEACOO^- + H_3O^+ \rightarrow MEA + CO_2 + H_2O$

Reaction 1 represents a basic equation of amine protonation. The standard water dissociation process is given in reaction 2. Reaction 4 gives the first dissociation of CO_2 to form HCO_3^-, while reaction 3 gives the second dissociation of CO_2 forming CO_3^{2-}. Reaction 5 is the opposite of reaction 4. One of the most important reactions is number 6, representing the reaction between MEA and CO_2 forming carbamate (MEACOO$^-$). Reaction 7 represents the carbamate reversion which takes place in the desorber column.

The CO_2-MEA reaction is exothermic, thus it is preferable to have low temperatures in the absorber column, whereas higher temperatures are preferred in the desorber column to reverse the reaction. This can also be seen from the vapor-liquid equilibrium graph which is given in Chapter 4.2. Since the CO_2-MEA reaction produces energy, the temperature in the absorber column will rise. It can be hypothesized that a temperature bulge occurs with the greatest rate of absorption. When there is excess solvent relative to the inlet CO_2, the greatest absorption will occur at the bottom of the column, giving the temperature bulge there. The opposite happens if there is insufficient solvent such that the greatest absorption rate happens at the top of the column, giving the temperature bulge there [15]. The temperature bulge, with various locations in the column, can be seen in the different temperature profiles given in the results section of this thesis.

3 Literature Review

A significant amount of research has been done on carbon capture and storage in recent years because of the growing interest in and knowledge about global warming and the effects of an increased concentration of greenhouse gases in the atmosphere. As noted above, IPCC have stated that CO_2 is the largest contributor to the enhanced greenhouse effect, and therefore is the main target in combating climate change.

The focus of this thesis is on post-combustion capture by absorption using 30wt% MEA as solvent. However, there are also other possible solvents on the market, and there is ongoing research to develop new solvents and solvent blends, mainly to reduce the process energy demand.

3.1 Possible process design

The general process flow diagram shown in Figure 2-1 is the one most frequently reported as being used. However, there are other process designs. One of which is the UOP's (Universal Oil Products LLC) Amine Guard FS^{TM} system. In this system the absorber operates at a higher pressure than atmospheric, and the rich solution is flashed after the absorber. The liquid phase is preheated before entering the stripper, while the gas phase is directly mixed with the CO_2 stream leaving the top of the stripper [16]. A flow diagram of this system is shown in Figure 3-1.
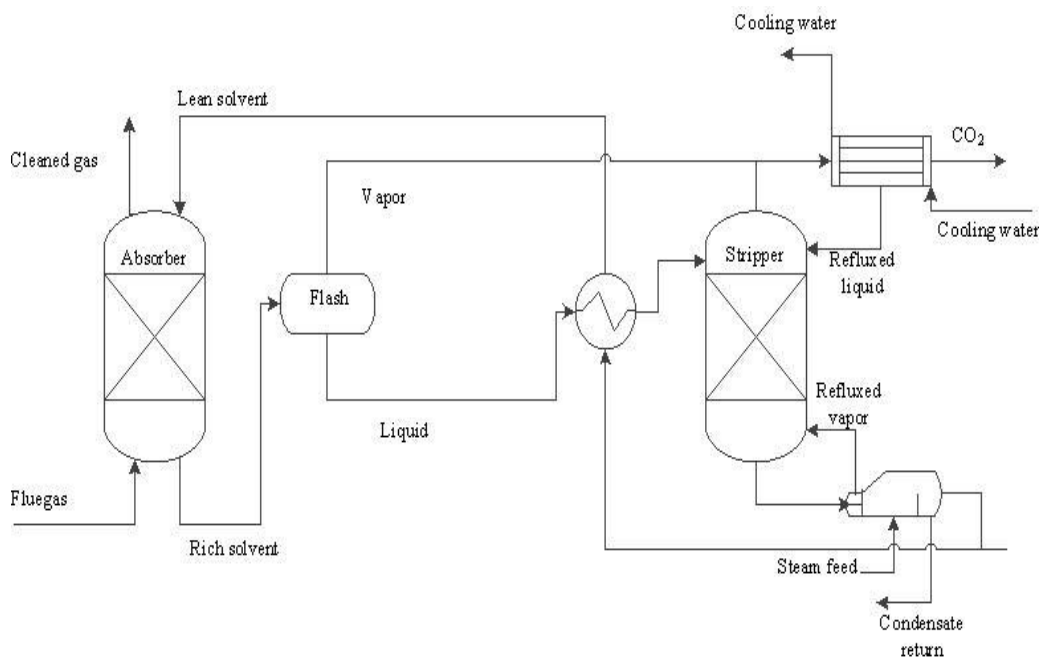
Figure 3-1 Process flow diagram of UOP's Amine Guard FS^{TM} system

Another possible process design is the Kerr-McGee/ABB (Asea Brown Boveri Ltd.) Lummus Global MEA absorption process. This process uses an "energy saving design", where the rich solution is flashed after the heat exchanger. The liquid phase is fed to the stripper, while the gas phase is mixed with the CO_2 stream leaving the top of the stripper [16]. The flow diagram for this system is shown in Figure 3-2.
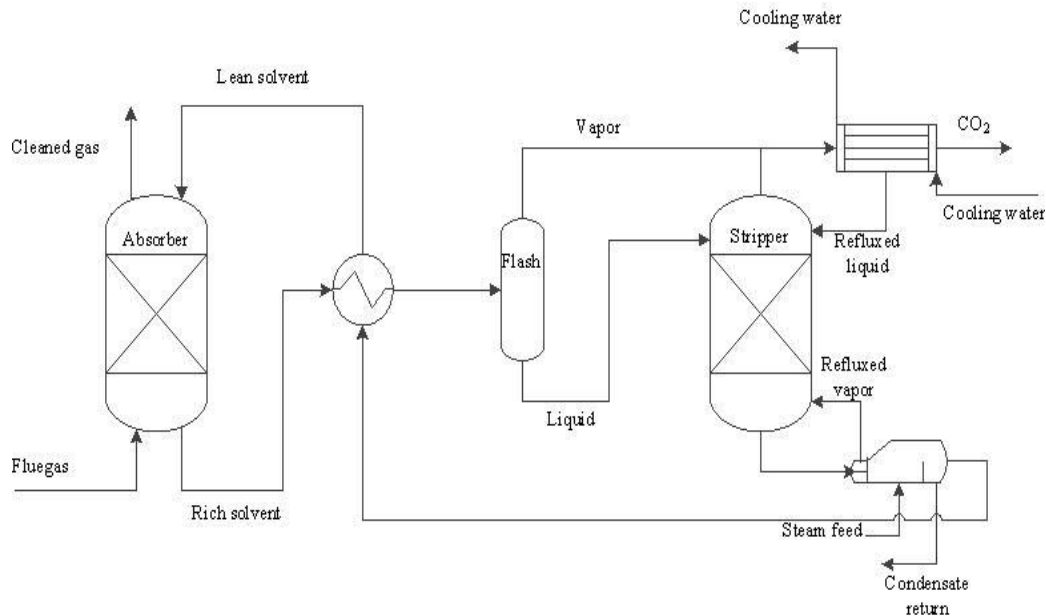
Figure 3-2 Process flow diagram of Kerr-McGee/ABB Lummus Global MEA absorption process

Feliu and Soave proposed a design where only parts of the rich solution are sent through the heat exchanger in order to significantly reduce the reboiler duty. In this process the part of the rich solvent that is not heated is fed to the top of the stripper, while the part of the rich solvent that is heated is fed to the middle of the stripper [17]. A flow diagram of the proposed design is given in Figure 3-3.
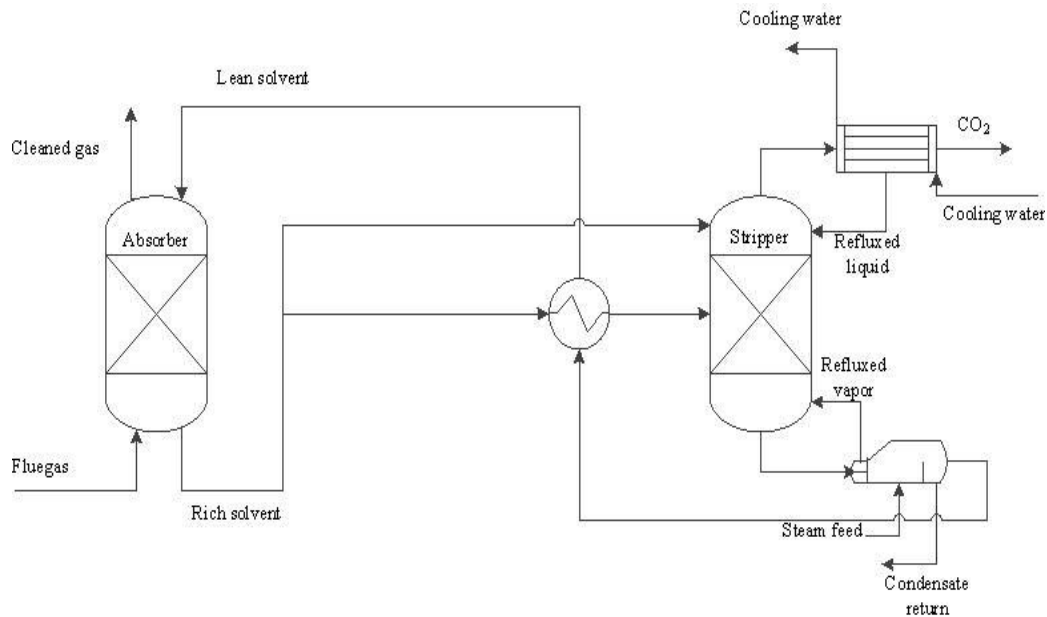
Figure 3-3 Process flow diagram of the proposed process design by Feliu and Soave

In the pilot plant at Jaworzno II Power Plant in Poland, both inter-stage absorber cooling and split flow systems have been tested. In inter-stage cooling, the rich solution is split and sent to two separate heat exchangers, similar to the design proposed by Feliu and Soave. The flow diagram for this process is shown in Figure 3-4. In the split flow process, both a lean solution and a semi-lean solution are extracted from the stripper, and heat exchanged with the rich solution before they are fed to the absorber in two separate streams. The lean solution is fed to the top of the absorber and the semi-lean solution to the middle of the absorber. The flow diagram for this process is shown in Figure 3-5. These two options are also ways of reducing the energy demand of the amine based carbon capture process, and have shown good results during testing [18].
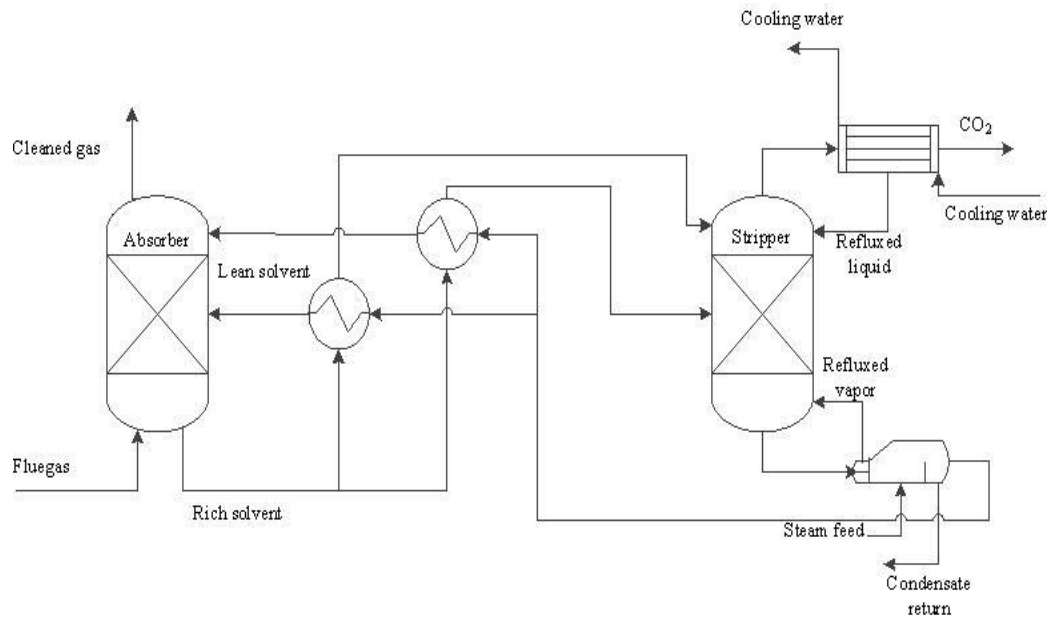
Figure 3-4 Process flow diagram of the inter-stage cooler cooling process at Jaworzno II Power Plant
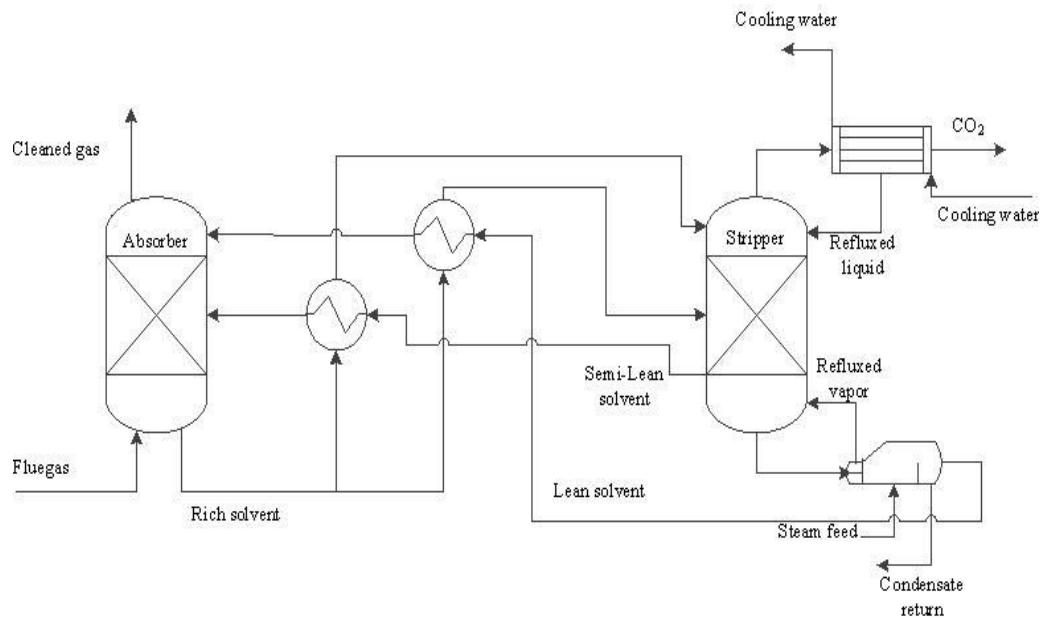
Figure 3-5 Process flow diagram of the split feed process at Jaworzno II Power Plant

3.2 Published Pilot Campaigns with 30wt% MEA

A number of papers have been published regarding CO_2 capture using 30wt% MEA related to pilot operation where the general process design shown in Figure 2-1is used. The papers are written with some different objectives, and not all publications include necessary data such that it can be used for process simulation. The focus in this thesis was to make a simulation model of the absorber part and desorber part of the process separately. The papers presented below gives an insight in literature that is published with 30wt% MEA solvent and process design similar to that shown in Figure 2-1.

"*Experimental validation of a rigorous absorber model for CO_2 postcombustion capture*" [19]. The pilot plant used in the experimental work is located at NTNU, and absorber data for 20 runs are published in the paper by Tobiesen et al. (2007). The absorber column has a diameter of 0.15 m and a packing height of 4.36 m. The packing material in the absorber column is Sulzer Mellapak 250Y. During the experiments, a synthetic gas was used. The objective of the work was to develop a rigorous rate-based model and to validate it against mass-transfer data.

"*Experimental validation of a rigorous desorber model for CO_2 post-combustion capture*" [12]. The pilot plant used in the experimental work is located at NTNU, and desorber data for 19 runs are published in the paper by Tobiesen et al. (2008). The desorber column has a diameter of 0.1 m and a packing height of 3.89 m. The packing material in the desorber column is Mellapak 250Y. During the experiments, a synthetic gas was used. The objective of the work was to develop a rigorous rate-based model and to validate it against mass-transfer data.

"*CO_2 post combustion capture with a phase change solvent. Pilot plant campaign*" [20]. The pilot plant located at NTNU is used also in the experimental work performed by Pinto et al. (2014). The absorber column diameter is the same, 0.15 m, but the packing height and packing material are changed to 4.23 m and Sulzer BX packing. The desorber column diameter is 0.1 m and the packing height is 3.57 m, also packed with Sulzer BX. A synthetic gas has been used during the experiments, and data for 6 runs have been published. However, there is not published enough data to perform process simulations. The objective of the work

was to compare the performance of a new class of solvents, DEEA/MAPA, with MEA solvent.

"*A new pilot absorber for CO_2 capture from flue gases: Measuring and modelling capture with MEA solution*" [21]. The pilot plant used in this experimental work is located at DTU, and data for 23 runs are published in the paper by Sønderby et al. (2013). The absorber column has a diameter of 0.1 m, and the packing height varies from 1.6 to 8.2 m depending on where the lean solvent enters the column. The packing material is Sulzer Mellapak 250 Y and also here a synthetic flue gas had been used. The objective of the work was to compare simulation results with pilot data changing three parameters: packing height, liquid flow rate and loading of lean solvent.

"*Post-combustion CO_2 capture by reactive absorption: Pilot plant description and results of systematic studies with MEA*" [22]. In the experimental work by Notz et al. (2012), the pilot plant from the EU CASTOR project located at the University of Kaiserslautern is used. The absorber column diameter is 0.125 m and the packing height is 4.2 m. The desorber column diameter is 0.125 m and the packing height is 2.52 m. In both the absorber and desorber column the packing material is Sulzer Mellapak 250Y. During the experiments, gas from a natural gas burner plus CO_2 from a gas bottle were used. The paper provides flow diagrams with data and information from 47 runs. The objective of the work was to present the plant and critically discuss its operation and the data evaluation by performing parameter studies.

"*Validation of mass transfer correlations for CO_2 absorption with MEA using pilot data*" [23]. The experimental work from this paper by Razi et al. (2013), is performed at the Esbjerg CESAR pilot plant. The absorber column diameter is 1.1 m and the packing height is 17 m. The desorber column has a total packing height of 10 m, but the desorber diameter is not given. The packing material is Sulzer Mellapak 2X in both the absorber and desorber column, and the flue gas is given from Dong Esbjerg power station. The paper provides some data from 4 runs, but not enough to perform process simulations. The objective of the work was to compare several design correlations available in literature and to perform a sensitivity

analysis to show the effect of the kinetic model and design correlations in a large-scale CO_2 capture process.

"Comparison of solvent performance for CO_2 capture from coal-derived flue gas: A pilot scale study" [24]. The pilot plant used in the experimental work by Liu et al. (2013) is located at the University of Kentucky. The absorber column diameter is 0.1 m and the packing height is 3.25 m. The desorber column diameter is 0.1 m, but the packing height is not given. The packing material is Plastic Pall ring random packing, and the flue gas used in the experiments is generated from a coal-based flue gas generator. Some data are published for 7 runs, but not enough to perform process simulations. The objective of the work was to compare the performance of a proprietary solvent (CAER-B2), which is an amine-carbonate blend, with 30wt% MEA under similar experimental conditions.

"A study of the CO_2 capture pilot plant by amine absorption" [25]. The pilot plant used in the experimental work by Shim et al. (2012) is located at Korea Electric Power Research Institute. The absorber column diameter is 0.4 m and the packing height is 23.5 m. The desorber column diameter is 0.35 m and the packing height is 17 m. Each of the towers was packed with ring-shaped stainless steel packing material (Intalox Metal Tower Packing). The flue gas used during the experiments is emitted from a coal fired plant. Neither this paper provides enough data to perform process simulations. The objective of the work was to study the absorption/regeneration process, and the CO_2 recovery as a function of flow rate and input location of absorbent, pressure and temperature of the stripper, and temperature of the flue gas.

"Novel full height pilot plant for solvent development and model validation" [26]. The pilot plant used in the experimental work by Mejdell et al. (2011) is built at SINTEF in Trondheim, and is a full height pilot. The absorber packing height is 19.5 m, and the packing type used is Mellapak 2X, a structured industrial packing. The packing height can however be reduced by alternatively feed the lean amine further down in the absorber column. The diameter of the absorber column is 0.2 m. The stripper column has an inner diameter of 0.162 m and a total packing height of 13.6 m, also filled with structured Mellapak 2X packing. A synthetic gas is used during the experiments. All together 71 runs were performed, but there is

not published enough data to perform process simulations. The objective of the work was to demonstrate the energy requirement and necessary absorber height to get the desired CO_2 removal, and to find optimal loading and circulation rate for different solvents. Additionally long-term degradation of amines and solvent replacement were studied.

In the evaluation of which of the published campaigns that could be used for the process simulation work in this thesis, the access to process information required by Aspen Plus was important. Inlet temperatures, pressures and flow rates had to be given, as well as the composition of the streams. This concerned both the flue gas and the lean solvent entering the absorber, and the rich solvent entering the desorber column. Also the reboiler duty and the temperature and pressure in the condenser had to be given. However, since the absorber and desorber were simulated separately, only information regarding one of the columns was needed.

3.3 Pilot Campaigns Simulated in the Thesis

3.3.1 Pilot Campaigns Absorber Part

----In this thesis, experimental data of the absorber from five different pilot campaigns, all with 30wt% MEA, were used to establish a simulation model in Aspen Plus. Experimental data retrieved from a pilot plant located at NTNU, Tobiesen et al. (2007) [19], were used to fit the model, and the other four campaigns were used for model validation. Simulation results are heavily influenced by the choice of mass transfer coefficients and kinetic parameters in the rate-based model. Thus it is important to validate the simulation model built, preferentially with experimental data from pilot plants with different packing height and diameter. Table 3-1gives an overview of the pilot campaigns used for absorber simulations in this thesis.

Table 3-1 Table giving an overview of the pilot campaigns used for simulation model fitting and validation in the absorber simulations

Pilot campaign	Tobiesen et al.	Pinto et al.	Enaasen et al.	Sønderby et al.	Notz et al.
Campaign Used For	Simulation model fitting	Validation	Validation	Validation	Validation
Absorber Specifications					
Column Internal Diameter [m]	0.150	0.150	0.150	0.100	0.125
Main Packing Height [m]	4.36	4.23	4.23	1.60-8.20	4.2
Packing Type (Experimental)	Sulzer Mellapak 250Y	Sulzer BX	Sulzer BX	Sulzer Mellapak 250Y	Sulzer Mellapak 250Y
Packing Type (Aspen Plus, Packing Rating)	Koch Flexipak 250Y	Koch Flexipak 500X	Koch Flexipak 500X	Koch Flexipak 250Y	Koch Flexipak 250Y

Flow Parameters

Fluegas Flow Rate [kg/h]	137.0-165.4	97.5-101.7	94.4-140.8	39.8-44.2	55.5-100.0
Lean Solution Flow Rate [kg/h]	187.9-579.1	198.6-206.6	142.1-240.9	130.5-565.6	75.0-350.3
L/G [mol/mol]	1.3-4.5	2.3-2.4	1.3-2.1	3.9-18.1	1.3-5.4
Lean Solution Loading [mol CO_2/mol MEA]	0.183-0.409	0.210-0.350	0.215-0.341	0.112-0.300	0.111-0.356
Temperature Fluegas [°C]	39-69	38-51	38-51	20-28	23-49
Temperature Lean Solution [°C]	40-66	41-41	41-58	20-28	30-50
Absorber Pressure [kPa]	99-104	104-106	102-106	101-104	100

As can be seen from the table above, the packing type specified in Aspen Plus differs from the packing type used in the experiments. In Aspen Plus rate-based simulations, packing rating is used to define the column diameter and packing height, and the packing parameters are used to calculate mass transfer rates and other parameters like the pressure drop. Aspen Plus has been provided with packing specifications from several vendors. However, Sulzer is not one of them, and therefore similar packings with similar size and pressure drop have been used as replacements during the simulations. Sulzer Mellapak 250Y, used in the Tobiesen et al., Sønderby et al. and Notz et al. experiments, has been replaced by Koch Flexipak 250Y. Both of these packings have surface area 250 m^2/m^3 and similar pressure drops. The choice of using Koch Flexipak 250Y was based on a recommendation by Reza Farzad at NTNU, who has worked with similar absorber simulations. As a replacement for Sulzer BX packing, Koch Flexipak 500X has been used. Also here the packings have equal surface area, 500 m^2/m^3 and is believed to have similar pressure drops. The choice of using Flexipak 500X as replacement was based on a trial-and-error approach. Different packings with surface area 500 m^2/m^3 was tested in the Pinto et al. simulations, and Flexipak 500X gave the best results when comparing simulation results with experimental measurements.

3.3.2 Pilot Campaigns Desorber Part

Furthermore, experimental data from four desorber pilot campaigns, all with 30wt% MEA, were used for model validation and consistency studies. Table 3-2 gives an overview of the pilot campaigns used in the desorber simulations in the thesis.

Table 3-2 Table giving an overview of the pilot campaigns used for simulation validation in the desorber simulations

Pilot campaign	Tobiesen et al.	Notz et al.	Enaasen et al.	Pinto et al.
Campaign Used For	Validation	Validation	Validation	Validation
Desorber Specifications				
Column Internal Diameter [m]	0.100	0.125	0.100	0.100
Main Packing Height [m]	3.89	2.52	3.57	3.57
Packing Type (Experimental)	Sulzer Mellapak 250Y	Sulzer Mellapak 250Y	Sulzer BX	Sulzer BX
Packing Type (Aspen Plus, Packing Rating)	Koch Flexipak 250Y	Koch Flexipak 250Y	Koch Flexipak 500X	Koch Flexipak 500X
Flow Parameters				
Rich Solution Flow Rate [kg/h]	183.5-569.7*	79.8-359.0	157.0-246.1	203.4-210.2
Rich Solution Loading [mol CO_2/mol MEA]	0.264-0.457	0.297-0.501	0.323-0.485	0.250-0.479
Temperature Rich Solution [°C]	103-118	106-117	100-110	102-112
Desorber Pressure [kPa]	194-216	200-230	169-190	175-177
Reboiler Duty [kW]	3.9-13.8	5.2-16.7	6.1-10.4	4.2-8.4

The rich solvent flow rate for the Tobiesen et al. campaign was reported in l/min. The kg/h numbers are taken from Aspen Plus.

As can be seen from the table above, the packing type specified in Aspen Plus differs from the packing type used in the experiments also in the desorber part. The same replacements as described for the absorber pilot campaigns in Chapter 3.3.1 are used.

3.4 Commercially Available Simulation Packages

Process simulators available today in the field of CO_2 absorption/desorption can be divided into two groups: rate-based models and equilibrium stage models. HYSYS from Aspen Tech is a stage based model, but includes rate-based mass transfer calculations through an estimation of tray efficiencies. The program has the capability of calculating most types of process equipment, but has shown some none-satisfactory results for specific amine treating units. Additionally, the amine package does not differentiate among the type of column packing during column calculation [27].

ProTreat from Optimized Gas Treating Inc. is a package especially developed for amine treating units. The model is fully rate-based, but limited in the number of absorbent systems included [27].

Aspen Plus also belongs to Aspen Tech, and has a rate-based model which uses the Chen NRTL equilibrium model. It is considered as the market-leading chemical process optimization software used for design, operation, and optimization of safe, profitable manufacturing facilities [28].

PRO II/Provision is another rate-based model. This process simulator uses the RateFrac module from Koch-Glitsch [27].

In addition, Tsweet can be mentioned as an equilibrium stage model [27].

It was decided to use the rate-based approach in the simulations in this thesis. This was preferred due to the nature of the rate-based framework. A scale-up from laboratory scale to industrial scale should not require any additional parameter fitting in these types of models. Hydraulic parameters will be recalculated for the new and larger systems, and adjusted accordingly. In the case of an equilibrium stage model, new tray efficiencies or residence time profiles need to be calculated, which may be a more demanding task [27]. Because Aspen Plus has the ability to handle solid, liquid, and gas processes, advanced electrolytes and equation oriented modeling mode, as well as having a good reputation, this process simulator was chosen.

4 Simulation Model of the CO_2 Absorption/Desorption Process in Aspen Plus

4.1 Aspen Plus Inbuilt Template

The CO_2 absorption/desorption process using MEA as solvent, was simulated in Aspen Plus version 8.6. As a basis for the simulation model, the inbuilt template, "ENRTL-RK_Rate_based_MEA_Model", was used. This is a rate-based inherent rigorous model that uses electrolyte Non-Random-Two-liquid (eNRTL)[3] to predict activities. The ENRTL-RK is a property method in Aspen Plus which can be chosen by the user. The method uses the Redlich-Kwong equation of state[4] to find vapor phase properties, and Henry's law[5] for electrolyte systems under unsymmetric reference state for ionic species. The Kent-Eisenberg method is used to find equilibrium constants and enthalpy. All simulations are performed in steady-state [32].

The inbuilt Aspen Plus model for CO_2 absorption/desorption using MEA solvent is developed in collaboration between Aspen Plus and the University of Texas at Austin. The model is based on pilot plant experiments with 30wt% MEA, and includes the required physical property and reaction parameters to simulate these types of systems [33]. In the development of the simulation model used in this thesis, the physicochemical properties package was used without any changes.

The property method ENRTL-RK is extended to accommodate interactions with ions in solution. Aspen Physical Property System contains binary and pair interaction parameters and chemical equilibrium constants for systems containing CO_2, H_2S, MEA and H_2O with temperatures up to 120 °C and amine concentrations up to 50wt%.

Both the absorber and the desorber column in the template are of the type RadFrac, which is a column selected from the Aspen Plus model bank. An extension of the RadFrac is Aspen Rate-Based modelling, which performs rate-based, non-equilibrium separation. It simulates actual packed columns rather than idealized representations. Aspen Rate-Based modelling treats separation as a mass and heat transfer rate process, instead of an equilibrium

---

[3] The eNRTL model is also known as the Chen electrolyte model. More information about this model can be found 29. Chen, C. and Y. Song, *Symmetric Electrolyte Nonrandom Two-Liquid Activity Coefficient Model*. Industrial & Engineering Chemistry Research, 2009. **48**.

[4] Redlich-Kwong equation of state 30. Adewumi, M. *Redlich-Kwong EOS (1949)*. 17.04.2015].

[5] Henrys Law 31. Zumdahl, S.a.S., *Chemistry*. Vol. Fifth edition. 2000: Boston, MA: Houghton Miffin Company.

process. This represents higher fidelity and gives more accurate simulation results than those attainable from equilibrium stage models. The degree of separation achieved between the contacting phases depends on the extent of mass and heat transfer between phases, and the transfer rates are strongly affected by the extent to which the phases are not in equilibrium. Aspen Rate-Based simulation assumes that thermodynamic equilibrium prevails only at the vapor liquid interface separating contacting phases[6].

Mass transfer correlations and the interfacial area method used in the Aspen Plus calculations are taken from Bravo et al. (1985). The heat transfer correlation is taken from Chilton and Colburn.

In the template the absorber column consists of 20 stages where the flue gas enters in the bottom, stage 20, as "Gas-only" and the lean solvent enters in the top, stage 1, as "Liquid-only". These feed stream conventions, "Gas-only" and "Liquid-only", in Aspen Plus means that the feed flows to the specified stage and is treated as being entirely in the phase specified. This means e.g. that the flue gas is entirely in gas phase, and enters in stage 20, and not in-between stage 19 and 20 which also is possibility. The cleaned gas leaves the column in stage 20, and the enriched solvent leaves the column in stage 1.

The desorber column also consists of 20 stages, where the bottom stage is the reboiler. The rich inlet stream is defined as "Vapor-Liquid", meaning that it is treated as a two-phase stream by Aspen Plus. The stream leaving the top of the desorber is led into a flash, where the cleaned CO_2 gas stream is separated, and the condensed stream is recycled back to the desorber column. The lean solution, stripped from CO_2, leaves the desorber column in the bottom.

The number of stages in the column and the feed stream conventions were kept constant for all simulated campaigns, except for some of the runs in the Sønderby et al. campaign. This will be specified in Chapter 6.3.

---

[6] Information about Aspen Rate-Based simulations is taken from the Aspen Plus help function.

4.2 Vapor Liquid Equilibrium

Equilibrium curves for CO_2 in 30wt% MEA were generated in Aspen Plus by flash tank simulations to examine the ability of the model to predict vapor liquid equilibrium (VLE). VLE determines the operating characteristics of the process and should therefore be correct to ensure that the simulations are fairly good. The simulation results were compared to experimental data from Jou et al. [34], which is often used to fit models with CO_2 in 30wt% MEA. The result can be seen in Figure 4-1 and Figure 4-2.
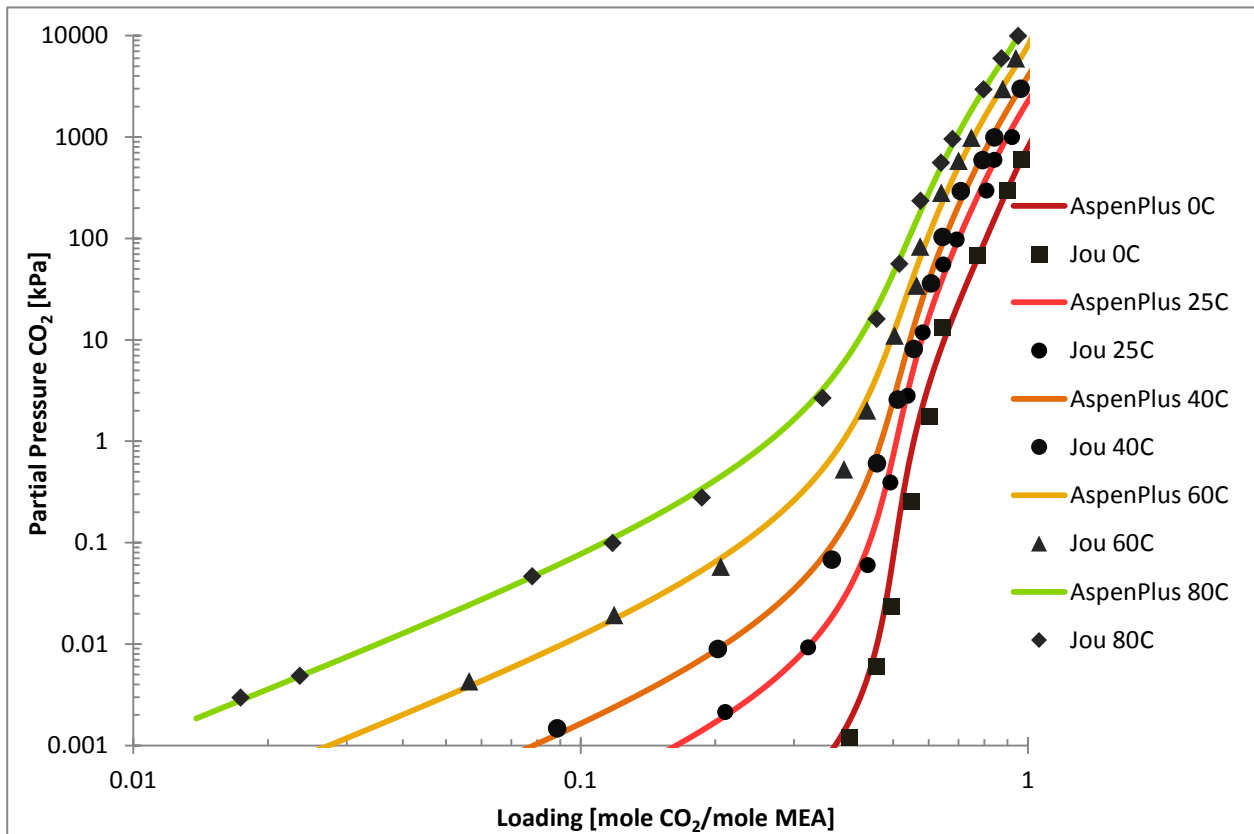
Figure 4-1 Log-Log Plot of CO_2 partial pressure versus loading for temperatures 0°C to 80°C, comparing simulation and experimental data

31
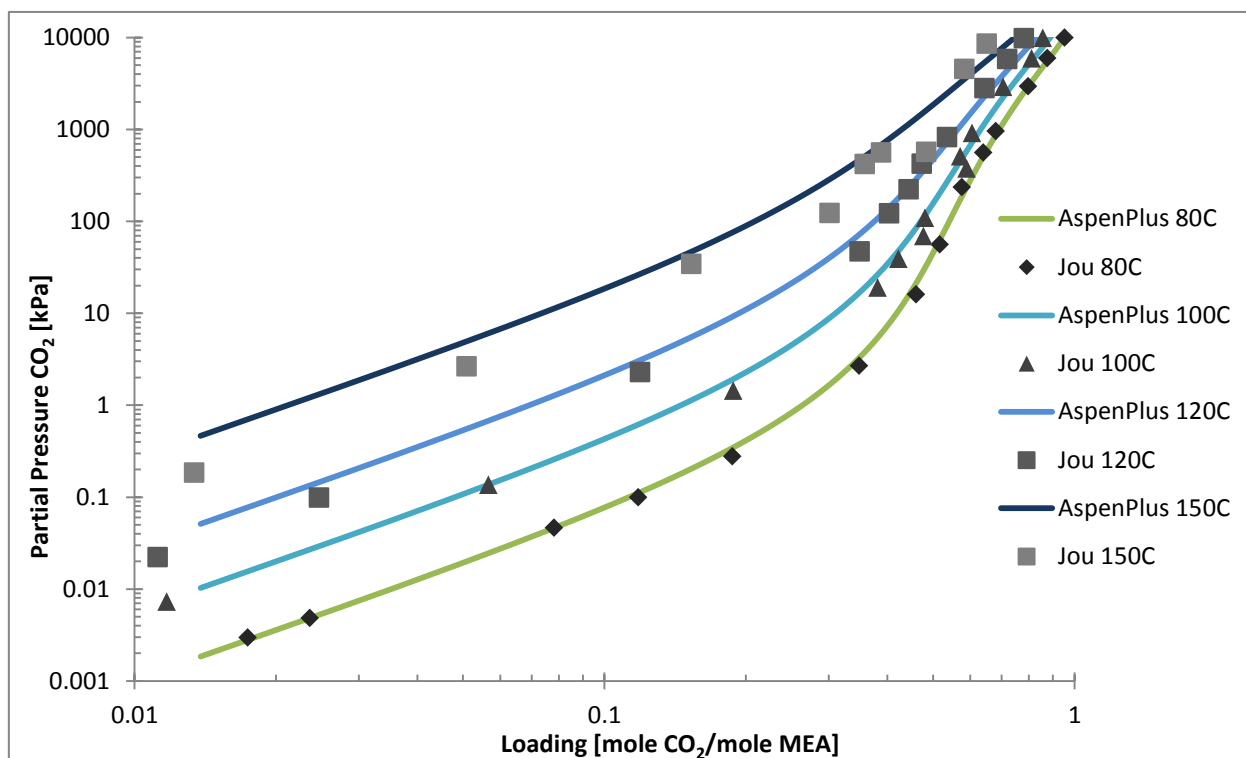
Figure 4-2 Log-Log Plot of CO_2 partial pressure versus loading for temperatures 80°C to 150°C, comparing simulation and experimental data.

As can be seen from the plots in Figure 4-1 and Figure 4-2, the simulations fit very well with the experimental values for all temperatures. It was taken a closer look at the higher temperatures, 80 °C, 100 °C and 120 °C, since these temperatures are most important for the desorber simulations. As mentioned, the reactions in the desorber take place so rapidly that it can almost be considered as equilibrium. Thus it is very important to have precise predictions of the VLE curves at these temperatures to ensure a precise performance of the simulation model. This plot can be seen in Figure 4-3.
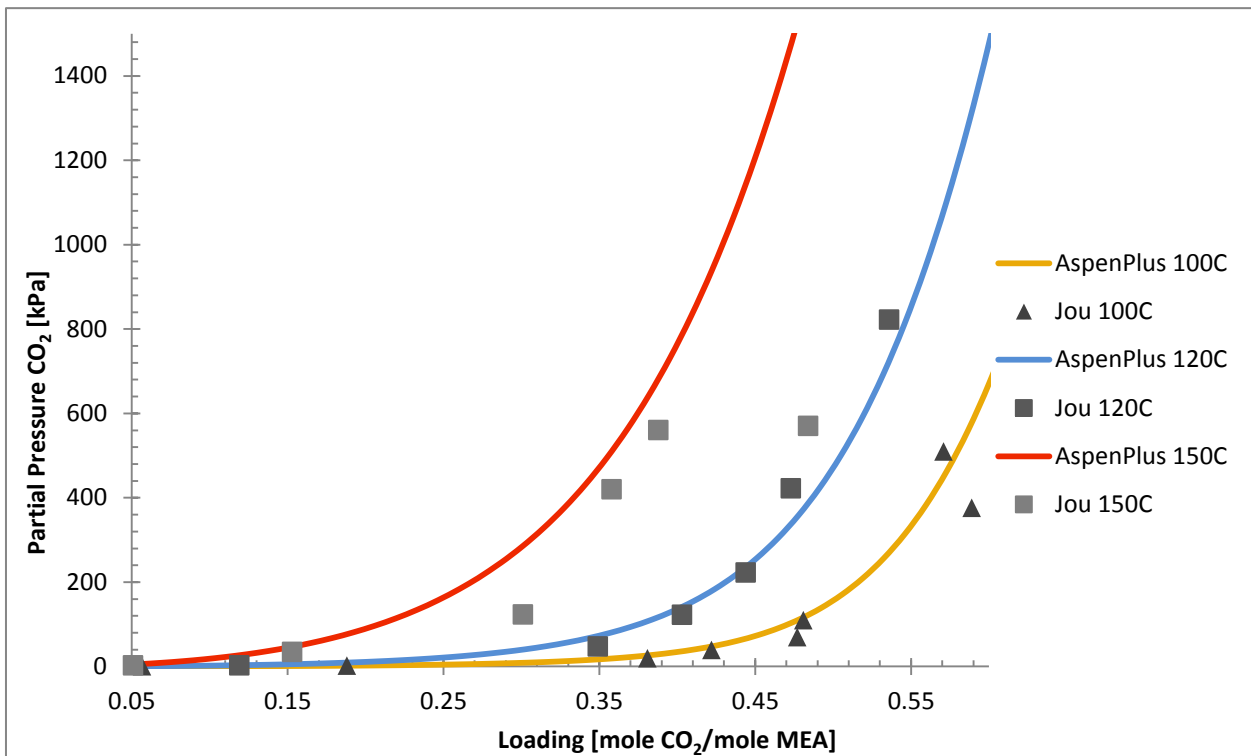
Figure 4-3 Plot, on normal scale, of CO$_2$ partial pressure versus loading for temperatures 100°C, 120°C and 150°C, comparing simulation and experimental data

As can be seen from the plot, the prediction of the simulation model fits well with experimental data from Jou et al. also for high temperatures. The vapor liquid equilibrium behavior of the Aspen Plus model was therefore considered to be precise enough for both the absorber and desorber simulations.

4.3 Comparing Experimental and Simulated Data

4.3.1 Absorber Simulations

The following experimental data was used in the absorber simulations:

- Incoming liquid and gas streams to the absorber: molar flow rate, F; component molar fraction, x_i; temperature and pressure, T and p.

- Outlet liquid and gas streams from the absorber: molar flow rate, F; component molar fraction, x_i; temperature and pressure, T and p.

- Temperatures throughout the absorber packing to yield a temperature profile.

- CO_2 measurements throughout the absorber column to yield a CO_2 profile when possible.

Incoming liquid and gas streams were used as inputs in the absorber simulation model. The outlet flows, temperature profiles, and when possible CO_2 profiles, were compared to the simulation results. The CO_2 absorption rate found from the simulations was compared with experimental data to determine the performance of the model. Generally it is assumed that liquid measurements are more accurate than gas measurements in the absorber column, thus the reported liquid measurements are used for comparison. The percentage deviation between the simulated and experimental absorption rate was calculated from Equation (1). Note that the absorption rate is a small number (typically 3-6 kg/h), and thus small deviations between the experimental and simulated value will give larger percentage deviations.

$$x_i = \frac{v_{sim} - v_{exp}}{v_{exp}} \times 100 \tag{1}$$

In the equation v_{sim} and v_{exp} are the CO_2 absorption rate in kg/h found from the simulations and experimental data respectively.

The percentage deviation was further used to find the average deviation (AD) and absolute average deviation (AAD), which were calculated using the following formulas:

$$AD = \frac{1}{n} \sum_{i=1}^{n} |x_i| \tag{2}$$

$$AAD = \frac{1}{n} \sum_{i=1}^{n} |x_i - \bar{x}| \tag{3}$$

$$\bar{x} = \frac{\sum_{i=1}^{n} x_i}{n} \tag{4}$$

4.3.2 Desorber Simulations

The following experimental data was used in the simulations:

- Incoming enriched solvent stream to the stripper: molar flow rate, F; component molar composition, x_i; temperature and pressure, T and p.

- Outlet liquid and gas streams from the desorber: molar flow rate, F; component molar fraction, x_i; temperature and pressure, T and p.

- Reboiler heat duty, Q; and condenser temperature and pressure, T and p.

- Temperatures throughout the desorber packing to yield a temperature profile.

- CO_2 measurements throughout the desorber column to yield a CO_2 profile when possible.

Incoming enriched solvent stream was used as input in the desorber simulation model. The outlet flows, temperature profiles, and when possible CO_2 profiles, were compared to the simulation results. The CO_2 desorption rate found from the simulations was compared with experimental data to determine the performance of the model. In the desorber case, there were some uncertainties in the publications whether the reported gas or liquid measurements were most accurate. However, generally the gas measurements have been used for comparison to the simulation results, but this will be specified for the individual campaigns. The percentage deviation between the simulated and experimental desorption rate was calculated from the same expression as for the absorber shown in Equation (1) Chapter 4.3.1. The same applies to the average deviation and absolute average deviation, Equation (2) and (3) in Chapter 4.3.1. Also the desorption rate is a small number, in the same range as the absorption rate. Thus, small deviations between the simulated and experimental value will give larger percentage deviations also here.

5 Absorber Simulation Model Fitting

During the first simulation round, the Aspen Plus template was used without any changes except the conditions of the inlet streams, and the packing type and packing height in the absorber column. The results were compared to experimental data from Tobiesen et al. (2007) presented in Chapter 3.3.1. The reported vol% of CO_2 in the flue gas is given on a dry basis. For the simulations, the wet vol% of CO_2 was calculated assuming the flue gas was saturated with water. The amount of H_2O entering the absorber was found using Raoults law[7]. The rest of the gas stream entering the absorber was set to be N_2. A print screen of the Aspen Plus flowdiagram can be seen in Figure 5-1.
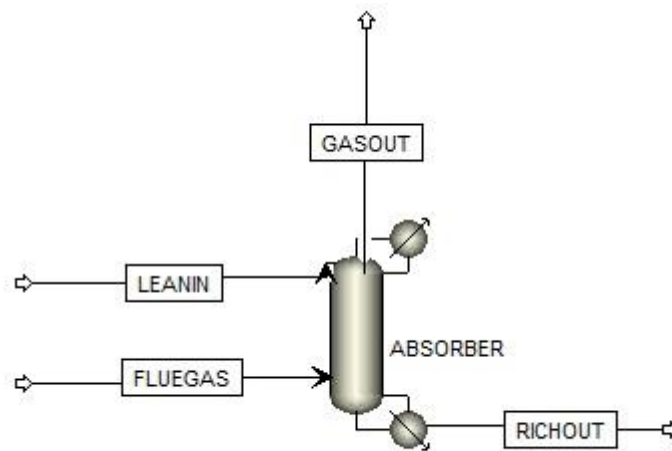
Figure 5-1 Print screen of Aspen Plus flow diagram showing the absorber column with associated in- and outflows.

Data from the pilot plant located at NTNU were collected from experiments which were run continuously over a 3 month period divided into 20 acquisition periods. The operation was divided into three loading ranges defined as 1-3, having the loading 0.20-0.30, 0.30-0.40, and 0.40-0.45, respectively. Absorber specifications and flow parameters can be found in Table 3-1.

---

[7] Raoults law: $P_0 = x_0 P$, where x_0 and P_0 is the fraction and partial pressure of component 0 respectively, and P is the total pressure.

5.1 Simulation Results

Some of the simulation results, including loading and absorption rate for the 20 runs, are listed in Table A.1 in Appendix A, section A1.1. In that table, experimental and simulated outlet loading for the individual runs are listed. However, comparing simulated and experimental outlet loading do not give a clear indication of model accuracy. The sensitivity to errors is low, and data shown in this fashion may conceal significant discrepancies. A better approach is to compare experimental and simulated CO_2 absorption rates. From the results in Table A.1, it can be seen that the percentage deviation between simulated and experimental absorption rate generally increases with increased lean loading.

In addition, the ratio between the simulated CO_2 absorption rates in kmol/h was compared with the experimental values calculated for each run. If there is total agreement between them, the ratio is one. By plotting this ratio against different values like lean solvent loading, vol% CO_2 in the flue gas and the inlet temperatures of the streams, systematic errors can be detected.

In Figure 5-2 the ratio between the simulated and experimental CO_2 absorption rates (kmol/h) is plotted against lean solvent loading, vol% CO_2 in the flue gas and the inlet temperatures of the flue gas and the lean solvent stream for the 20 runs by Tobiesen et al. (2007). As can be seen from these figures, the error between the simulated and experimental data increases with increased lean solvent loading, increased vol% CO_2 in the flue gas and also with increased inlet temperatures of the streams. It other word; the CO_2 absorption rate is over-predicted in the simulations in cases with high loading, large amount of CO_2 and high temperatures. The AD between the experimental and simulated results is calculated to be 19.4% and AAD is found to be 13.4%.
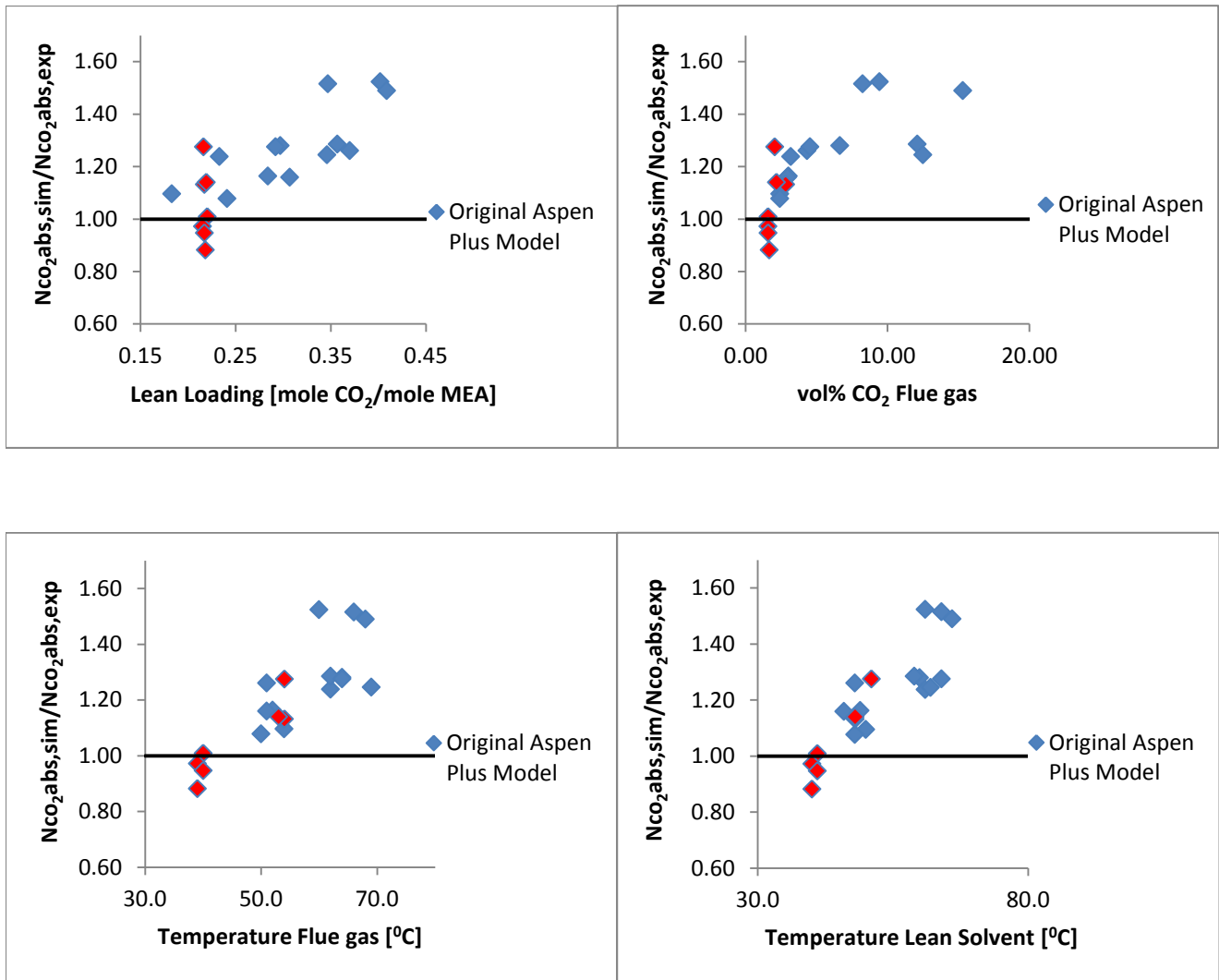
Figure 5-2 Four figures showing the ratio between the simulated and experimental CO$_2$ absorption rates plotted against lean solvent loading, vol% CO$_2$ in the flue gas and the inlet temperatures of the flue gas and the lean solvent for the 20 runs. Run 1, 2, 3, 4, 5, 10 and 11 are marked in red.

It is worth noticing that for lean solvent loading from 0.215 to 0.220 there are 7 experimental points. These are marked in red (run 1, 2, 3, 4, 5, 10 and 11) in Figure 5-2. Some of these points are under-predicted and some are over-predicted in the simulations. However, if one look at other parameters like inlet temperatures, concentration of MEA or vol% CO$_2$ in the flue gas for these runs, there is nothing that sticks out as the reason for this spread. It is therefore assumed that this is partly due to experimental deviations.

The experimental data also provides five temperatures throughout the absorber packing. These data were plotted against the temperature profile for the interface given from the simulations. The most sensitive part of the temperature profile is at the temperature bulge,

where most of the absorption takes place, giving the largest change in temperature. However, for most of the runs, the temperature profiles agreed well with a deviation between experimental measurements and simulations below 2 °C. This is illustrated by the temperature profile for run 1, shown in Figure 5-3. It is worth noticing that the temperature profiles fitted best for the runs with lower lean loading.

Especially for run 5 and 17, the dissimilarities between the simulated temperature profile and the experimental data throughout the whole column is large. In run 5, the deviation between the experimental measurement and the simulation at the bulge are almost 5.5 °C. In run 17, the deviation is about 4 °C. Temperature profiles for these runs are given in Figure 5-3. However, there was not found any reason why exactly these two runs should show these large deviations from the experimental measurements. Thus this can be assumed to be caused by errors in the measurements, and not in the simulations. It is worth noticing that it is unknown if the temperature is measured for the gas or liquid phase, or a blend of these phases during the experiments.
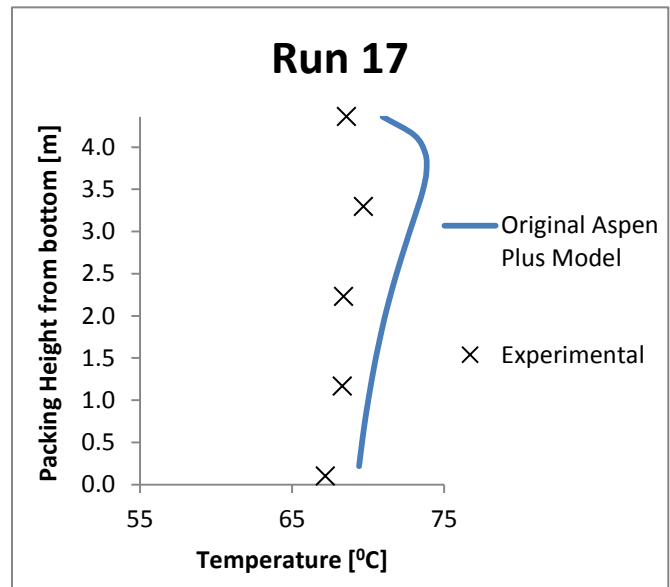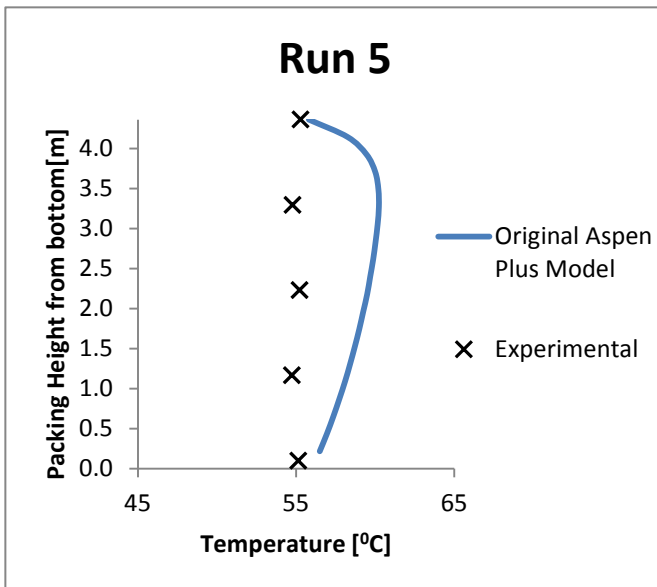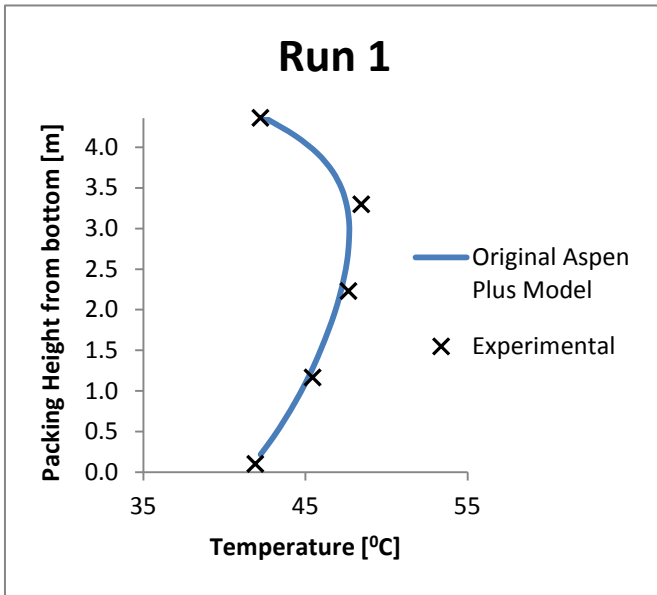
Figure 5-3 Plot of the temperature profile for run 1 in the upper left corner, and the temperature profile for run 5 and 17 in the lower left and right corner respectively.

5.2 Modifying the Aspen Plus Template

After comparing the simulation results with the experimental data from Tobiesen et al. (2007), the next step was to modify the simulation model such that the simulations fitted better with the experimental data. Two different approaches were used; changing the effective interfacial area and changing the kinetic constant for the MEA carbamate reaction, reaction number 6 from Chapter 2.3.

5.2.1 Changing the Effective Interfacial Area

The effective interfacial area in Aspen Plus can be changed either by the Stichlmair parameter or by the interfacial area factor. The Stichlmair et al. correlation predicts liquid holdup in all kinds of packings. One of these parameters gives the specific area of the packing, and this parameter can be changed in Aspen Plus. The interfacial area factor is a scaling factor for the interfacial area. The effective interfacial area predicted by a correlation in Aspen Plus is found by multiplying the specified interfacial area by this factor[8].

Changing either one of these parameters gives approximately the same effect. Changing the effective interfacial area changes the effective mass transfer area, and thus the absorption of CO_2. This will thereby influence all the runs in a similar way, meaning that more or less CO_2 is absorbed for each single run in the simulations, depending on whether the effective interfacial area is increased or decreased.

The effect can be illustrated by the experimental runs of 2 and 17. The simulated value for the CO_2 absorption rate in run 2 is close to the experimental, but the simulated value in run 17 is over-predicting quite much. It was therefore desirable to change the effective interfacial area to reduce the over-predicting in run 17. Thereafter, the same changes were performed on run 2, and the effect was as expected, reducing the absorption rate also in this run.

As can be seen from Table 5-1 and Table 5-2, quite large reductions in the surface area or the interfacial area factor was needed to reduce the deviation in run 17. Reducing the surface area by 61% reduced the deviation in the absorption rate by 31.1%. Reducing the interfacial area factor from 1 to 0.3, corresponding to a reduction in the effective interfacial area by 70%, reduced the deviation 45.7%. As expected, the same changes for run 2 resulted in an under-prediction of the absorption rate, and a large deviation from the experimental value in this run. The effect of changing the Stichlmair Surface Area in run 2 and 17 are given

---

[8] Information about the Stichlmair correlation and the interfacial area factor is found from the help function in Aspen Plus.

in Table 5-1, and the effect of changing the Interfacial Area Factor in run 2 and 17 are given in Table 5-2.

Table 5-1 Table showing the effect of changing the Stichlmair Surface Area on absorbed CO_2 for Run 2 and Run 17

	Sichlmair Surface Area [m^2/m^3]	CO_2 abs. rate, exp [mol/h]	CO_2 abs. rate, sim [mol/h]	%dev, x_i
Run 2	250	0.06	0.07	-1.8
	100	0.06	0.04	-46.6
Run 17	250	0.09	0.13	47.5
	100	0.09	0.10	16.4

Table 5-2 Table showing the effect of changing the Interfacial Area Factor on absorbed CO_2 for Run 2 and Run 17

	Interfacial Area Factor [m^2/m^3]	CO_2 abs. rate, exp [mol/h]	CO_2 abs. rate, sim [mol/h]	%dev, x_i
Run 2	1	0.06	0.07	-1.8
	0.3	0.06	0.03	-57.8
Run 17	1	0.09	0.13	47.5
	0.3	0.09	0.09	1.8

43

5.2.2 Changing the Kinetic Constant

Changing the parameters in the kinetic constant can be a better option in improving the simulation model: it can remove or at least decrease the over-prediction seen in higher temperatures (Figure 5-2). This is because the kinetic constant is temperature dependent.

In Aspen Plus the kinetic model is defined as:

$$Kinetic\ constant = kT^n e^{-E/RT} \tag{5}$$

Where k is a constant, T is the temperature, n is the temperature exponent, E is the activation energy and R is the gas constant.

The seven chemical reactions defined in the Aspen Plus template is given in Table 2-1, Chapter 2.3. Four of these reactions are kinetic, and the most important for the CO_2 absorption is probably reaction 6, the MEA carbamate reaction. The values given by the Aspen Plus template for this reaction, are the following:

$$
\begin{aligned}
k &= 3.02 \times 10^{14} \\
n &= 0 \\
E &= 17.7404 MBtu/lbmol \\
[Ci] &basis: Mole\ gamma
\end{aligned}
\tag{6}
$$

5.2.2.1 Changing the activation energy

As was seen in Figure 5-2, the first simulation model over-predicted the CO_2 absorption rate for most of the runs. In order to get closer to the experimental data, it was tried to alter the activation energy, *E*, from the original value defined in the kinetic constant for the MEA carbamate reaction, shown in Equation (6). This was done using a trial-and-error approach, and the best option found was for *E*=18.4 *MBtu/lbmol*.

The effect of changing the activation energy is illustrated in Figure 5-4, by plotting the same four plots as earlier: the ratio between the simulated and experimental CO_2 absorption rates against lean solvent loading, vol% CO_2 in the flue gas and inlet temperatures of flue gas and lean solvent. The points from the first simulation round are also shown in the figures for comparison. In addition, some of the simulation results, including the deviation in the absorption rate for each single run, are listed in Table A1.2 in Appendix A, section A1.2.
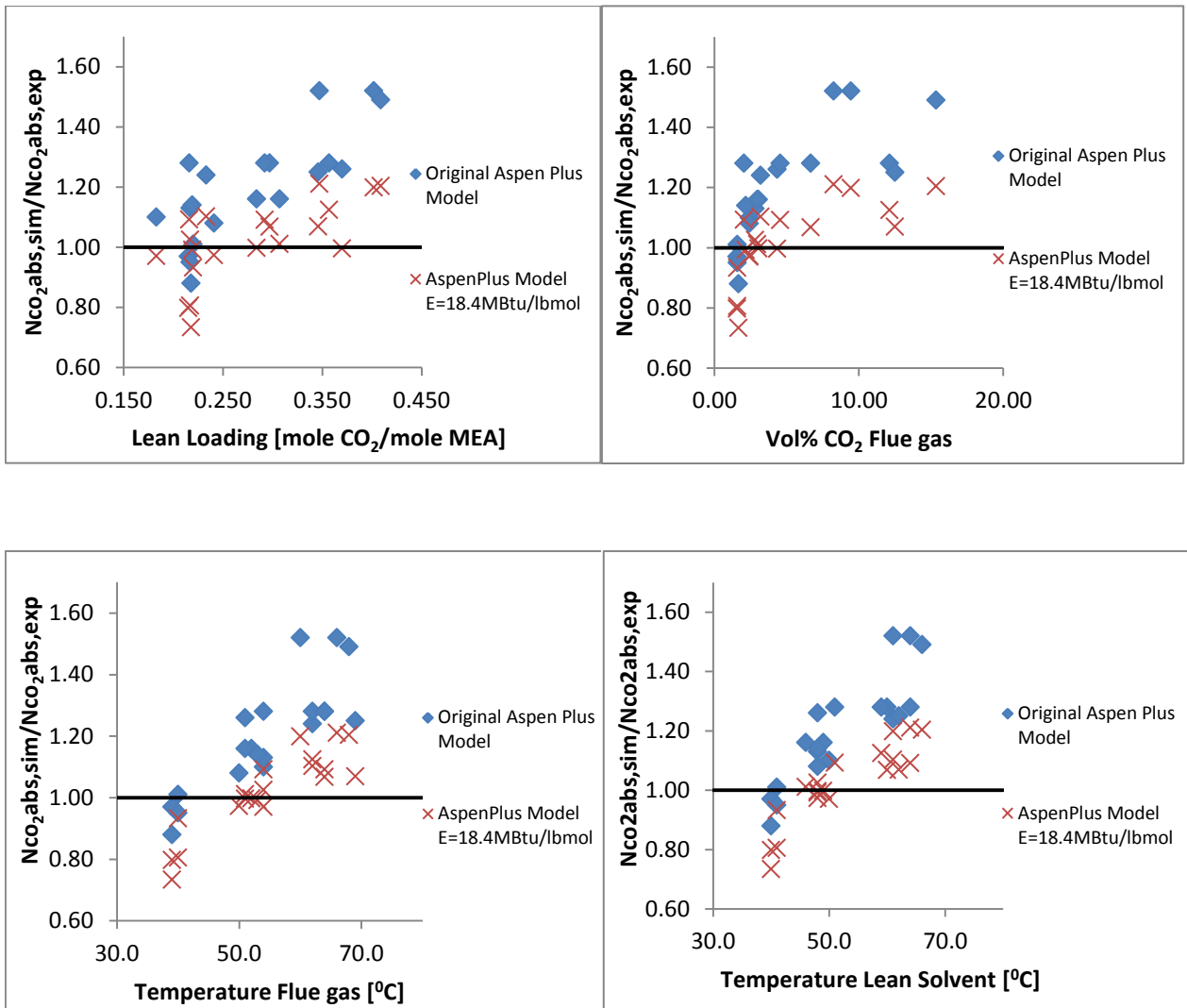
Figure 5-4 Four figures showing the ratio between the simulated and experimental CO₂ absorption rates plotted against lean solvent loading, vol% CO₂ in the flue gas and the inlet temperatures of the flue gas and the lean solvent for the 20 runs. The simulation results using the Aspen Plus template are shown in blue and the new simulation results are shown in red crosses.

As can be seen from the plots, all points are shifted downwards from the original model, and thereby the simulated and experimental data fit better. In the model with changed activation energy, both AD and AAD are reduced to 10.5%, which is still quite high. It can also be seen that the largest deviations using this model is found for the runs with low CO_2 content and low inlet temperatures.

5.2.2.2   Using the kinetic constant from Aboundheir et al.

Changing the activation energy in the original kinetic constant for the MEA carbamate reaction, did not give a satisfactory result. Therefore a kinetic constant from literature was tested. The kinetic constant was taken from a paper by Aboundheir et al. (2003) [35]. The new parameters in the kinetic constant were as following:

$$k = 4.61 \times 10^9$$

$$n = 0$$

$$E = \frac{4412 * 8.314}{1000} = 36.7 kJ/mole \quad\quad (7)$$

$$[Ci] basis: Molarity$$

Also for this case four plots were made, and these are shown in Figure 5-5. From the figures below it can be seen that the new kinetic model shifts the points downwards from the original Aspen Plus model. However, the change between the original model and the new model is different for each single point. For most of the runs, except run 16 and 17 which are marked in orange, the simulations are under-predicting the absorption rate compared to experimental data. However, based on the figures it seems that the new kinetic model is a bit better than the original Aspen Plus model, since the spread between the points are smaller. The AD and AAD using the new kinetic model was found to be 13.1% and 5.9% respectively. Some of the simulation results are also listed in Table A.3 in Appendix A, section A1.3, including the percentage deviation for each single run.

Figure 5-5 Four figures showing the ratio between the simulated and experimental CO₂ absorption rates plotted against lean solvent loading, vol% CO₂ in the flue gas and the inlet temperatures of the flue gas and the lean solvent for the 20 runs. The simulation results using the Aspen Plus template are shown in blue and the new simulation results are shown in yellow, run 16 and 17 in orange.

5.2.2.3 Changing the activation energy in the Aboundheir et al. model

Based on the results using the kinetic constant from Aboundheir et al. (2003) [35], it was assumed that this kinetic model could give an even better result than the original kinetic model when the activation energy was altered. Also here a trail-and-error approach was used, and the best result was found when the activation energy was reduced from 36.7 kJ/mole to 36.0 kJ/mole. The results are presented in Figure 5-6. In addition, some of the simulation results including the percentage deviation for each single run are listed in Table A.4 in Appendix A, section A1.4.

Figure 5-6 Four figures showing the ratio between the simulated and experimental CO$_2$ absorption rates plotted against lean solvent loading, vol% CO$_2$ in the flue gas and the inlet temperatures of the flue gas and the lean solvent for the 20 runs. The simulation results using the Aspen Plus template are shown in blue and the new simulation results are shown in green.

As can be seen from the plots, the modified new kinetic model fits very well with the experimental data. The AD and the AAD was found to be 8.5% and 7.4% respectively, which is deemed satisfactory. It is worth noticing that there are several points which have

approximately the same lean solvent loading and/or vol% CO_2. This can indicate errors in the experimental data, as mentioned earlier in Chapter 5.1.

Temperature profiles for the modified Aboundheir model were also made to compare the performance of this model with the performance of the original Aspen Plus model. It was shown that for lower CO_2 loadings like run 1, the original Aspen Plus model predicted the temperature profile most accurate, as illustrated in Figure 5-7. However, for medium and high loading ranges like run 12, the modified Aboundheir model performed best, as illustrated in Figure 5-8. For most of the runs, the simulations overlapped the experimental data well, with a deviation from the experimental data below 2 °C in all runs, except run 5 and 17. Both an over-prediction and/or an under-prediction of the temperature throughout the column were seen in the individual runs.

As mentioned, the simulation results from run 5 and 17 were still quite poor. The modified Aboundheir model performed slightly better than the original Aspen Plus model. Nevertheless, the simulated temperature profiles are still quite far from the experimental values, with an over-prediction of approximately 5 °C at the bulge in run 5 and 2°C at the bulge in run 17. This can indicate errors in the experimental values for these runs.
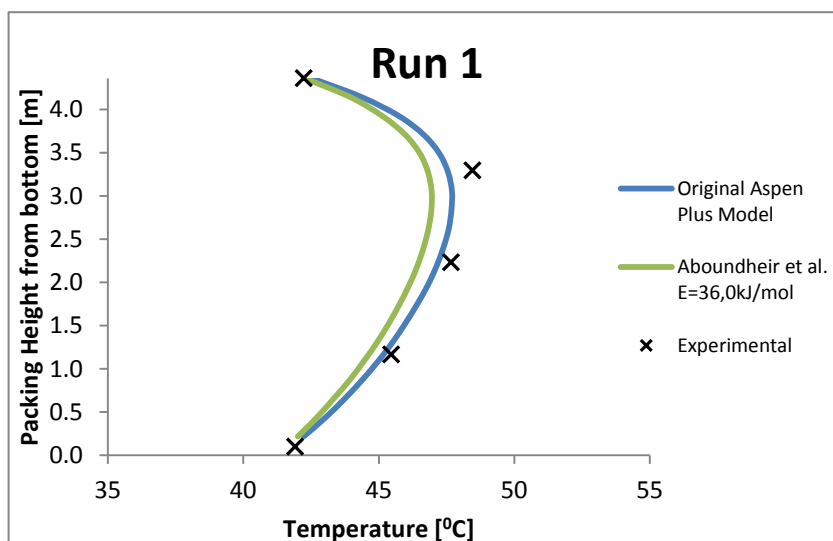
Figure 5-7 Figure giving the temperature profile for run 1, lean solvent loading 0.281 mol CO₂/mol MEA
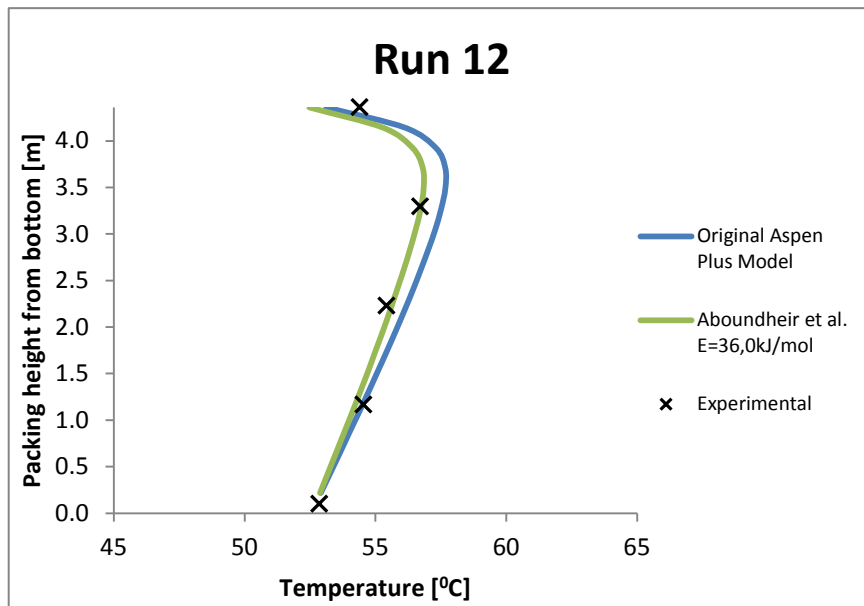
Figure 5-8 Figure giving the temperature profile for run 12, lean solvent loading 0.317 mol CO₂/mol MEA

5.2.2.4 *Summary of results by changing the kinetic model*

To get an overview of the changes made to the Aspen Plus template, a plot showing all four simulation results are made. In Figure 5-9 the blue marks is the results using the original Aspen Plus model without any changes in the kinetic constant, the red marks gives the results when the activation energy is changed in the kinetic constant for the MEA carbamate reaction, the yellow marks gives the results using the kinetic constant from Aboundheir et al. (2003), and the green marks gives the results when the activation energy for the MEA carbamate reaction in this model is changed.

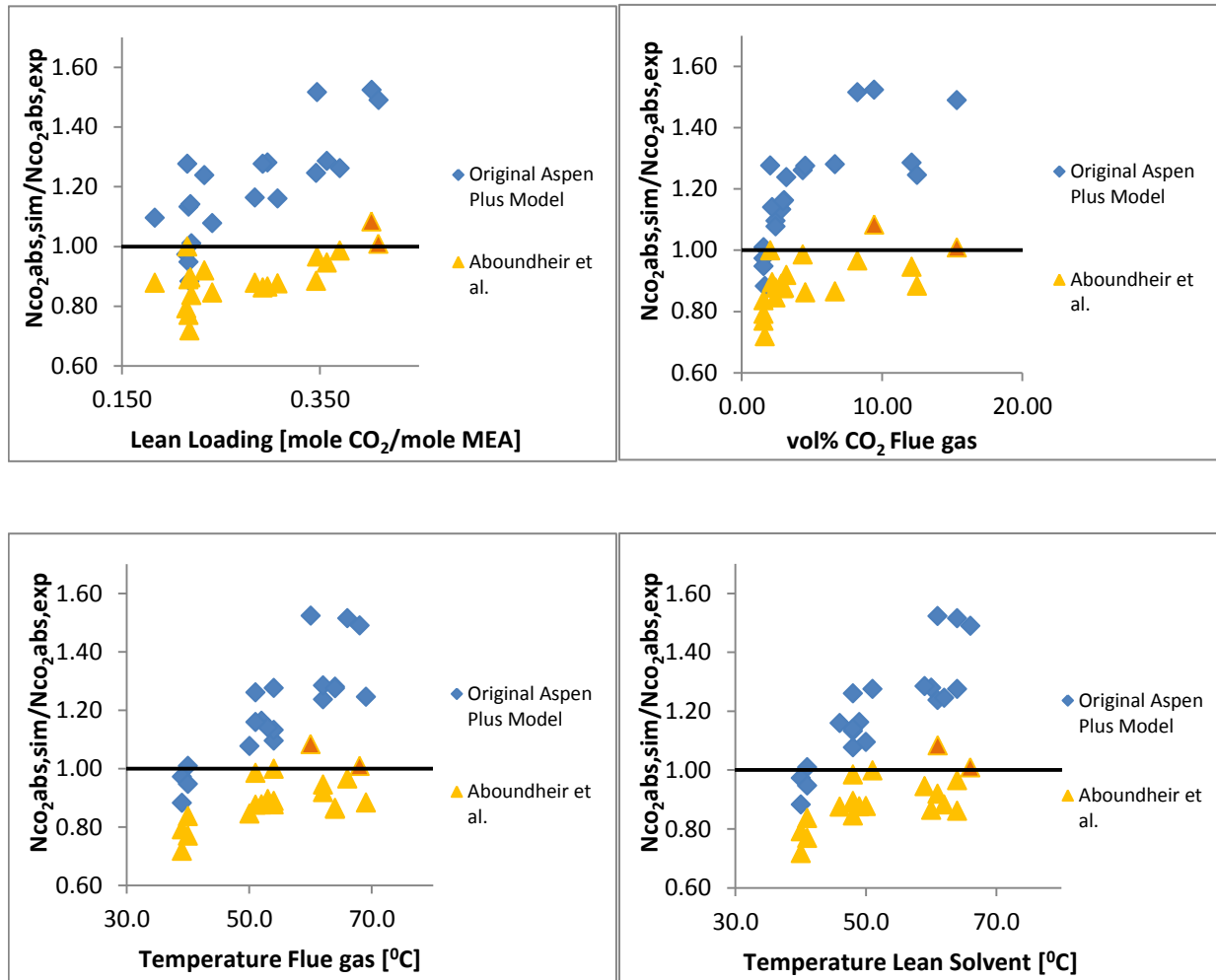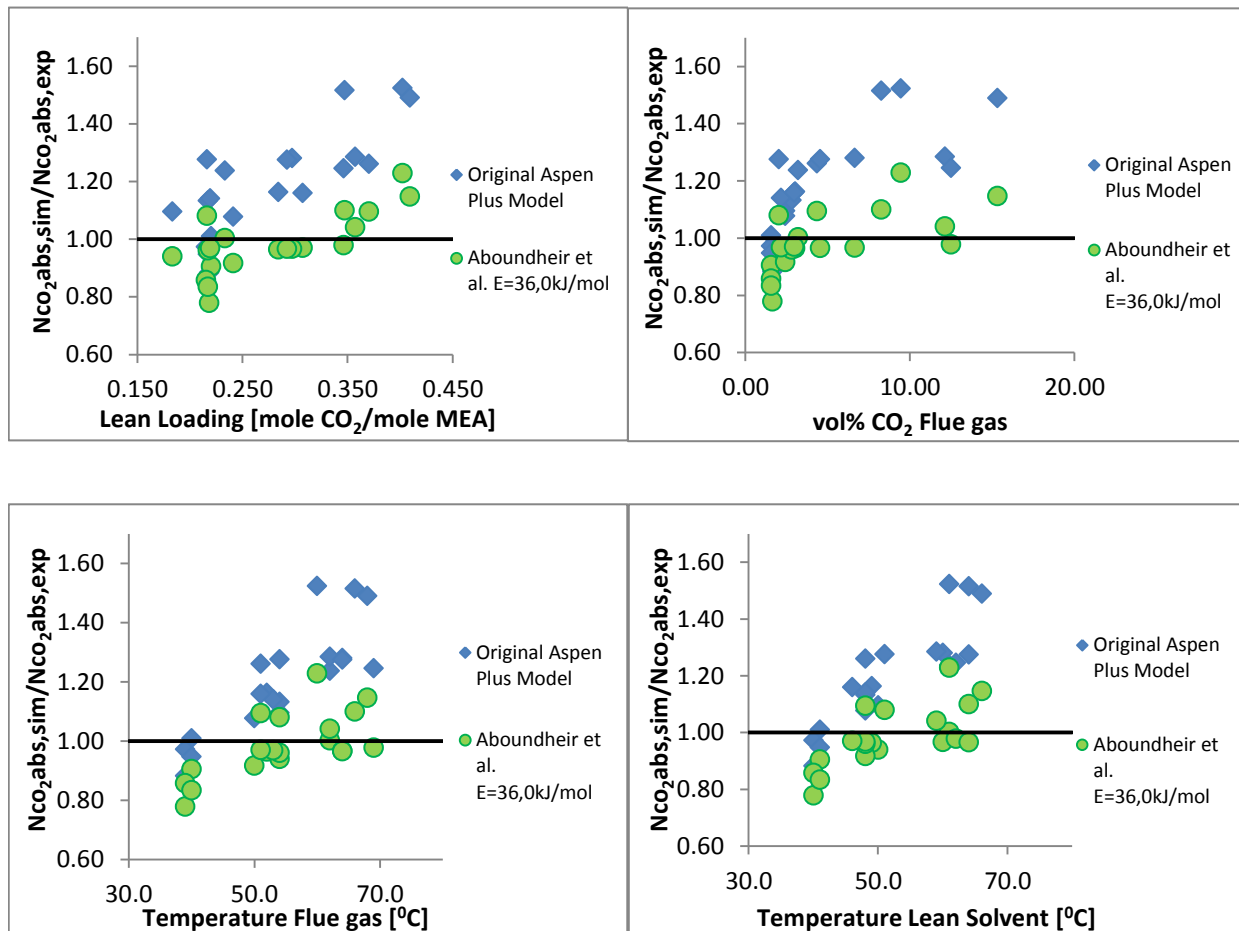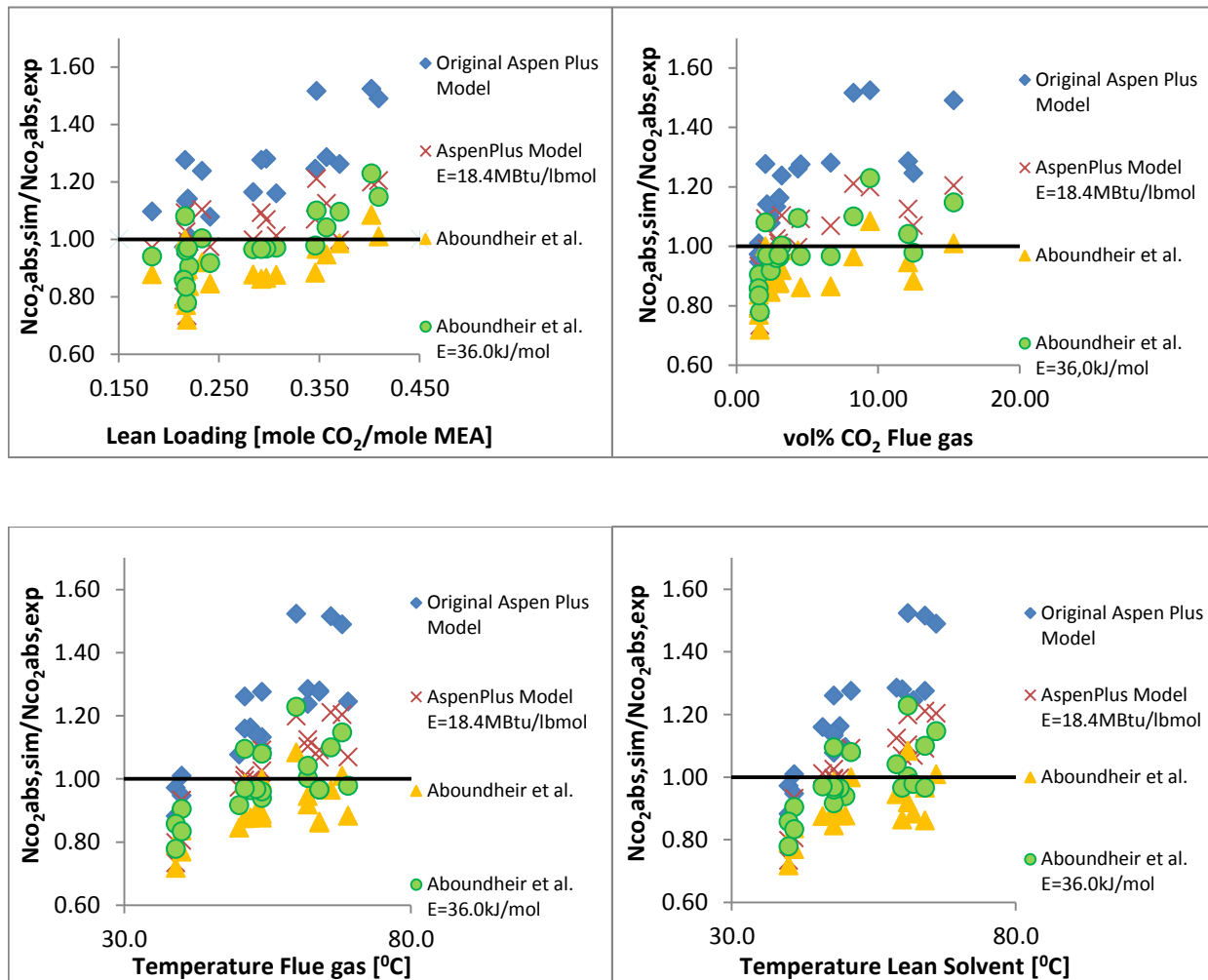**Figure 5-9 Four figures showing the ratio between the simulated and experimental CO_2 absorption rates plotted against lean solvent loading, vol% CO_2 in the flue gas and the inlet temperatures of the flue gas and the lean solvent for the 20 runs. The simulation results using the Aspen Plus template are shown in blue and the modified kinetic models are shown in red, yellow and green respectively.**

As can be seen from the green marks in the figures, the deviation is not increasing with increasing lean loading, increasing vol% CO_2 and increasing temperatures of the flue gas and the lean solvent for the modified Aboundheir model, which was the case using the

original Aspen Plus model. However, the results using the modified Aboundheir model, also called the new kinetic model, are both under-predicting and over-predicting the CO_2 absorption rate compared to experimental measurements. It looks like the new kinetic model under-predicts in cases with lower lean loading, lower vol% CO_2 and lower inlet temperatures, and over-predicts in cases with higher lean loading, higher vol% CO_2 and higher inlet temperatures. Nevertheless, the overall deviation between the CO_2 absorption rate in the simulations and experiments are decreased quite much using the new kinetic model compared to the original Aspen Plus Model.

The improvements can also be illustrated by the decrease in average deviation and absolute average deviation given in Table 5-3 below.

Table 5-3 Table showing the average deviation, AD, and absolute average deviation, AAD, found for the four different simulation models.

Model	AD [%]	AAD [%]
Original Aspen Plus Model	19.4	13.4
Aspen Plus Model E=18.4 MBtu/lbmol	10.5	10.5
Aboundheir et al. model	13.1	5.9
Aboundheir et al. E=36.0 kJ/mol	8.5	7.4

As can be seen from Table 5-3 and Figure 5-9, the deviation between experimental measurements and simulation results are least for the modified Aboundheir model. In the validation of the simulation model using the other four campaigns listed in Table 3-1, the modified Aboundheir model (new kinetic model) is therefore used.

The simulation results found using the modified Aboundheir simulation model can also be compared with the simulation results reported in the publication by Tobiesen et al. (2007). In the publication, a rate-based simulation program implemented in Fortran 90 was developed and validated against the experimental data. Tobiesen et al. report that the mass-transfer trends using their simulation model are deemed satisfactory over the whole loading range, with AD of 6.16% and AAD of 6.24%. The relative deviation between simulated and experimental absorption rate for single runs varied from 19% to -9.6%, and there was no systematic deviation to be found. In the temperature profiles it seemed to be a slightly under-prediction of the heat evolved in the experiments with low loadings, whereas a small over-

prediction could be seen for loading range 3 (rich loading > 0.40). This was in spite the fact that the predictions of absorption rate were equally good over the whole loading range.

The simulation results found using the modified Aboundheir simulation model shows a relative deviation between simulated and experimental absorption rate for single runs varying from -18.5% to 19%, with AD of 8.5% and AAD of 7.4%, slightly worse than the rate-based model used by Tobiesen et al. For the temperature profiles, the trend is somewhat opposite for the modified Aboundheir simulation model, where there is a slightly over-prediction for low loadings and a slightly under-prediction for high loadings. However, mostly the agreement between the temperature profiles is deemed satisfactory.

6 Model Validation

6.1 Pilot Data from Pinto et al. (2014)

The fitted simulation model presented in the previous chapter was validated using experimental data from Pinto et al. (2014) [20]. These experiments are performed in the same pilot plant located at NTNU, however with a different packing type and packing height, as listed in Table 3-1.

The simulation results from this campaign can be presented by the same plots as was made for the simulation results from Tobiesen et al. in the previous chapter. Thus the ratio between the simulated and experimental CO_2 absorption rate was plotted against lean solvent loading, vol% CO_2 in the flue gas and the inlet temperatures of the streams for the 6 runs. The plots can be seen in Figure 6-1. Additionally, some of the simulation results can be found in Appendix A, section A2, including the percentage deviations in each single run.
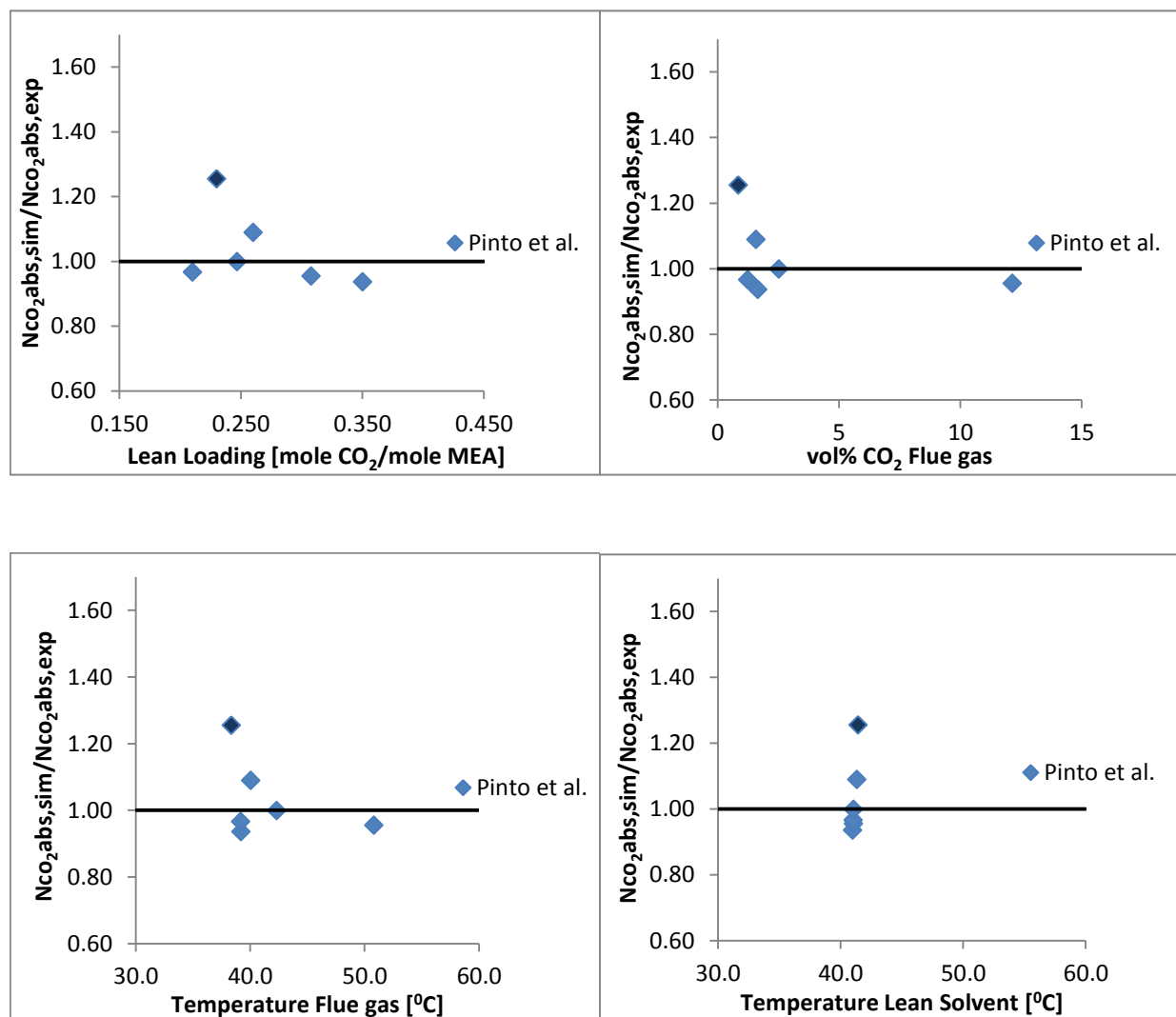
Figure 6-1 Four figures showing the ratio between the simulated and experimental CO₂ absorption rates plotted against lean solvent loading, vol% CO₂ in the flue gas and the inlet temperatures of the flue gas and the lean solvent for the 6 runs. Run 3 is marked in dark blue.

As can be seen from the figures, the simulation model predicts well the experimental values also when the packing type is changed. There is only one outlier, marked in dark blue, which over-predicts the absorption rate with about 25%. Except for this point, all other points are inside 10% deviation, where the relative deviation between simulated and experimental absorption rate for single runs varies from -6.6% to 9.1%. The simulated results are compared with experimental liquid phase measurements because these measurements are considered to be most accurate. However, if the gas measurement was used instead for the point with 25% deviation, the error would be reduced to 2%.

The publication by Pinto et al. (2014) includes simulation results using the NTNU/Sintef in-house code CO2SIM in experiments using DEEA/MAPA solvent, but not in experiments

using 30wt% MEA. Therefore a comparison between their simulation model and the modified Aboundheir simulation model was not possible.

Also the experimental data from this campaign gives temperature measurements throughout the absorber column. These measurements were used to create and compare temperature profiles. The experimental data were compared with the temperature profile for the interface given from the Aspen Plus simulations. For each of the runs in this campaign, the temperature profiles disagreed quite much, as illustrated in Figure 6-2, showing the temperature profiles for run 1 and 2. It is not known why there is such large disagreement for this data set, and it is assumed that the reported temperature values are wrong or from another place in the column than indicated in the data. This is also supported by the fact that the simulation model predicts the CO_2 absorption rate well, and also is able to predict the temperature profiles from the other campaigns. It is worth noticing that also here it is unknown if the temperature is measured for the gas or liquid phase, or a blend of these phases.
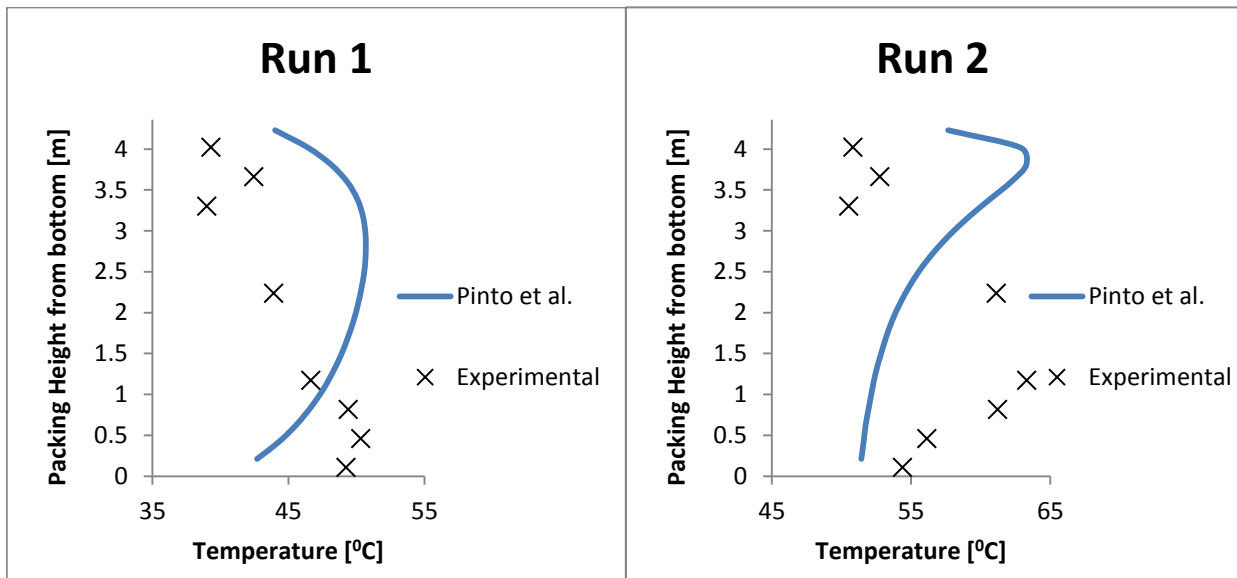
Figure 6-2 Temperature profiles for run 1 to the left and for run 2 to the right.

6.2 Pilot Data from Enaasen et al. (2015)

The simulation model was also validated using experimental data from Enaasen et al. (2015). Also this campaign was run in the pilot plant located at NTNU, and with the same packing type and packing height as for the Pinto et al. (2014) campaign. The column specifications can be seen in Table 3-1.

The simulation results from this campaign can be presented by the same plots as was made for the other simulated campaigns. Thus the ratio between the simulated and experimental CO_2 absorption rate was plotted against lean solvent loading, vol% CO_2 in the flue gas and the inlet temperatures of the streams for the 8 runs. The plots can be seen in Figure 6-3. Additionally, some of the simulation results, including the percentage deviation in each single run, can be found in Appendix A, section A3.
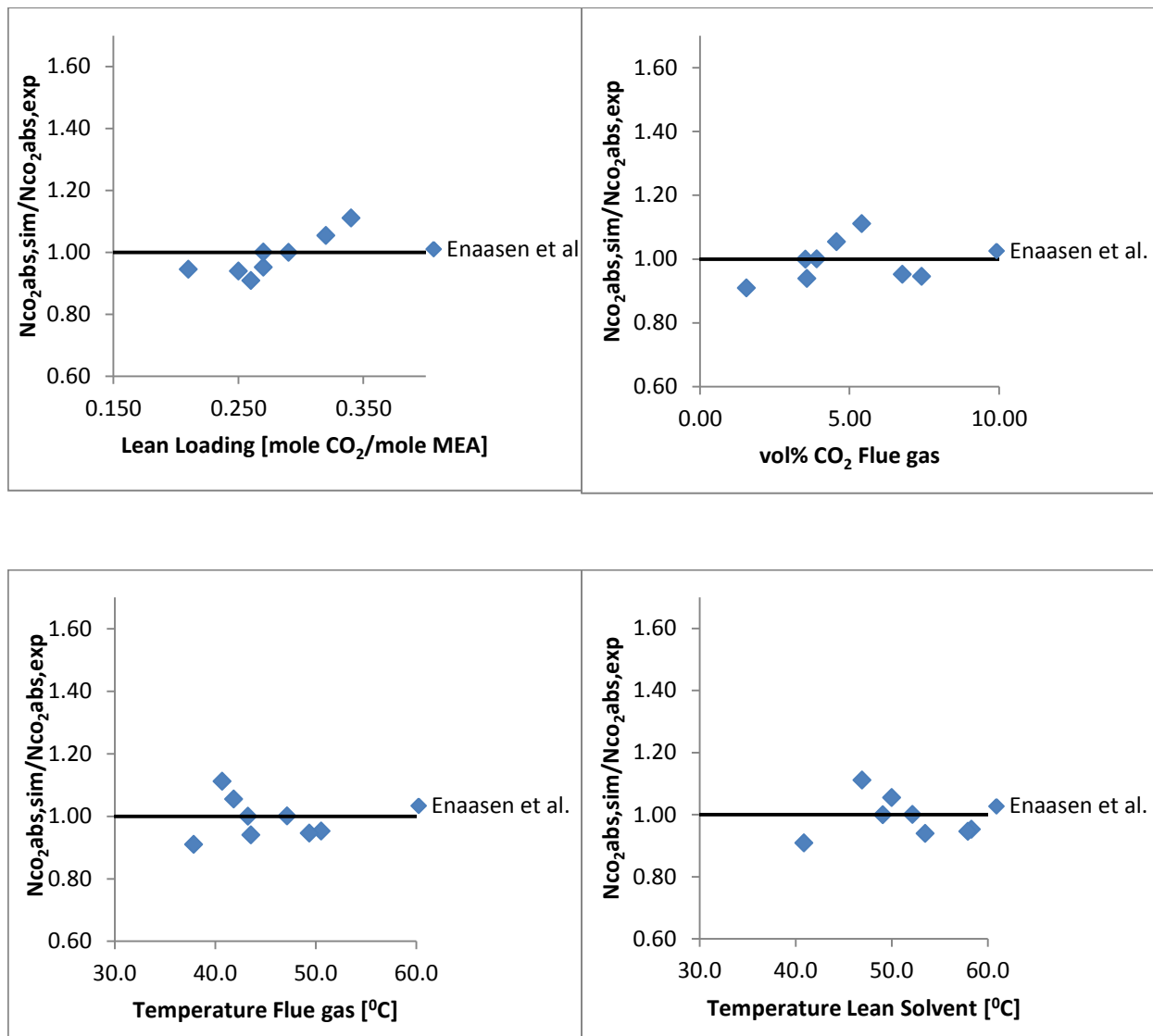
Figure 6-3 Four figures showing the ratio between the simulated and experimental CO$_2$ absorption rates plotted against lean solvent loading, vol% CO$_2$ in the flue gas and the inlet temperatures of the flue gas and the lean solvent for the 8 runs.

As can be seen from these figures, the simulation model predicts the experimental runs performed by Enaasen et al. very well. It looks like the simulation model under-predicts the absorption rate at lower lean loadings, and over-predicts the absorption rate at higher lean loadings. This was also the case in the Tobiesen et al. campaign, shown in Figure 5-6. However, in this case all simulations are inside 12% deviation from the experimental values, where only one point has more than 10% deviation.

The experimental data from this campaign have been provided by my supervisor Hanna Knuutila and is not taken from a publication. A comparison between simulation results using another simulation model was therefore not possible for this campaign.

Also the experimental data from this campaign provides temperature measurements throughout the absorber packing used to create temperature profiles. The recorded temperatures have the same "flow diagram mark" as the temperatures reported in the data from Pinto et al. (2014), and should therefore measure at the same places in the absorber column. However, when the experimental data were compared with the temperature profile for the interface given from the Aspen Plus simulations, the simulated and experimental profiles fitted well for most of the runs here. This is illustrated by the temperature profile for run 1 shown in Figure 6-4.

For this campaign, the tendency was that the simulation model over-predicted the temperature compared to experimental measurements, and the largest deviations were found at the top of the column. Nevertheless, the agreement was not equally accurate for every single run. In some cases, like in run 6 shown in Figure 6-5, the simulations over-predicted the temperature with about 4 ℃ compared with the experimental measurements throughout the whole packing. As mentioned for the other campaigns using the pilot plant located at NTNU, it is unknown if the temperature is measured for the gas or liquid phase, or a blend of these phases.
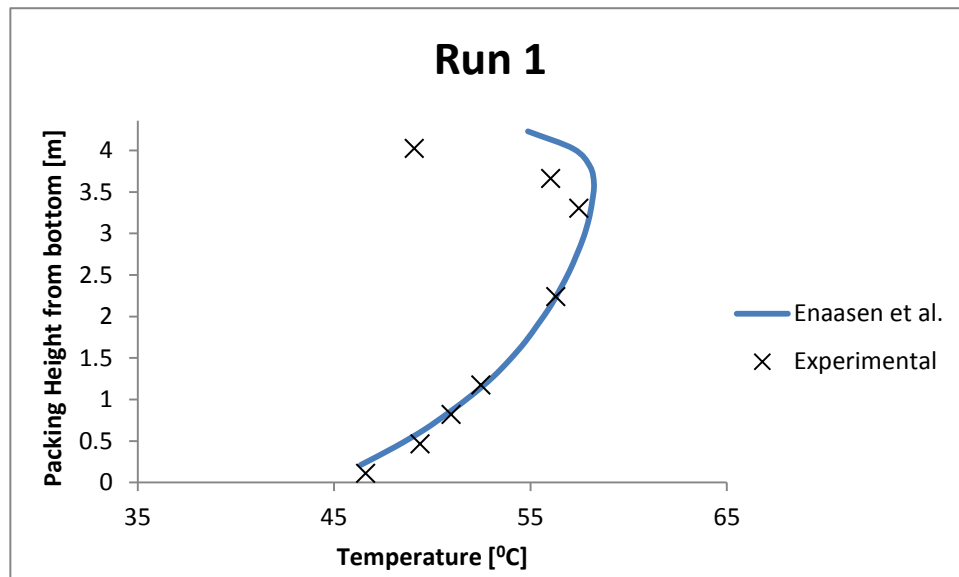
Figure 6-4 Figure giving the temperature profile for run 1
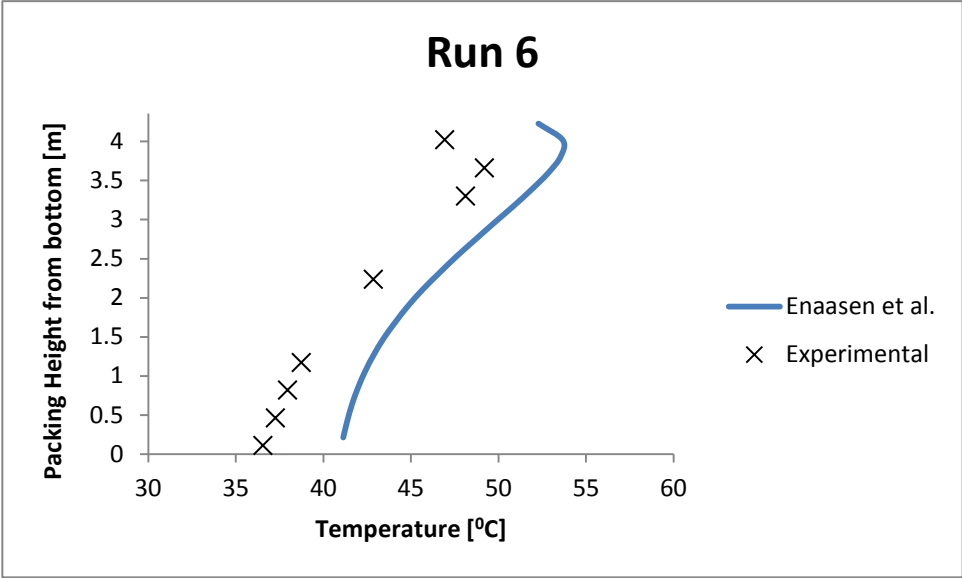
Figure 6-5 Figure giving the temperature profile for run 6

6.3 Pilot Data from Sønderby et al. (2013)

As mentioned, it is important to validate the simulation model since the performance is heavily influenced by the choice of mass transfer coefficients and kinetic parameters in the rate-based model. To ensure a reliable and robust simulation model, it is important to test the model against data from other pilot plants which have different heights and diameters. The simulation model was therefore validated using experimental data from Sønderby et al. (2013). The column specifications can be seen in Table 3-1, where it also can be seen that the packing type in the Sønderby et al. campaign was the same as in the Tobiesen et al. campaign. A flow diagram of the absorber column can be found in Figure 6-6.
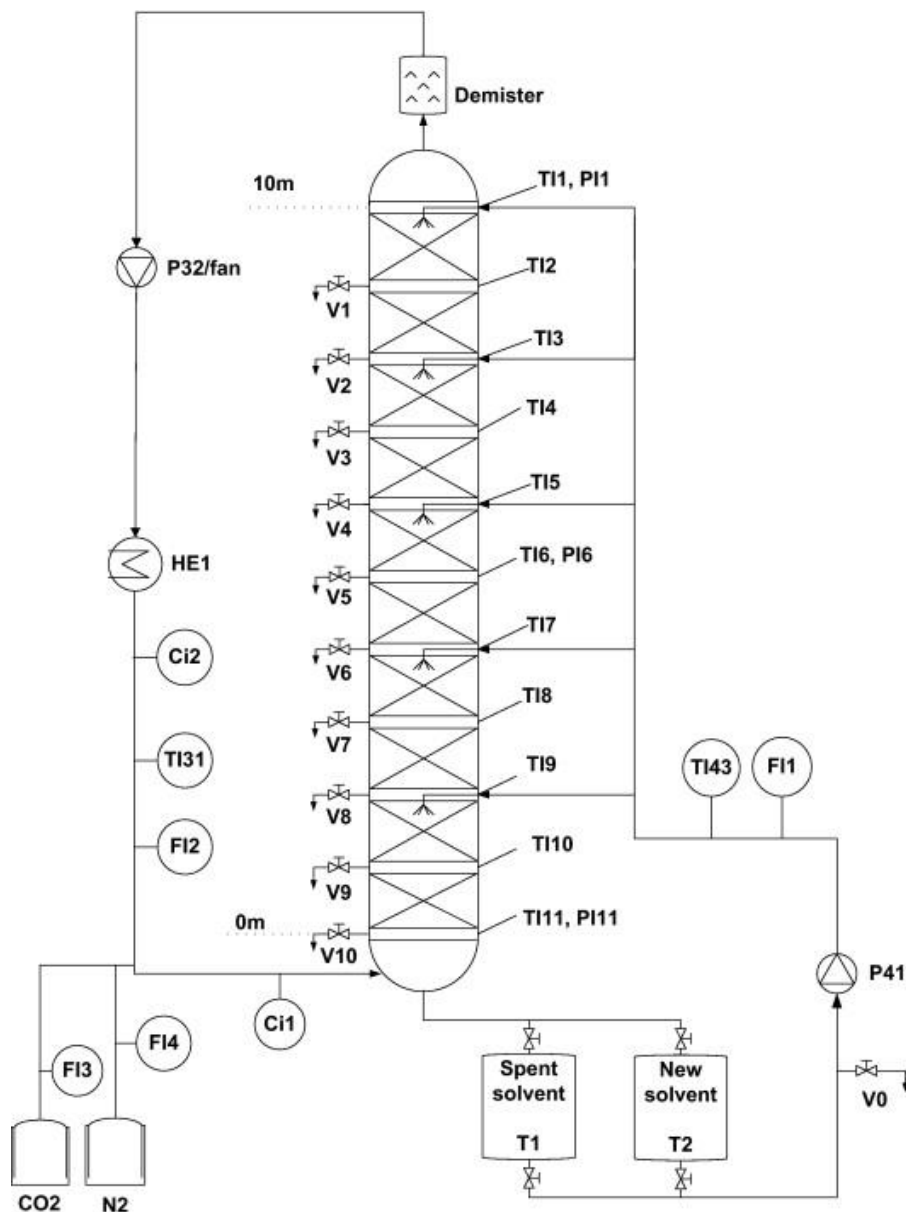
Figure 6-6 Flow diagram showing the absorber column used in the Sønderby et al. campaign

In the first five runs, the packing height is 8.2 m. In the next five runs, the packing height is decreased to 6.6 m, and in the following six runs the packing height is 4.9 m. Thereafter the packing height is 3.3 m for three runs, and 1.6 m for one run. At last, the packing height is 8.2 m for the remaining three runs performed. When the packing height is 8.2 m, the column is simulated with 20 stages in Aspen Plus. However, when the packing height is decreased, the column is simulated with 15 stages where the packing is defined to be from stage 6 to 15. This was done to get the simulation to converge.

As can be seen from Figure 6-6, the cleaned outlet gas is recycled back to the bottom of the column, and mixed with a CO_2 stream and N_2 stream to get the desired composition of the flue gas. The composition of the flue gas was calculated in the same way as described in Chapter 5.

The simulation results from this campaign are presented by the same plots as was made for the other simulation results. Thus the ratio between the simulated and experimental CO_2 absorption rate was plotted against lean solvent loading, vol% CO_2 in the flue gas and the inlet temperatures of the streams for the 23 runs. The plots can be seen in Figure 6-7. Additionally, some of the simulation results, including the percentage deviation for each single run, are given in Appendix A, section A4.
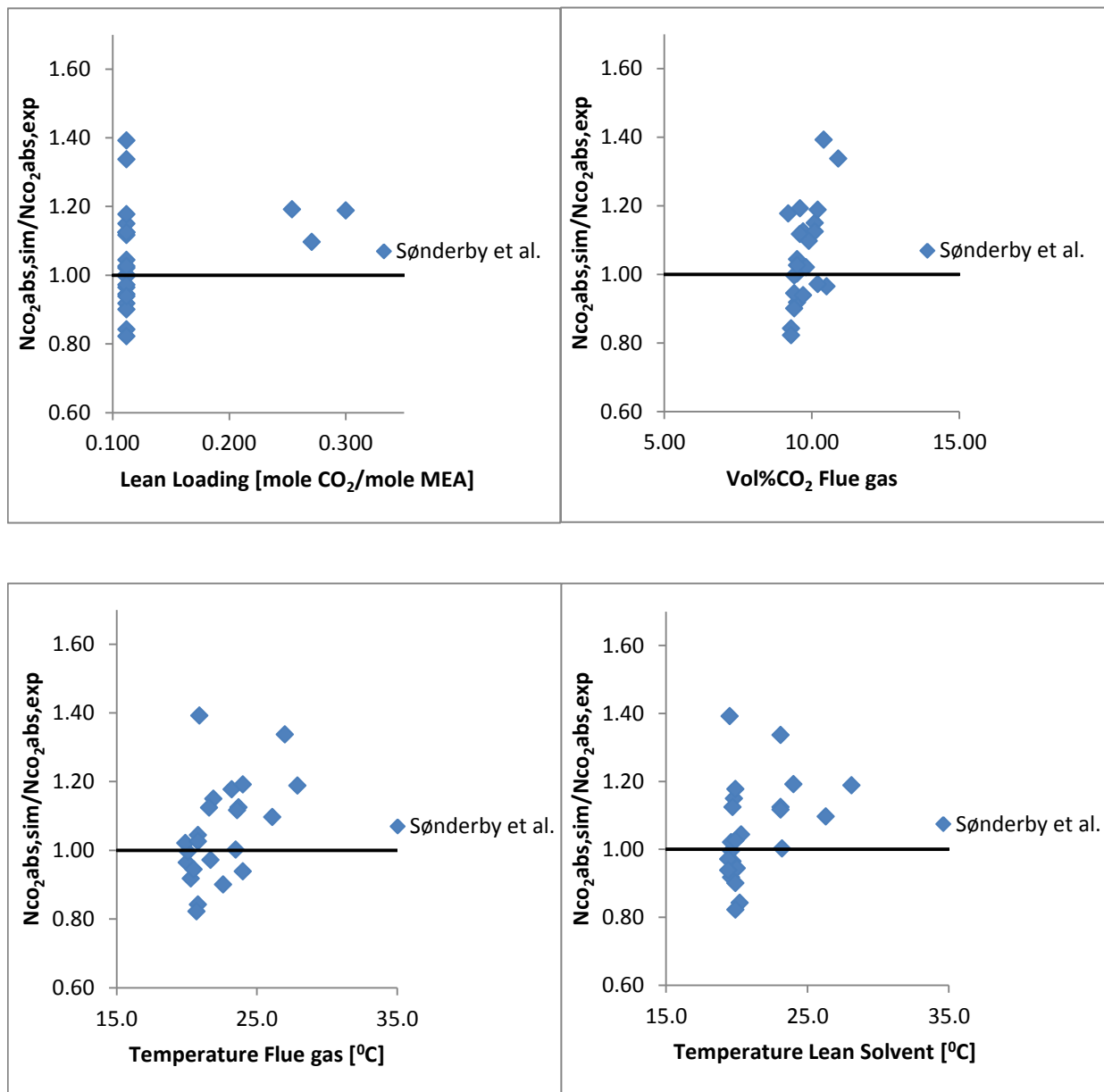
Figure 6-7 Four figures showing the ratio between the simulated and experimental CO$_2$ absorption rates plotted against lean solvent loading, vol% CO$_2$ in the flue gas and the inlet temperatures of the flue gas and the lean solvent for the 23 runs.

As can be seen from the figures, the simulation model predicts quite well the experimental data also for this campaign. Only two points over-predicts the absorption rate with more than 20%. One of these points, having 33.7% deviation, plus one point having 17.7% deviation, are performed with packing height 3.3 m. The other point, having 39.2% deviation, is performed with packing height 4.9 m. Four out of five other runs performed with this packing height also deviates quite much, 10-15% from the experimental data. In cases with lower packing heights, the results are more sensitive to the performance of the model, thus this might explain why the results are poorer in these cases.

There are also two points with about 19% deviation between the simulated and experimental absorption rate. For these two points, the lean loading is 0.254 and 0.300 respectively, which is in the higher loading range for this campaign. Remembering the simulation results of the Tobiesen et al. (2007) campaign, the model over-predicted with increased lean loading, increased temperatures and increased amount of CO_2 in the flue gas. Also for these two points the vol% of CO_2 is high, about 10%, but the temperatures of the inlet flows are lower than what was the case in Tobiesen et al. data.

As can be seen from the plot with lean loading on the x-axis, almost all the experimental runs were performed with the same lean loading. During these experiments, only the packing height and liquid flow rate was varied. This might explain why the results are spread, both over-predicting and under-predicting the absorption rate, even though the inlet conditions are similar for the individual runs.

Sønderby et al. used a rate-based model, originally developed by Gabrielsen et al. and modified by Faramazi et al., to perform simulations of their campaign. The results showed good agreement between experimental values and model predictions with respect to temperature, CO_2-loading and CO_2 gas phase concentration. The difference between model predictions and experimental values for the CO_2 concentration was less than 5% (based on experimental values) for all except 3 of the runs which exceeded this limit – the cases of very low absorption height. Thus, Sønderby et al. found the same trend as what was found in the Aspen Plus simulations. However, with the modified Aboundheir model, the relative deviation between simulated and experimental absorption rate for single runs varies from -17.8% to 19.2%, if the two points that is over-predicted with more than 20% are disregarded. The simulation results using the model developed by Gabrielsen et al. therefore predicts the CO_2 absorption rate better.

The experimental data from Sønderby et al. also gives several temperatures throughout the absorber packing, as well as over the packing section. These data were plotted against the temperature profile for the interface given from the simulations. The agreement between the experimental and simulated profiles was somehow varying, both under-predicting and over-predicting compared to experimental measurements, mostly with 2-4 °C.

For run 6, 11 and 17 there were a clear over-prediction of 10-20 °C in the simulations. In these cases it looks like the temperature bulge is assumed to be higher in the column in the simulation than what was found experimentally. The liquid flow rate in these runs was lower,

meaning that also the L/G ratio was lower, compared to the other runs. Low liquid flow can give dry spaces in the column, and thereby reduce the mass transfer efficiency. This might be clearer in the experiments than in the simulations, giving an over-prediction in the simulated temperature profiles. The plot for run 17 can be seen in Figure 6-9.

Even though the height of the packing was varying during the experiments, the agreement between the simulated and experimental profiles was quite accurate for several of the runs. This is illustrated by showing one temperature profile for each of the different packing heights, shown in Figure 6-8, Figure 6-9 and Figure 6-10. In run 20, the packing height is only 1.6 m, and there is hard to see how the temperature profile actually looks. Nevertheless, it was clear that when the lean solvent loading was increased for the last three runs, run 21, 22 and 23, the simulation under-predicted the temperature bulge with 2-4 °C compared to the experimental values. This is illustrated with the plot of run 21 shown in Figure 6-10.

Sønderby et al. report accurate agreement in cases with higher packing heights (8.2 m) and high L/G ratio (17-18), but a greater deviation between the experimental values and model predictions at lower packing height (4.9 m or lower) and low L/G ratio (3.9), in their simulations. In the simulations using the modified Aboundheir model, it also seems like low L/G ratio in combination with lower packing heights gives larger deviations than higher L/G ratios.
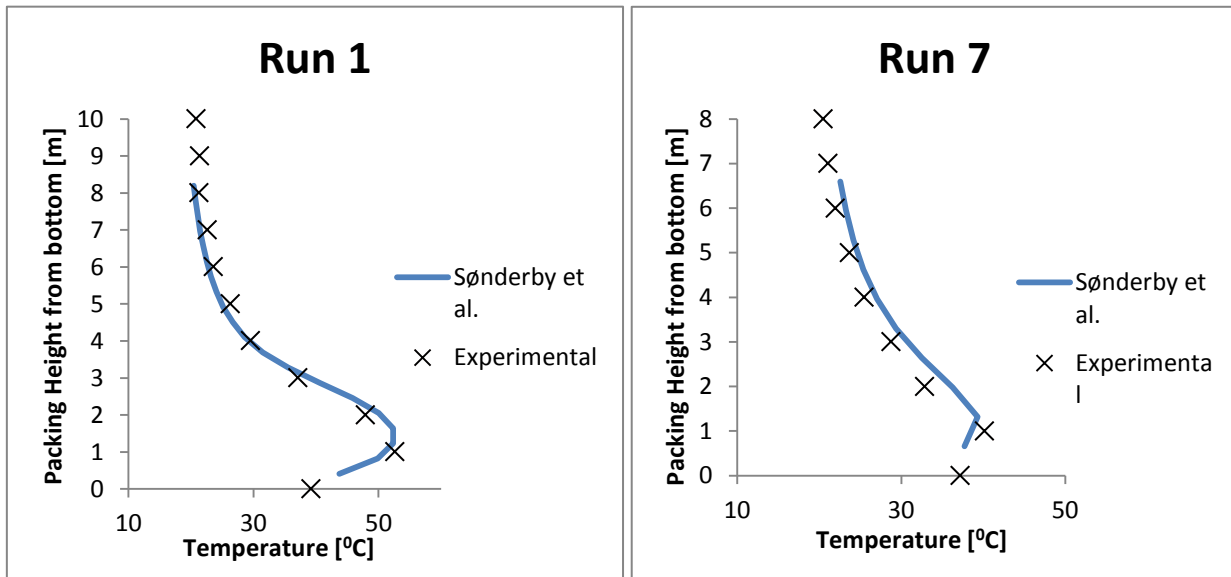
Figure 6-8 The temperature profile for run 1, with packing height 8.2 m, can be seen to the left. The temperature profile for run 7, with packing height 6.6 m, can be seen to the right.
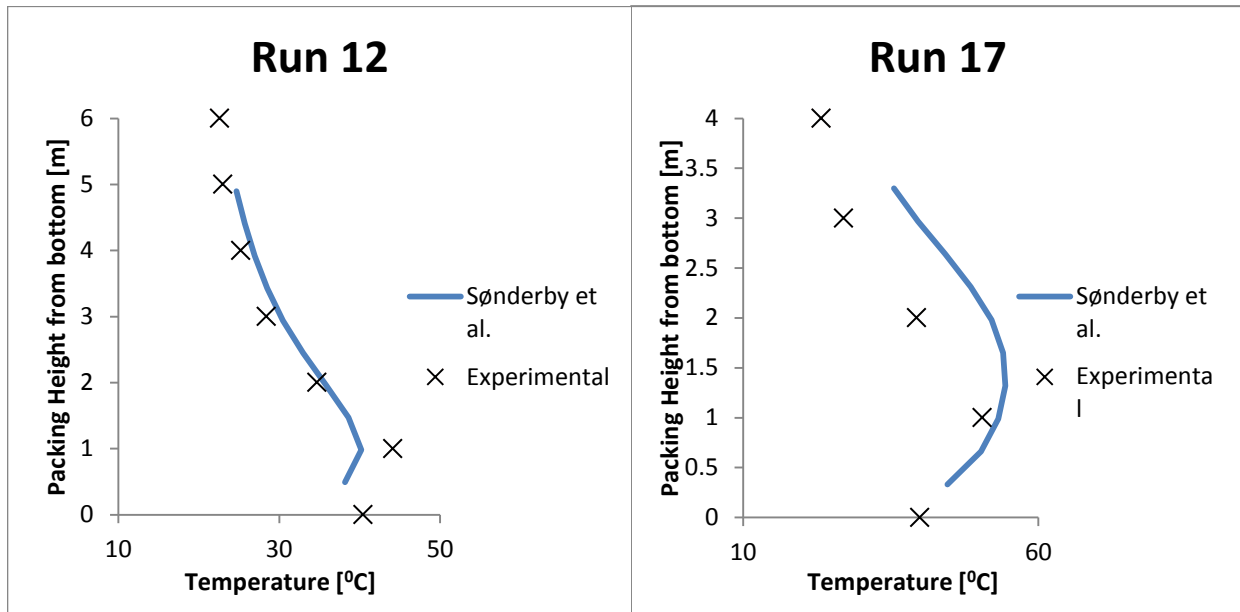
Figure 6-9 The temperature profile for run 12, with packing height 4.9 m, can be seen to the left. The temperature profile for run 17, with packing height 3.3 m, can be seen to the right.
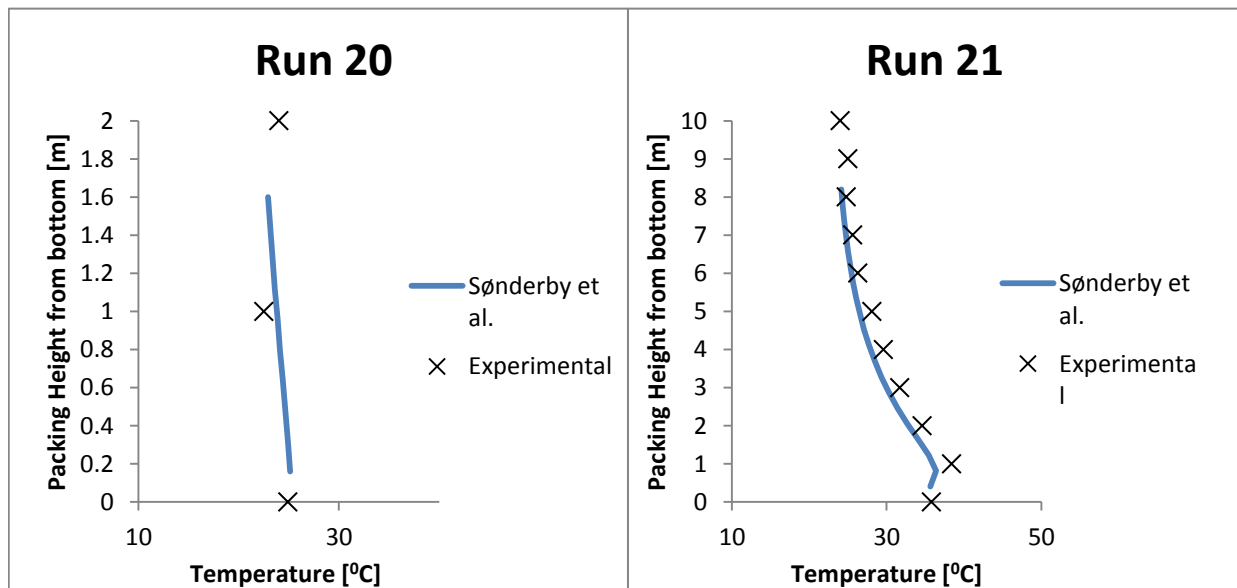
Figure 6-10 The temperature profile for run 20, with packing height 1.6 m, can be seen to the left. The temperature profile for run 21, with packing height 8.2 m and lean loading 0.254 mole CO_2/mole MEA, can be seen to the right.

6.4 Pilot Data from Notz et al. (2012)

The simulation model was also validated with experimental data from Notz et al. (2012). This campaign was run at the pilot plant used in the EU CASTOR project, and is located at the University of Kaiserslautern. The column specifications can be found in Table 3-1.

The absorber column is divided into six packing sections, where the sixth section is a water wash. Nevertheless, the column was simulated in the same way as the other columns, so the water wash section was disregarded. A part of the flow diagram given by Notz et al., showing only the absorber part, is shown in Figure 6-11.
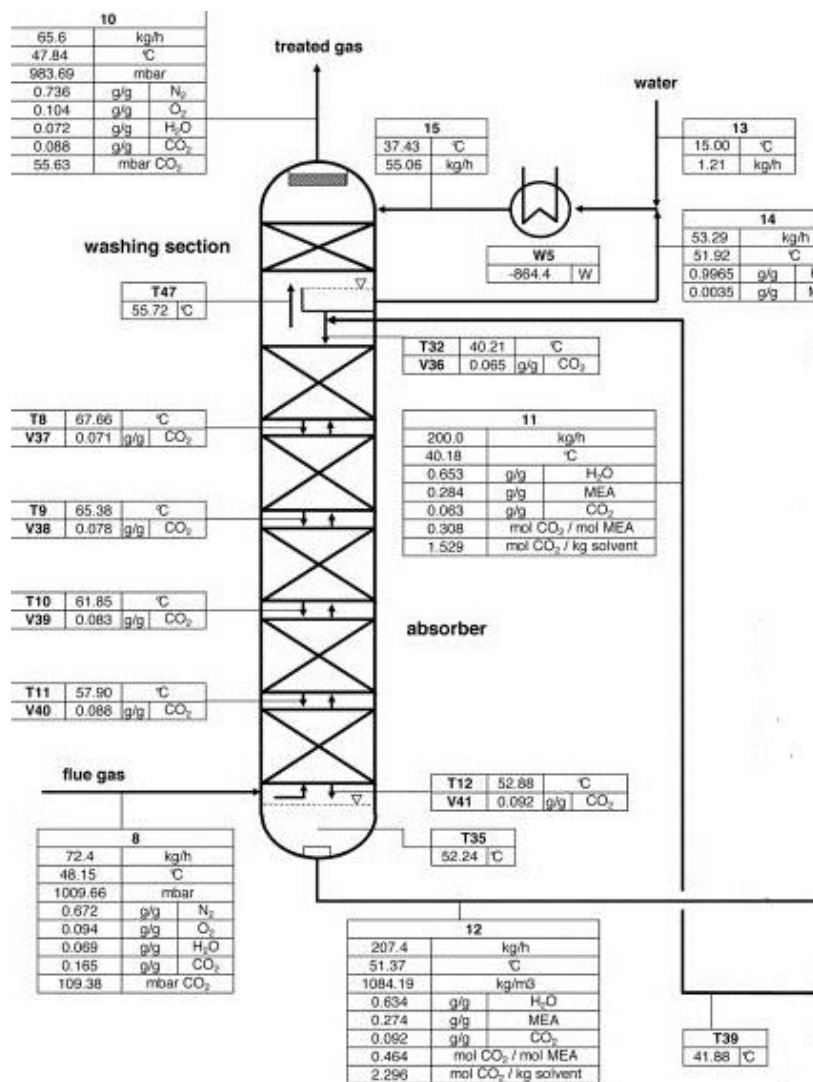
Figure 6-11 A part of the flow diagram provided by Notz et al. showing the absorber column with specifications of the streams

For this campaign, the composition of the flue gas was taken directly from the flow diagrams, which give the mass fraction of CO_2, H_2O, N_2 and O_2. The experimental

measurement of the CO_2 fraction is done on a dry basis, and it is given that the flue gas is assumed to be saturated with water. The temperature measurement on the top of the packing was used to calculate the fraction of water. By assuming that the N_2 and O_2 mole fraction was constant from the inlet, the composition of the cleaned gas was found. For run 30-47, the temperature measurement is missing, so for these runs the vol% CO_2 in the cleaned gas is not found. However, the absorption rates could still be compared. CO_2 measurements along the absorber are given for several of the runs, and therefore it has been possible to also create CO_2 profiles for comparison in this campaign.

The simulation results from this campaign are presented by the same plots as were made for the other simulation results. Thus the ratio between the simulated and experimental CO_2 absorption rates was plotted against lean solvent loading, vol% CO_2 in the flue gas and the inlet temperatures of the streams for 46 runs (one, run16, did not converge). However, since there was so much data, the data set was divided into run 1-25 and run 26-47. The plots can be seen in Figure 6-12. Additionally, some of the simulation results, including the percentage deviation for each single run can be found in Appendix A, section A5.
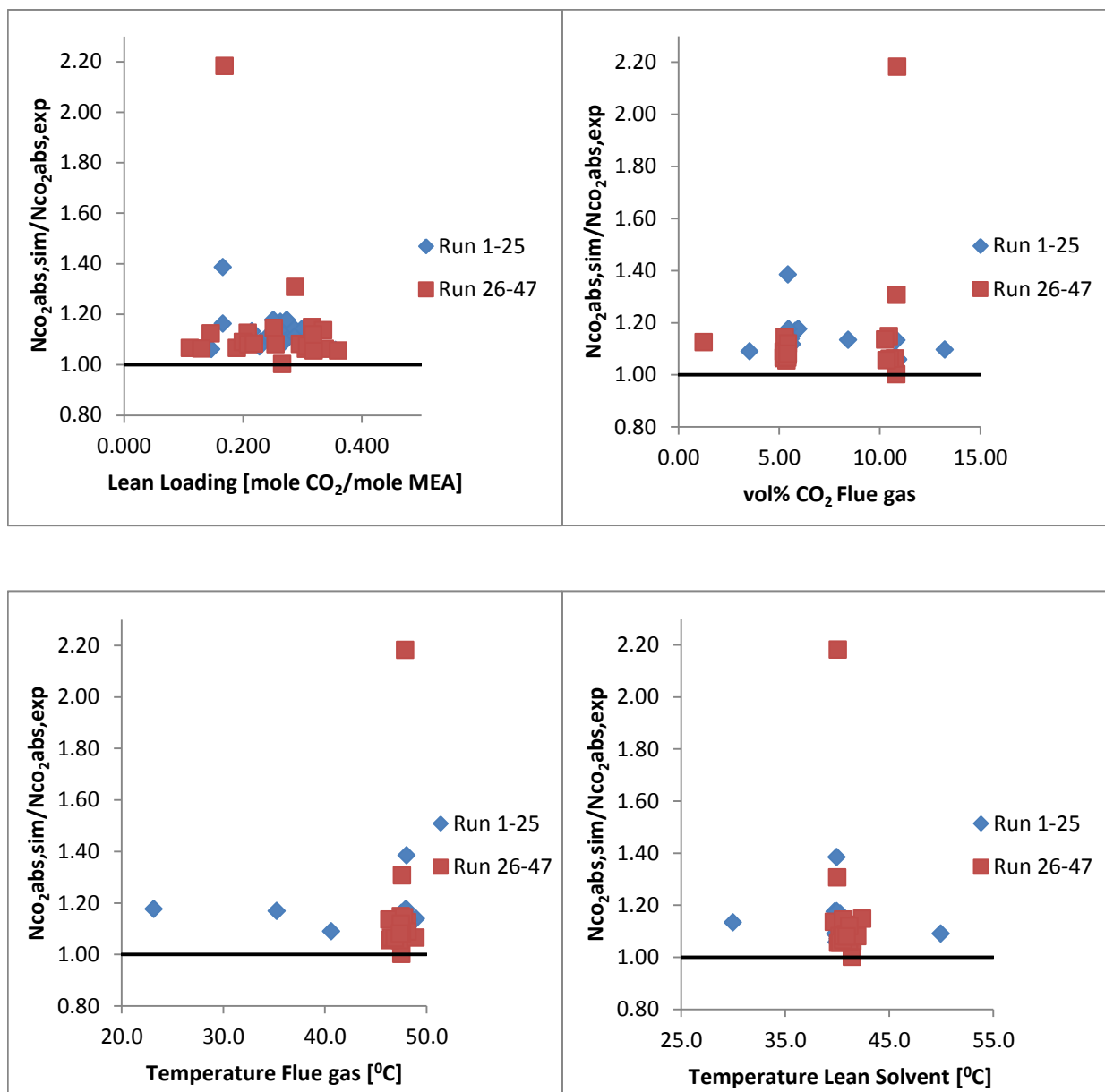
Figure 6-12 Four figures showing the ratio between the simulated and experimental CO₂ absorption rates plotted against lean solvent loading, vol% CO₂ in the flue gas and the inlet temperatures of the flue gas and the lean solvent for the 47 runs. Run 1-25 are marked in blue and run 26-47 are marked in red.

As can be seen from the figures, also here the simulation model predicted well the experimental results. The points are stable, over-predicting the CO₂ absorption rate for all runs, even though there is a large spread in loading, vol% CO₂ and inlet temperatures.

It is worth noticing that the simulation model over-predicts every point, which is not the case for the other campaigns. This might indicate that calibration of the equipment here is performed in another way than for the other campaigns.

It can also be seen that there is only three points that over-predicts the absorption rate with more than 20%. When investigating this closer, if was found that this was run 25, 26 and 27. It can therefore be assumed that there might be experimental errors here, for instance in calibrations of the equipment.

The focus in the Notz et al. publication was to present the plant and critically discuss its operation, as well as performing parameter studies. Therefore this publication has not published any simulation results, neither for the CO_2 absorption nor the temperature profiles, which can be used for comparison with simulations results found using the modified Aboundheir model.

However, the experimental data from Notz et al. also gives several temperature measurements throughout the absorber column. These data were plotted against the temperature profile for the liquid phase given from the Aspen Plus simulations. The liquid phase was used since it looks from the flow diagrams that the measurements are performed on this phase. The agreement between the experimental and simulated profiles was satisfying for almost every run from this campaign. For run 25 and 27 the simulation model over-predicted the temperature with about 2 °C and 10 °C respectively throughout the column. As mentioned earlier, it may be calibration errors in run 25, 26 and 27. However, this may only affect the CO_2 measurements, and do not have to affect the temperature measurements.

Figure 6-13, showing the temperature profiles for run 1 and 10 respectively, illustrates how well the simulation model predicts the experimental temperature measurements. This was the case for most of the runs in this campaign. However, for the runs where the simulation disagrees with the experimental data, both under-prediction and over-prediction was found. For run 30, shown in Figure 6-14, the simulation model under-predicts the temperature with about 6 °C throughout the column, except at the top. This was also the case for run 28 and 29, where the simulation model under-predicted the temperature with about 5 °C and 3 °C respectively. For run 33, the simulation model predicts the temperature bulge at the top of the column, while the experimental measurements predict the bulge in the bottom. The temperature profile for this run is shown in Figure 6-14. The same result was found for run 39.
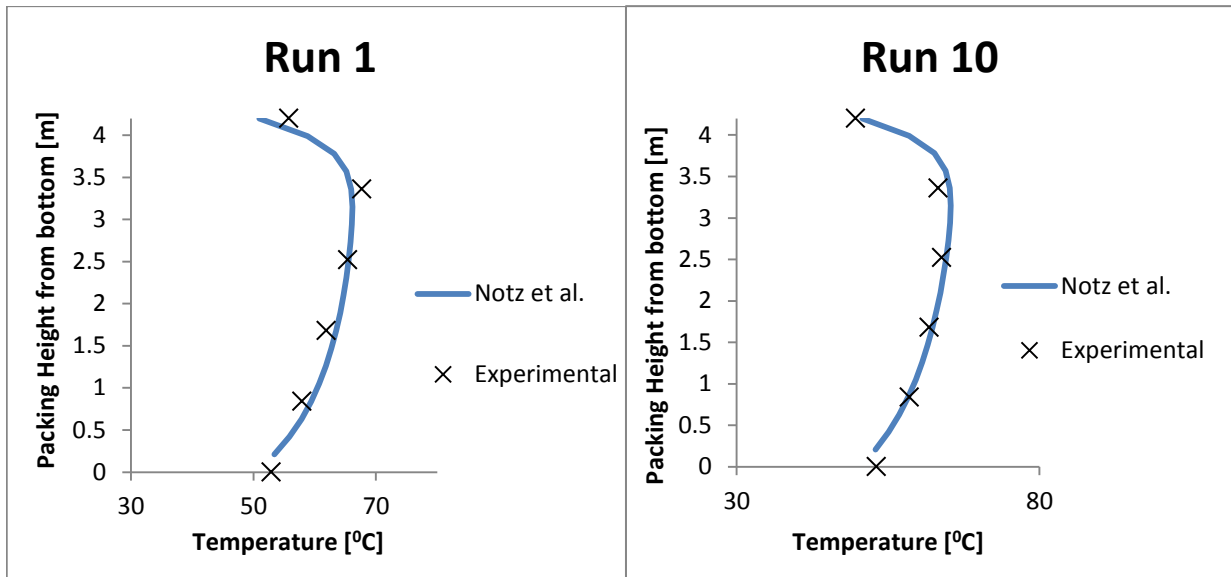
Figure 6-13 The temperature profile for run 1 can be seen to the left, and the temperature profile for run 10 can be seen to the right.
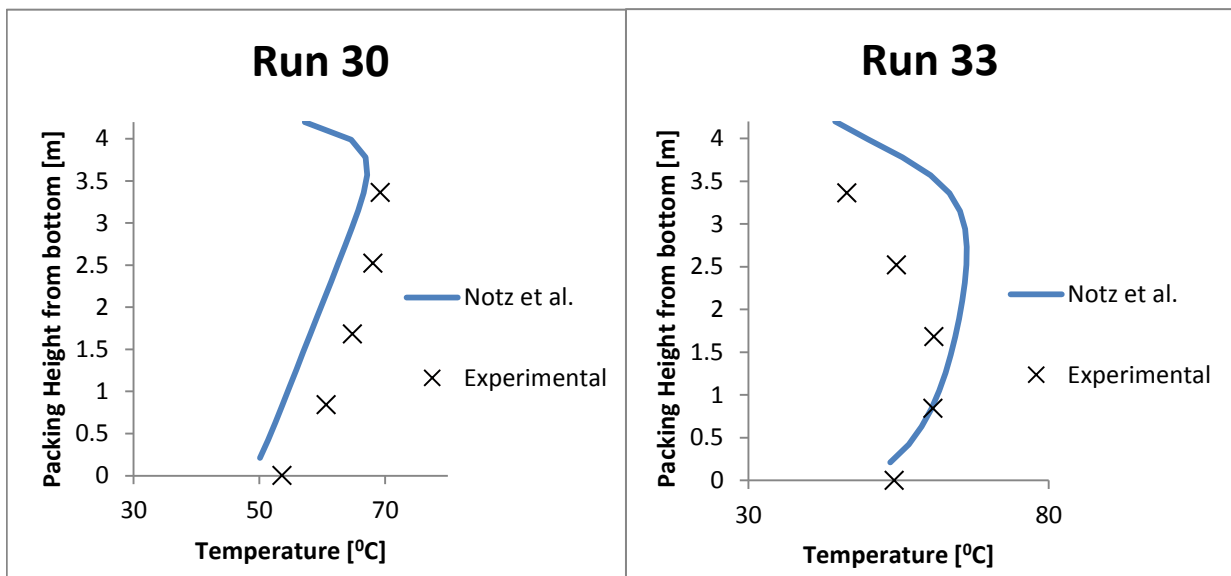
Figure 6-14 The temperature profile for run 30 can be seen to the left, and the temperature profile for run 33 can be seen to the right.

As mentioned, the experimental data from Notz et al. also gives CO_2 measurements throughout the absorber column. These data were plotted against the CO_2 profile for the liquid phase given from the simulations, since it looks from the flow diagrams that the measurements are performed on the liquid phase. There was not given measurements for every run, but for the ones given, the experimental data and simulated data were compared. It

was shown that the agreement between the experimental and simulated profiles was satisfying for almost every run. Below the CO_2 profile for run 1 and 24 are given in Figure 6-15.
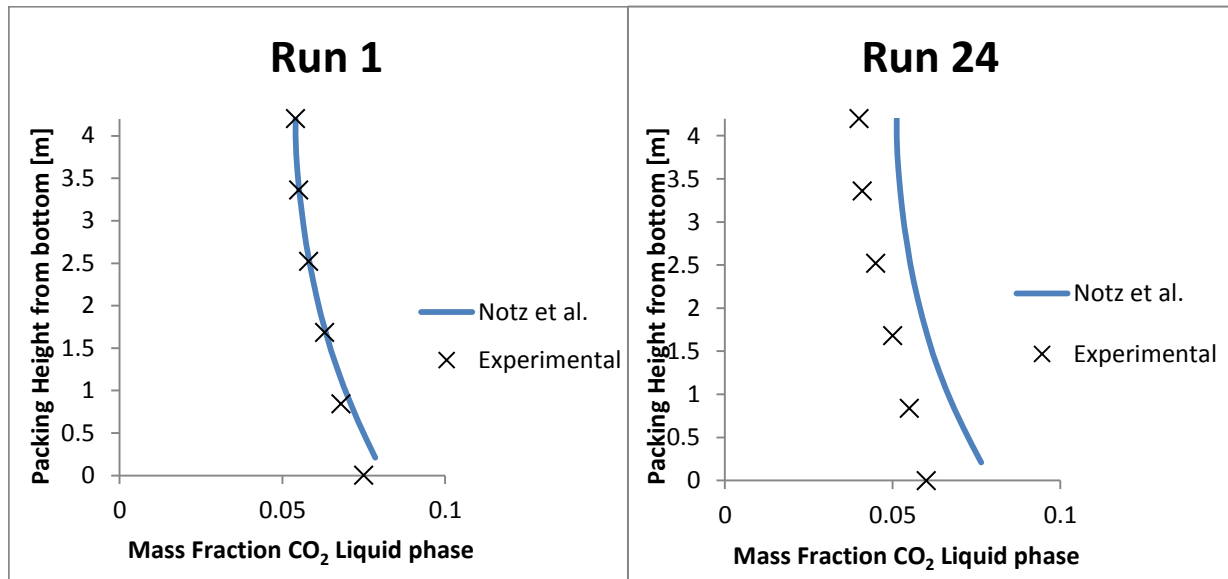
Figure 6-15 The CO_2 profile for run 1 is given to the left, and the CO_2 profile for run 24 is given to the right.

7 Desorber Simulations

In the desorber simulations the performance of the simulation model was varying for the different campaigns, and thus several factors that could explain the model performance were investigated. The reactions in the desorber column occur so rapidly that it is almost in equilibrium. The performance of the original Aspen Plus model was therefore compared to the performance of an equilibrium model for the Tobiesen et al. campaign. In addition, the performance of the new kinetic model, the modified Aboundheir model, was tested for the Tobiesen et al. and Notz et al. campaigns.

The reboiler is, maybe, the most important part of the desorber column and the solvent regeneration process. It is closely related to the heat loss in the column, which also is very important. If the heat loss in the desorber column is not properly taken into account, the simulation results can be heavily influenced. In the experimental data from Notz et al., the reported heat loss in the column had a large spread in the experimental runs. Therefore the effect of increasing the heat loss in some of the runs was looked closer into. For the Enaasen et al. and Pinto et al. campaigns, the heat loss was not reported. A heat loss of 0.5 kW was therefore introduced in the individual runs for these campaigns, based on the Tobiesen et al. (2008) publication from the same pilot plant.

At the end of this chapter, the simulation results from the different campaigns are compared to each other. It was attempted to identify trends in the performance of the simulation model, as well as examining the consistency of the campaigns.

7.1 Pilot Data from Tobiesen et al. (2008)

The desorber column located at NTNU used in the Tobiesen et al. (2008) campaign consists of 3.89 m Mellapak 250Y packing, with a reboiler at the bottom and a condenser at the top of the column. Since it was desired to only specify the reboiler duty in Aspen Plus, the column was simulated using a RadFrac column consisting of 20 stages, with no condenser and a kettle reboiler at the bottom, stage 20. The gas leaving the top of the stripper where sent through a flash with the given condenser temperature and pressure from the experimental data as specifications. Thus, the flash tank in the simulation represented the condenser in the real column. The condensate out of the flash was recycled to the reboiler. A flow diagram of the pilot plant can be seen in Figure 7-1, and campaign specifications can be seen in Table 3-2.
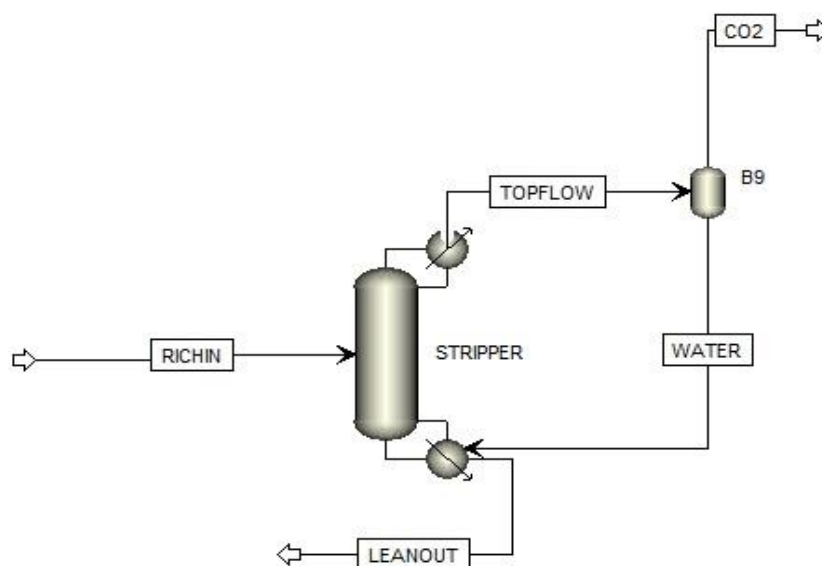
Figure 7-1 Aspen Plus Flow diagram illustrating the desorber part of the pilot plant located at NTNU.

In the first simulation round, the original Aspen Plus model was used, and the rich solvent flow was specified as a two-phase "Vapor-Liquid" stream using volume flow basis (l/min). The results from this simulation round were poor. When the simulated desorption rate was compared to the experimental gas measurements, the average deviation was found to be 16.3% and the absolute average deviation was found to be 18.1%. From the results it was seen that the deviation between experimental and simulated desorption rate increased with increased vapor fraction in the inlet stream. Note that the vapor fraction is calculated by Aspen Plus and not specified by the user. The percentage deviations between simulated and

experimental desorption rates and vapor fractions for each single run can be seen in Appendix B, section B1.1.

Based on the paper by Tobiesen et al. (2008), it was decided to test to define the inlet stream as "Liquid-Only" instead of "Vapor-Liquid". In the development of the simulation model used by Tobiesen et al., it was discussed as an option to define the inlet stream as a one phase stream, and therefore it was tested also here. The comparison of the simulation results from the two cases, having the rich inlet stream as "Vapor-Liquid" or "Liquid-Only", can be found in Appendix B, section B1.2. It can be seen that the overall deviation between experimental measurements and simulation results for the CO_2 desorption is far less when the rich inlet stream is defined as "Liquid-Only" compared to "Vapor-Liquid". Five of the runs have quite large differences, where the decrease in the deviation using "Liquid-Only" is from -56.0% to -8.1%, -51.7% to -15.6%, -61.3% to -11.4%, -60.6% to -6.6% and -35.6% to 1.5%. It is also worth noticing that the total outlet flow from the top of the stripper, including the condensate and CO_2 stream, is decreased when the rich inlet flow is defined as "Liquid-Only". This is as expected since it requires more reboiler duty to get the same vapor fraction in the desorber when the flow is only liquid compared to a combination of both vapor and liquid.

The simulation results using a "Liquid-Only" inlet stream was found to be interesting and thus looked closer into to understand the reason for the improvements. It was therefore examined whether the problem lay in the simulation of the desorber column itself. This was done by sending the rich stream in run 17 and 18 through a flash separating the gas and liquid stream, before the liquid stream entered the desorber column. Run 17 and 18 were chosen because the vapor fraction in these streams was largest, 0.0118 and 0.0140 respectively, and because the deviation in these streams was high -61.3% and -60.6%. The flow diagram from these simulations can be seen in Figure 7-2.
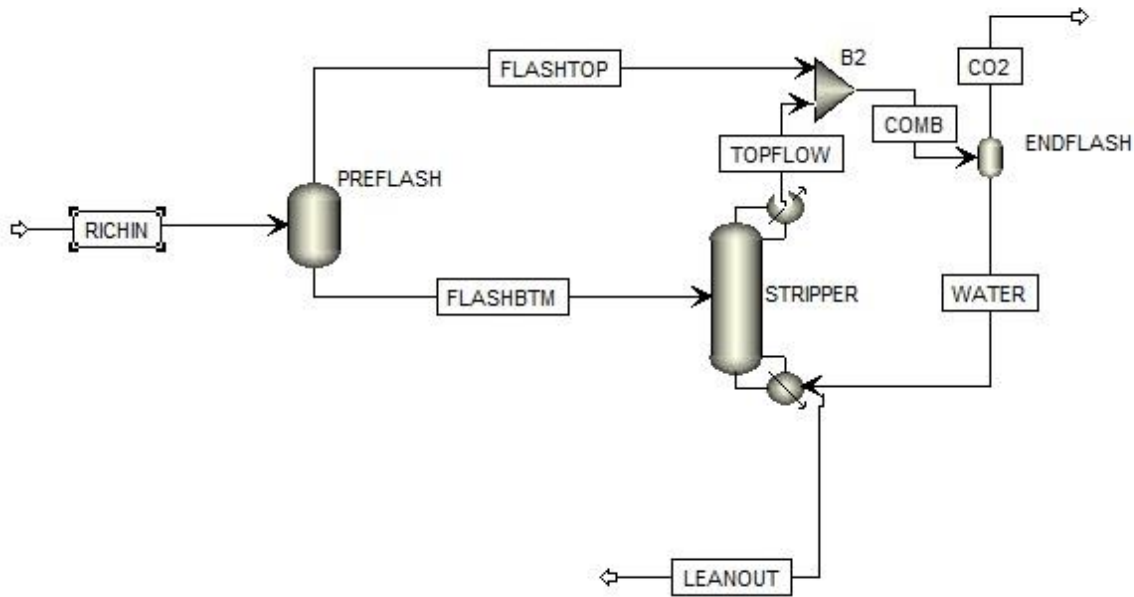
Figure 7-2 Flow diagram from the desorber simulation with a flash before the desorber column.

The results from these simulations gave the same results as the simulation where the rich inlet stream was defined as "Vapor-Liquid", i.e. giving 61.3% deviation in run 17 and 60.6% deviation in run 18. This indicates that the simulation problem is not in the desorber column itself.

Nevertheless, the simulation results found using "Liquid-Only" indicated that the problems may lay in the specifications of the inlet stream. This was investigated closer by comparing the rich mass flow (kg/h) and the density of the rich stream (kg/m^3) for the cases with "Vapor-Liquid" and "Liquid-Only" inlet stream. Both of which sizes, the mass flow and density, were given from Aspen Plus. From these sizes, which can be found in Appendix B, section B1.2, it could be concluded that when the flow is defined as "Vapor-Liquid" and specified on a volume basis (l/min), Aspen Plus does not consider that the original volume flow is a liquid flow, but that it is a sum of liquid and vapor. In other words, Aspen Plus first calculates a flash and thereafter the density (kg/m^3) and mass flow (kg/h) from the outlet liquid, and thus the results will be wrong. When the flow is specified on a mass basis on the other hand, Aspen Plus will calculate a flash of the total amount, including both the gas and liquid phase, and thus the results for the mass flow and density will be correct.

As a result of this, the next simulation round was performed with a "Vapor-Liquid" inlet flow and the flow that was specified on a mass basis (kg/h), instead of volume basis (l/min) as it was originally. The result of this improved the simulation results drastically, and the AD and AAD was reduced from 16.3% and 18.1% to 5.3% and 5.2% respectively. This is also a significantly improvement of the simulation results found by Tobiesen et al., which was 9.9% for both AD and AAD. Some of the simulation results from this round, including the percentage deviations in the desorption rates between simulated and experimental values, can be seen Appendix B, section B1.3.

Additionally it was examined whether the experimental gas measurements or liquid measurements fitted best with the simulation results for the CO_2 desorption rate. There is not given a mass balance for the experimental data comparing gas and liquid measurements in the paper by Tobiesen et al., but AAD and AD for the mass balance was reported as 4.2% and 4.5% respectively. Tobiesen et al. have further reported the following about the quality of the gas measurements compared to the liquid measurements of the CO_2 desorption rate:

"*The liquid side CO_2 removal in the desorber is calculated as the difference between the CO_2 rate in the incoming liquid to the desorber and in the liquid exit from the reboiler. The gas side CO_2 production is measured with a mass flow meter downstream the condenser. For most points the mass balance agreement between the gas and liquid sides is good, within 3%, and only for two points the deviation is more than 10%. It is difficult to tell which data set is better (liquid or gas).*" [12].

When the gas and liquid measurements are compared to the simulated values for the desorption rate of CO_2, it varies whether the gas or liquid measurement agrees best with the simulated values. If the measurement, either gas or liquid, which agrees best with the simulations are used, AD is reduced to 3.7% and AAD is reduced to 3.8%. This is a slightly improvement of the results found using only the gas measurements, which gave AD 5.3% and AAD 5.2%. The results from this can be found in Appendix B, section B1.4.

Further, the performance of an equilibrium model and the new kinetic model, the modified Aboundheir model that was used in the absorber simulations, was compared to the performance of the original Aspen Plus model. The results are summarized in four figures, showing the ratio between the desorption rate in the simulations and the desorption rate found in the experiments as a function of rich solvent loading, rich solvent flow rate, the inlet

temperature of the rich solvent and the reboiler duty. The plots can be seen in Figure 7-3 and a table presenting some of the results can be found in Appendix B, section B1.5 and B1.6.
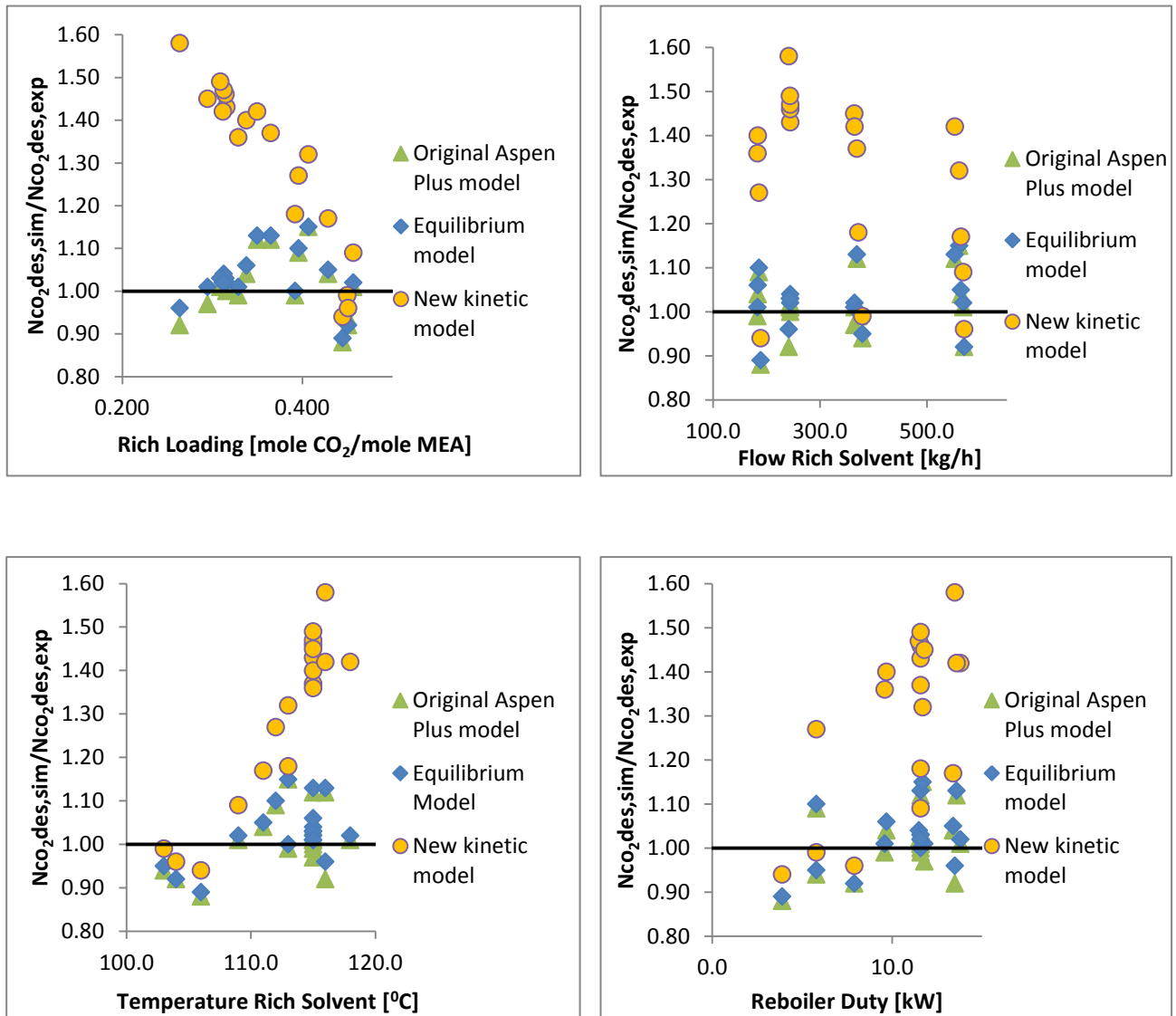
Figure 7-3 Four figures showing the ratio between the simulated and experimental CO_2 desorption rates plotted against rich solvent loading, rich flow rate, the inlet temperature of the rich solvent for the 19 runs.

As can be seen, there is no significant difference in the results found using the original Aspen Plus model compared to the equilibrium model. This is as expected since the reactions in the desorber column occur rapidly. The performance of the original Aspen Plus model and the equilibrium model are deemed satisfactory, with a relative deviation between simulated and experimental desorption rate for single runs varying from -11.8% to 15.4%. If one compares the results found using the original Aspen Plus model with the new kinetic model, it can be seen that the new kinetic model shifts all points upwards. It can be seen that the overall

performance of the new kinetic model is much less reliable than the performance of the original Aspen Plus model, with a deviation for single runs varying from -5.8% to 58.0%. In theory, a kinetic model should give desorption rated equal to, or lower than, an equilibrium model in cases with rapid reactions. As could be seen in Chapter 4.2, the VLE prediction by Aspen Plus is satisfactory. However, there is not found an explanation for the results seen here, but this should be analyzed closer.

Especially for the two plots with rich solvent loading and temperature of the rich solvent on the x-axis, it looks like the new kinetic model follows a trend with decreasing over-prediction with increasing solvent loading, and increasing over-prediction with increasing temperature. This trend is not equally clear in the simulations with the original Aspen Plus model or the equilibrium model. Nevertheless, since the original Aspen Plus model gives the best, and most reliable, results, this is used in the further investigations of the simulation model.

7.1.1 Sum up Tobiesen et al. desorber simulations

To sum up the Tobiesen et al. desorber simulations, it is found that the performance of the original Aspen Plus model is best, but approximately equal to the equilibrium model. In the simulations using the original Aspen Plus model, all runs are inside 15% deviation for the CO_2 desorption rate, which is deemed satisfactory. There is not found a clear trend regarding the performance of the simulation model based on the conditions (flow rate, temperature, loading, etc.) for the original Aspen Plus model. However, based on the results from the "Liquid-Only" simulation round, it is found that the rich inlet stream must be specified on a mass basis (kg/h) and not on a volume basis (l/min). There are some deviations in the experimental mass balance between gas and liquid measurements, but this does not have a significant effect on the simulation results.

7.2 Pilot Data from Notz et al. (2012)

The desorber column located at the University of Kaiserslautern has a little different configuration than the desorber column located at NTNU. At NTNU the condensate is recycled to the reboiler in the bottom of the column. However, at Kaiserslautern, there is a water wash section on the top of the packing, and the condensate is recycled to the top of this section. The Aspen Plus flow diagram used for simulating this campaign is shown in Figure 7-4, and the campaign specifications can be found in Table 3-2.
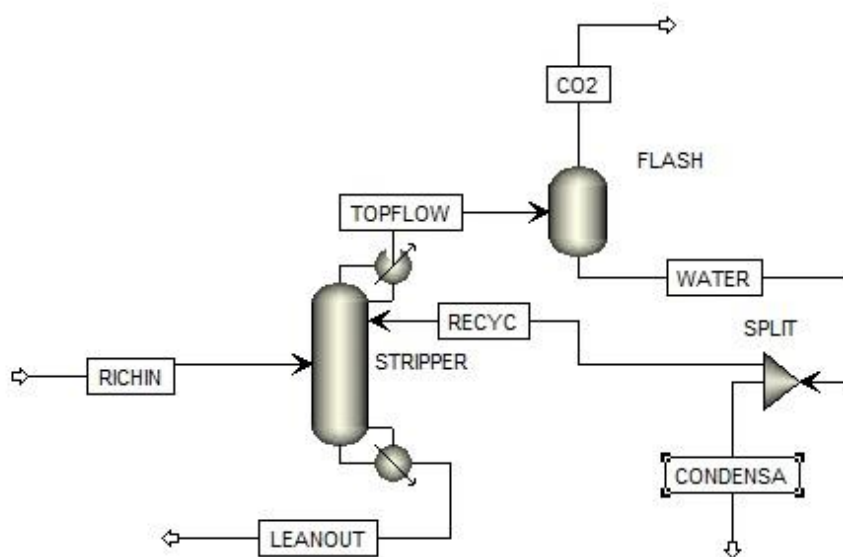
Figure 7-4 The Aspen Plus flow diagram used for simulating the Notz et al. campaign.

Notz et al. report that the gas measurements of the CO_2 desorption is most trustworthy, and therefore these are used when comparing with simulation results. However, when a mass balance on the experimental data from the gas and liquid side is performed, the deviation varies from about 0 to 15%.

Also for this campaign, simulation results using the original Aspen Plus model were compared to simulation results using the new kinetic model, the modified Aboundheir model used in the absorber simulations. Two of the runs, run 10 and 11, are not included because of convergence problems in Aspen Plus. Four plots, showing the ratio between the desorption rate in the simulation and the desorption rate found in the experiments as a function of rich solvent loading, rich solvent flow rate, the inlet temperature of the rich solvent and the reboiler duty are made. These can be seen in Figure 7-5. Additional information about the rich

solvent loading and flow rate for the individual runs can be found in Table B.5 in Appendix B, section B2.1.
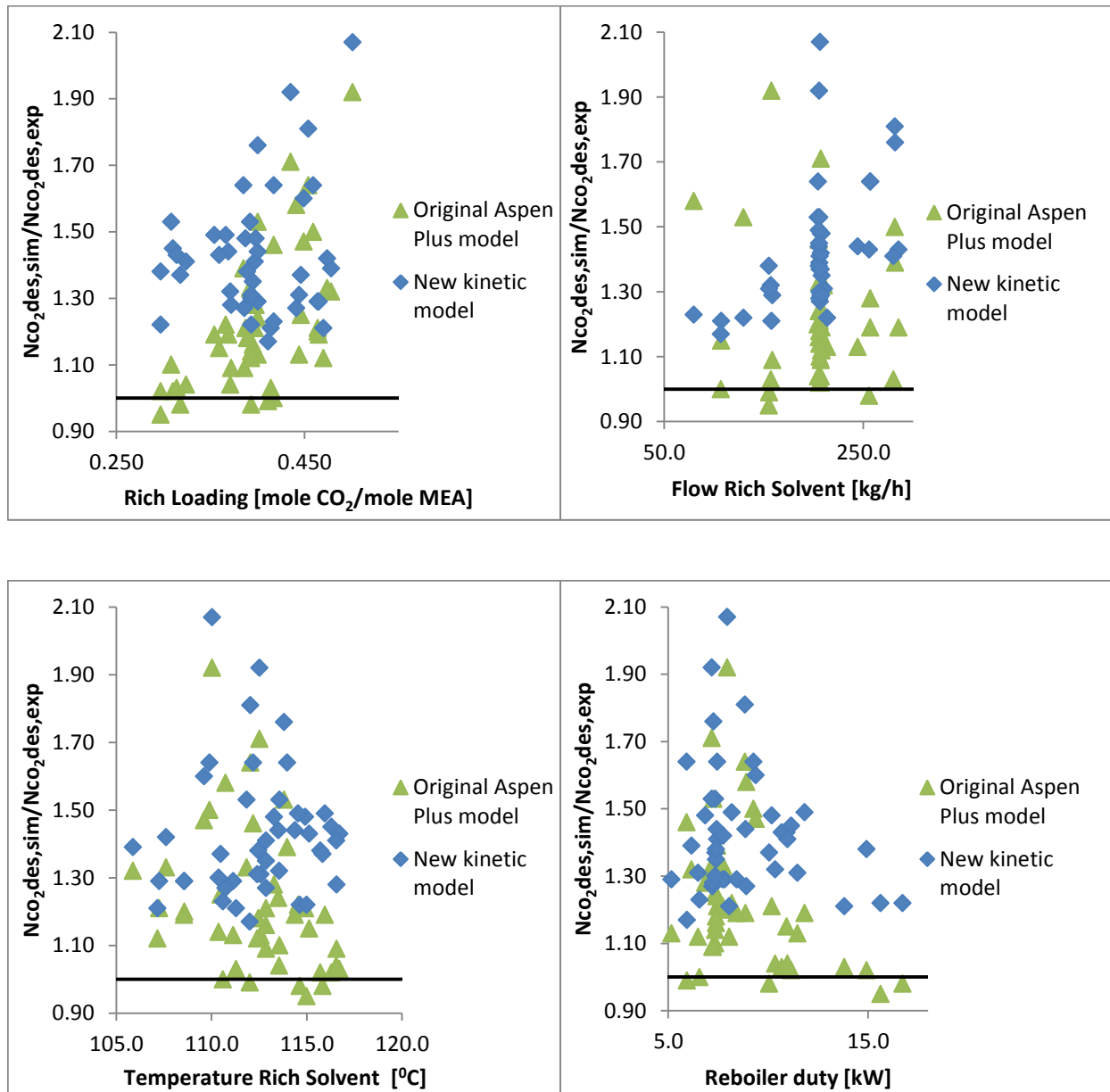
Figure 7-5 Four figures showing the ratio between the simulated and experimental CO₂ desorption rates plotted against rich solvent loading, rich flow rate, the inlet temperature of the rich solvent for the 45 runs.

As can be seen from the plots, also here all points are shifted upwards using the new kinetic model compared to using the original Aspen Plus model. The deviation between simulated desorption rate and experimental desorption rate using the original Aspen Plus model varies from -5.1% to 92.0% for single runs, which is a huge spread. It is worth noticing that three runs which are assumed to be wrong from the absorber part, run 25, 26 and 27, has

deviations of 71%, 33% and 92% respectively in the desorber simulations. This strengthens the assumption of errors in the experimental measurements for these runs.

In addition to run 25, 26 and 27, 6 other runs stands out as having large over-prediction of the CO_2 desorption rate. In all these runs, the experimental rich loading and the experimental lean loading are high compared to the other runs. This can be seen in Table B.8 in Appendix B, section B2.2. Also the rich solvent flow rate is relatively high for these runs compared to the other runs in this campaign, and in addition they have a relatively high vapor fraction.

It can be seen that several runs are performed at similar flow rates of about 200 kg/h. These runs give a large spread in the deviation between experimental measurements and simulation results for the CO_2 desorption rate, from a under-prediction of about 2% to an over-prediction of about 92%.

When the deviation in the experimental data are compared with the deviation between simulated and experimental values, there is no trend that large deviations in the experimental data gives large deviation between simulated and experimental values. Nevertheless, the AAD and AD using the original Aspen Plus model is found to be 16.0% and 22.8% respectively. This is very high numbers and usually refers to bad performance of the simulation model. However, large deviation in some of the points is mainly the reason.

7.2.1 Simulation without a Water Wash Section

As mentioned, the desorber column at the University of Kaiserslautern has a water wash section at the top of the desorber column. To try to understand the large deviations seen between the simulated and the experimental data, a similar flow diagram as used to simulate data from Tobiesen et al. (2008) was tested. In this option, shown in Figure 7-6, there is no water wash section and the condensate is recycled to the reboiler.
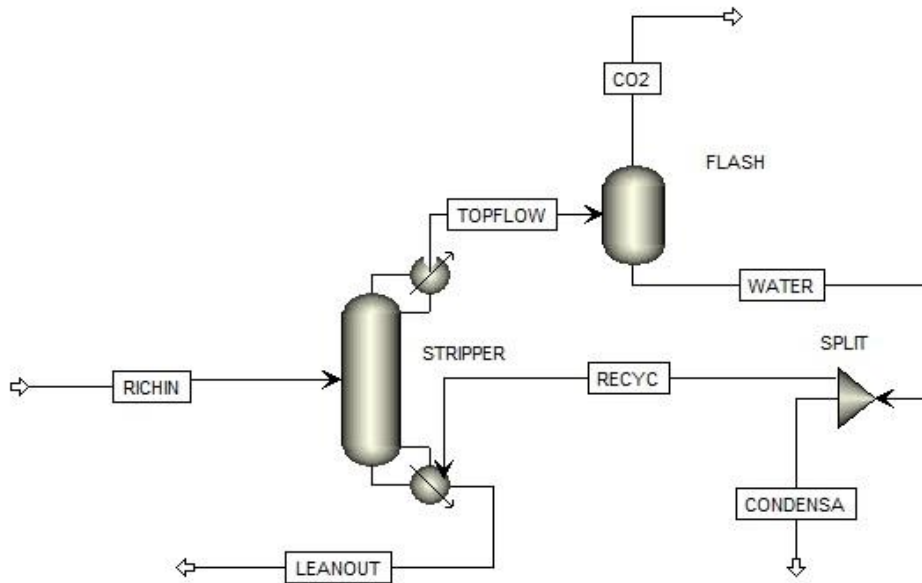
Figure 7-6 Aspen Plus flow diagram used to simulate the Notz et al. campaign when the water wash section are removed and the condensate are recycled to the bottom of the column.

The results from the simulation when the water wash section is removed gave slightly better results, giving a slightly lower desorption rate in all single runs. However, the difference is not significant and therefore the water wash section is not the reason for the large deviations seen. The simulation are illustrated graphically and can be seen in Appendix B, section B2.2.

Temperature profiles for these two options, having a water wash section or not, was also created and compared to experimental measurements. The biggest difference is found in the bottom of the column where the simulations without a water wash section gives results closest to the experimental measurements. The temperature profiles for run 1, 9, 31 and 46 are shown in Figure 7-7.
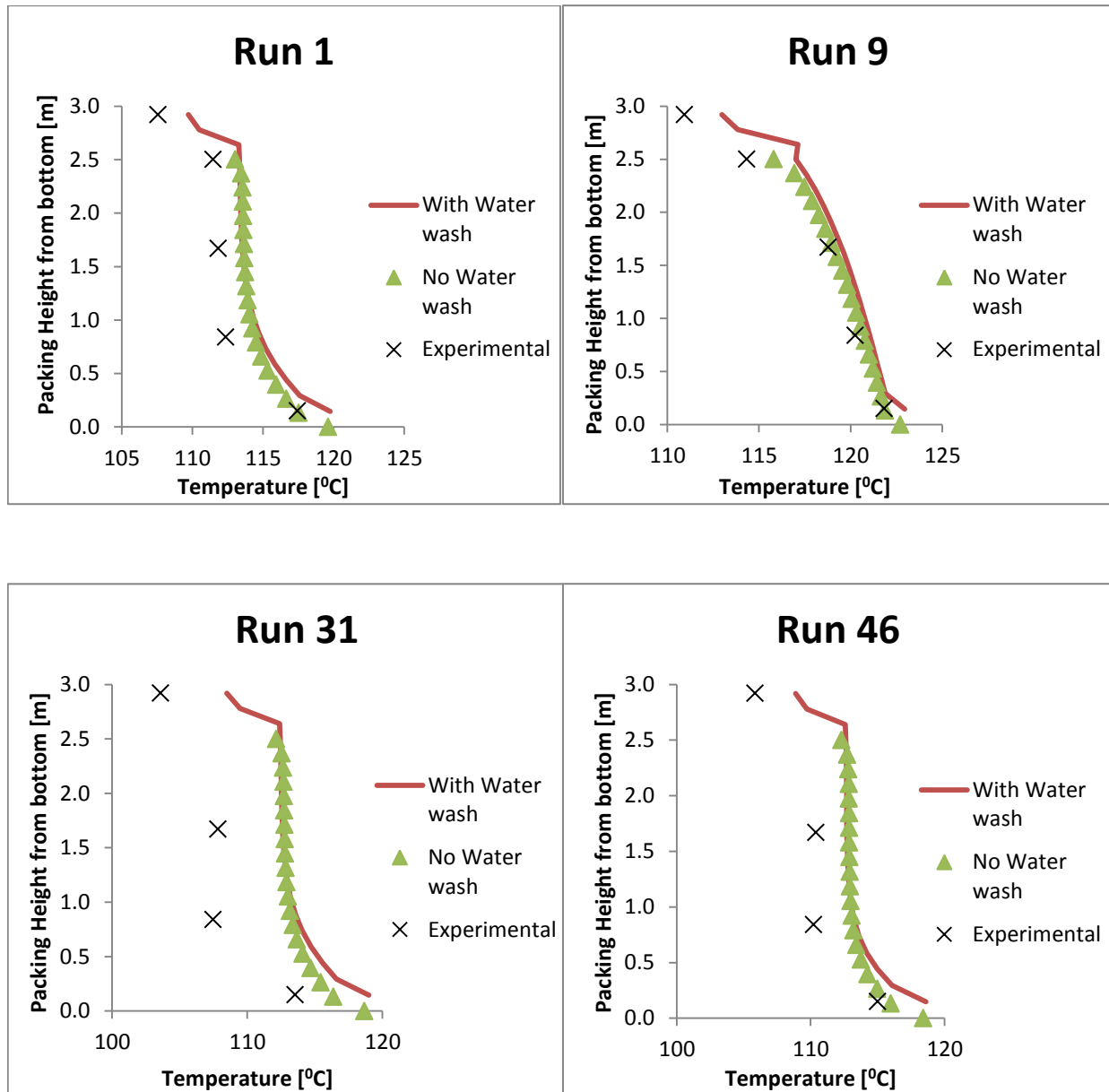
Figure 7-7 Temperature profiles for run 1, 9, 31 and 46, where the experimental points are marked in black and the simulations with a water wash section are marked with a red line and the simulations without a water wash section are marked in a green line.

As can be seen, the simulation model predicts the temperature quite well for run 1 and 9. For run 31 and 46 the deviation are larger, with an over-prediction of approximately 5 °C and 3 °C. However, also the CO_2 desorption is poorly predicted by the simulation model for these runs. Actually, the trend with 3-5 °C over-prediction of the temperature profiles regards all the six runs were also the CO_2 desorption was clearly over-predicted, namely run 30, 31, 32, 33, 39 and 46. Expect for these, the simulation model generally predicts the temperature profiles for the Notz et al. campaign quite well, with an over-prediction of 0-3 °C in most cases.

The publication by Notz et al. also provides several CO_2 measurements throughout the desorber column for some of the runs. These measurements were used to create and compare CO_2 profiles throughout the column. Also from these profiles it can be seen that the simulations without a water wash section and with a water wash section give almost identical results for all runs. The largest deviation is found for run 12-20. In these cases, the simulation with a water wash section gives results closest to the experimental measurements. Some of the CO_2 profiles are presented in Figure 7-8.
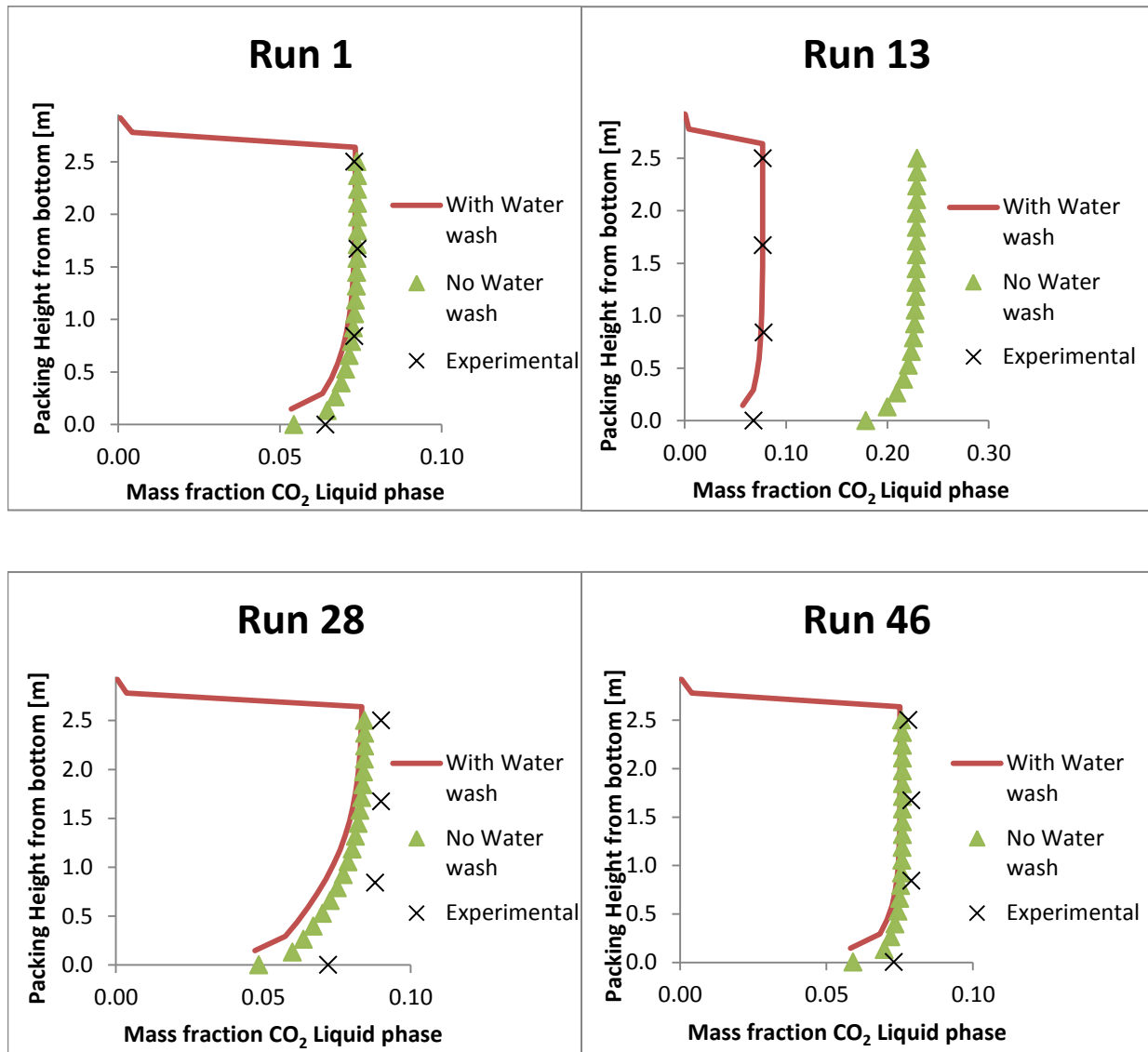
Figure 7-8 CO_2 profiles for run 1, 13, 28 and 46 showing the experimental measurements in black and the simulations with a water wash section in red and without a water wash section in green. All measurements are of the liquid phase.

Since the performance of the simulation model was not satisfactory, it was examined whether back-absorption in the water wash section at the top of the desorber column occurred

in the simulations. The CO_2 amount in the recycled stream in the simulation with a water wash section was therefore compared to the CO_2 amount in the recycled stream in the simulations without a water wash section. The results can be found in Appendix B, section B2.3, where it can be seen that there is no significant difference in the CO_2 amount in the recycled stream for the individual runs. Back-absorption in the water wash section is therefore not the reason for the large deviations between simulated and experimental CO_2 desorption rate.

As mentioned in the introduction to the desorber simulations, the heat loss in the desorber column should be properly taken into account in the simulations. This is because it can heavily influence the desorption rate of CO_2. The reported heat loss in the experimental data from Notz et al. varied from almost 0% to 14% based on the reported reboiler duty. Additionally, a value for "Evaporator power required to compensate heat losses" was reported, and also this number varied quite a lot, from 5% to 25% based on the reboiler duty.

To evaluate whether the varying heat loss in the reported data was the cause for the large deviation in the CO_2 desorption rate between simulated and experimental values, a heat loss of 10% (based on the reboiler duty for the single runs) were introduced in run 2, 8, 26, 27, 28, 29, 30, 31 and 32. These runs were chosen because the reported percentage heat loss in these runs was very low. The results and figures showing the percentage heat loss of the reboiler duty can be found in Appendix B, section B2.4. It was shown that the simulation results were improved when the percentage heat loss in these runs was increased to 10%. However, the improvements are only by 6% to 11% for the single runs, e.g. reducing the deviation between simulated and experimental CO_2 desorption rate from 50% to 42%. Therefore, the heat loss alone is not the reason for the bad prediction of the experimental data.

7.2.2 Sum up Notz et al. desorber simulations

To sum up, the performance of the original Aspen Plus model on experimental data from Notz et al. was not satisfactory. Eighteen out of the forty-five runs simulated deviated with more than 20% for the CO_2 desorption rate. The new kinetic model was attempted, but it gave results that were less reliable than the results found using the original Aspen Plus model. In addition it was tested to simulate the column without a water wash section at the top. This gave a slightly improvement of the simulation results. However, after comparing the temperature profiles and the CO_2 profiles, no clear conclusion can be drawn regarding which of these column structures are best for simulation purposes. There was not found any back-absorption in the water wash section that could explain the bad performance of the simulation model. Neither, the heat loss alone was found to be the reason.

7.3 Pilot Data from Enaasen et al. (2015)

The Enaasen et al. campaign was run at the same pilot plant as the Tobiesen et al. campaign, and therefore the configuration of the desorber column in Aspen Plus was the same as shown in Figure 7-1. However, the packing type in this column was Sulzer BX, and the packing height was 3.57 m. The campaign specification can be seen in Table 3-2.

There are not listen any heat loss in the desorber in the experimental data, so it was tested to reduce the reboiler duty by 0.5 kW, based on the paper by Tobiesen et al. [12]. A reduction in the reboiler duty will lead to lower mass transfer of CO_2. Based on the simulation results found without reducing the reboiler duty, is could be seen that a reduction would improve the results in seven out of eight runs. The results can be seen in Figure 7-9. The percentage deviation for single runs and the experimental mass balance can be found in Appendix B, section B3. In the comparison, the experimental gas measurements of the CO_2 desorption rate is used.
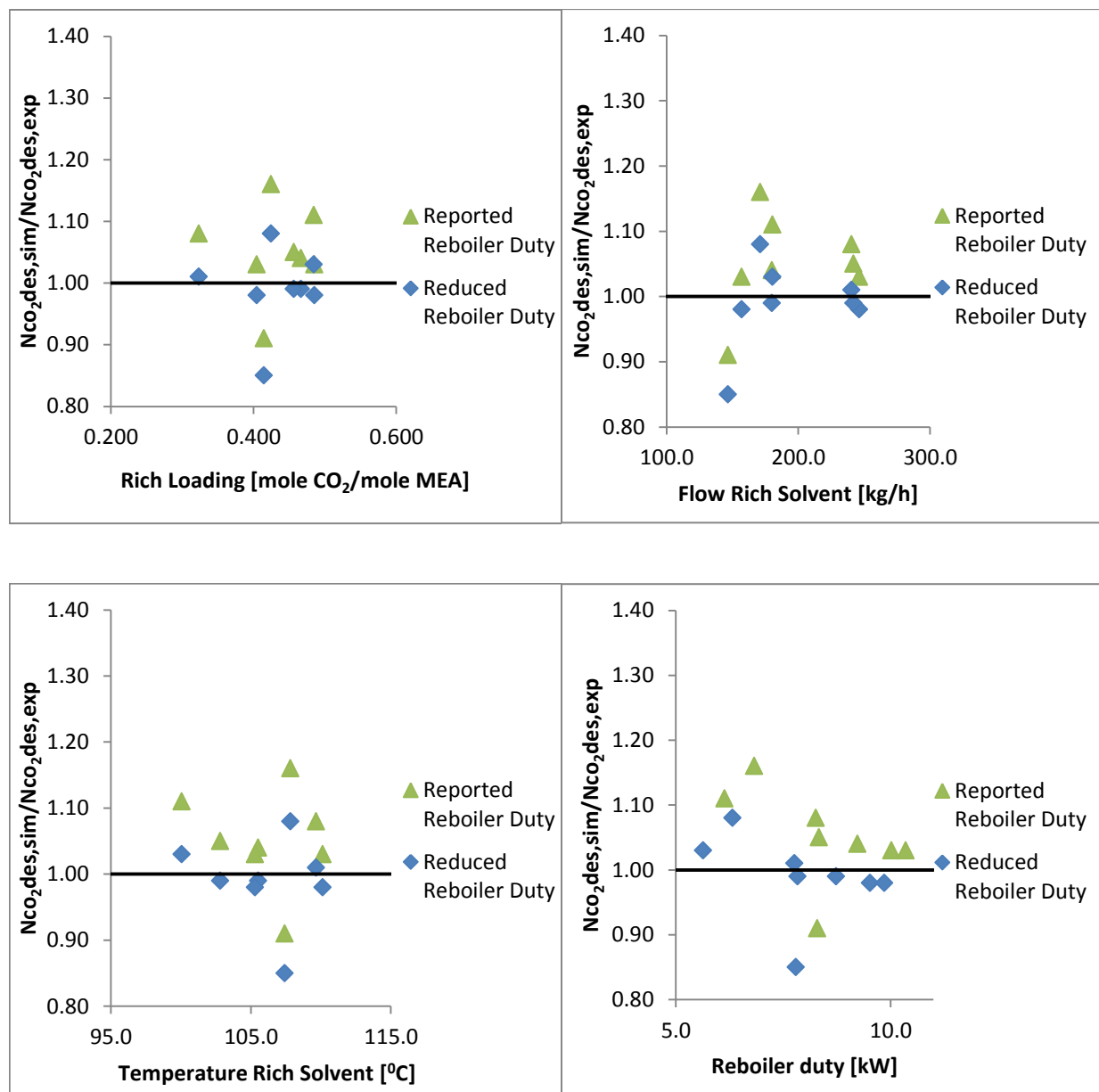
Figure 7-9 Four figures showing the ratio between the simulated and experimental CO₂ desorption rates plotted against rich solvent loading, rich flow rate, the inlet temperature of the rich solvent for the 8 runs.

The relative deviation between simulated and experimental desorption rate for single runs varies from -9.3% to 16.0% in the simulations using the given reboiler duty. In the simulations with reduced reboiler duty, the relative deviation between simulated and experimental desorption rate varies from -15.3% to 7.6%. The improvement by reducing the reboiler duty can also be expressed using AAD and AD. In the simulations with the given reboiler duty, AAD and AD was found to be 5.0% and 7.4%. In the simulations with reduced reboiler duty, AAD and AD was found to be 3.9% and 4.1%. Both of these results are deemed satisfactory.

As the simulation results show, there are already an over-prediction of the CO_2 desorption in most runs, thus the new kinetic model was not tested for this campaign since it would increase the over-prediction, and thus give poorer simulation results. It also performed poorly for the Tobiesen et al. and Notz et al. campaigns, and was therefore rejected as an option in the desorber simulation model.

Temperature measurements throughout the desorber column were provided, and therefore temperature profiles for the eight runs were created and compared. The profiles for run 2, 4, 6 and 8 are shown in Figure 7-10. As can be seen, there is no significant difference between the simulations using the reported reboiler duty and the simulations with reduced reboiler duty. The simulations also agree well with the experimental measurements.
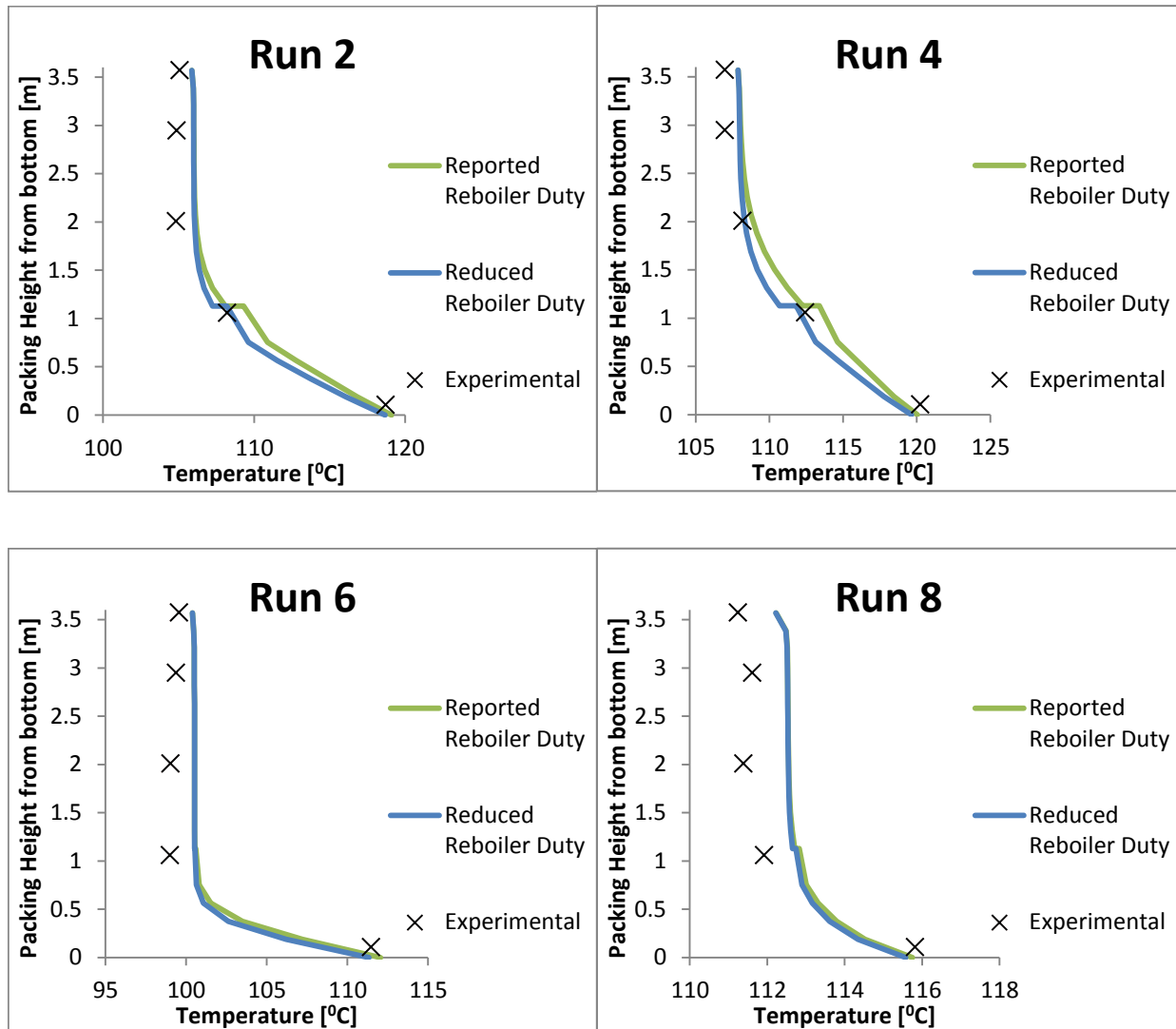
Figure 7-10 Temperature profiles for run 2, 4, 6 and 8 from the Enaasen et al, campaign. Experimental measurements are marked in black, and simulation results using the reported reboiler duty are marked in green while the simulation results with reduced reboiler duty are marked in blue.

As was seen from the simulation results presented in Figure 7-9, reducing the reboiler duty gave simulation results closer to the experimental measurements for all runs except one, run 4. Actually, in the simulations with reduced reboiler duty, run 4 is the one with largest deviation from the experimental CO_2 desorption rate. However, as can be seen, it has the best agreement for the temperature profile. Nevertheless, the simulated temperature profiles generally agree well with the experimental measurements, with a deviation below 2 °C in all runs. However, in some of the temperature profiles, like for run 2 and 4, it can be seen that there is a "shelf" in the profile approximately 1 m up in the column. This can indicate that there are convergence problems or problems in finding the optimal solution in Aspen Plus

here. However, Aspen Plus says that all calculations are completed normally, so it is not certain that this is a problem.

The deviation between simulated and experimental values for the CO_2 desorption rate in single runs can be compared to the mass balance in the experimental data between gas and liquid measurements. From this it can be seen that in cases with large deviation between simulated and experimental data, also the experimental mass balance are poor. Thus, if the liquid measurements where used instead of the gas measurement in some of the runs, e.g. run 1 and 4, the simulation model would perform even better. The recorded desorption rate of CO_2 in the liquid phase in run 1 was 4.63 kg/h compared to the gas phase where it was 4.39 kg/h. The simulations gave 5.09 kg/h, and thus closer to the liquid measurements. In run 4 the liquid measurement was 5.66 kg/h, the gas measurement was 6.50 kg/h, and the simulations gave 5.90 kg/h. However, in run 8 the liquid measurement was 2.93 kg/h, the gas measurement was 3.24 kg/h, and the simulations gave 3.49 kg/h.

7.4 Pilot Data from Pinto et al. (2014)

The Pinto et al. campaign was also run at the pilot plant located at NTNU, and with the same packing type and height as used in the Enaasen et al. campaign. The campaign specifications can be found in Table 3-2. Neither in this experimental data there is given any heat loss, and therefore it was tested to reduce the reboiler duty by 0.5 kW also in this case. However, as can be seen from Figure 7-11, four out of six runs already under-predict the desorption rate in the simulations with the given reboiler duty. Thus, a reduction in the reboiler duty will worsen the results. The percentage deviation for single runs and the experimental mass balance can be found in Appendix B, section B4. Also in this campaign, the experimental gas measurements of the CO_2 desorption rate are used.
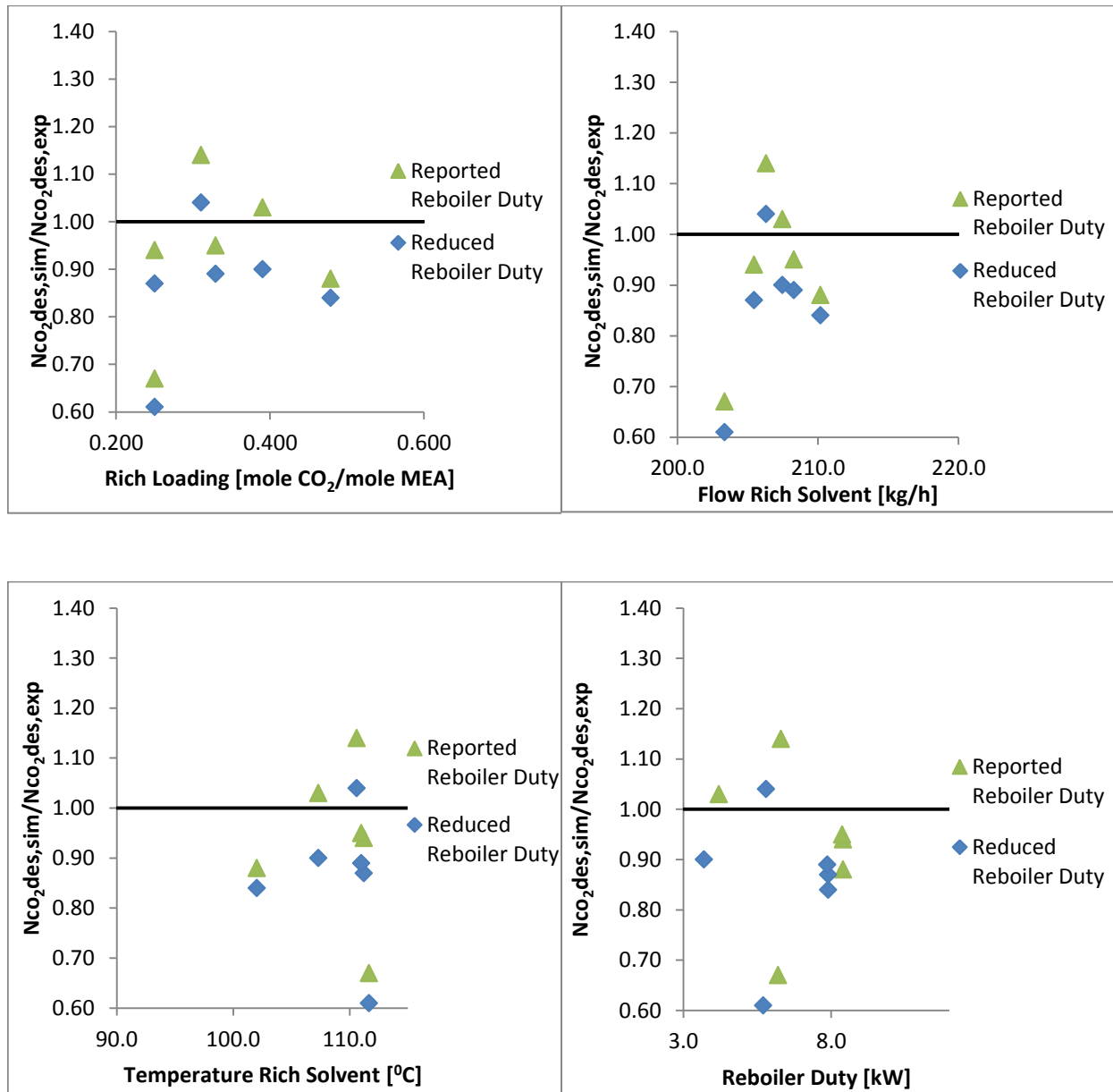
Figure 7-11 Four figures showing the ratio between the simulated and experimental CO₂ desorption rates plotted against rich solvent loading, rich flow rate, the inlet temperature of the rich solvent for the 6 runs.

As can be seen from the plots, 5 out of 6 runs agree well with the experimental data, and are all inside 15% deviation in the simulations with the given reboiler duty. Run 3 has the largest deviation, with -32.8% in the simulation with the given reboiler duty, and -39.2% in the simulation with reduced reboiler duty. However, if one look at the mass balance for experimental gas and liquid measurements for run 3, it can be seen that the deviation is 35.3% also here. Thus, if the liquid measurement for this run was used instead, the deviation would be reduced to -8.4% in simulation with the given reboiler duty and, -17.1% in simulation with reduced reboiler duty.

The AAD and AD can also be compared for the two cases, and these was found to be 10.4% and 12.0% in the simulation with the given reboiler duty, and 14.5% and 15.6% in the simulation with reduced reboiler duty. However, these large absolute deviations and absolute average deviations are mainly caused by the one point with large deviation, run 3. If this point is removed, AAD and AD will be reduced to 7.6% and 7.9% in the simulation with the given reboiler duty, and 9.0% and 10.8% in the simulation with reduced reboiler duty.

There are also provided several temperature measurements throughout the desorber column for this campaign. Thus temperature profiles are created and compared with experimental measurements. The profiles created in Aspen Plus for the two simulation cases, either with the given reboiler duty or with reduced reboiler duty, are almost identical. Temperature profiles for run 1, 2, 3 and 6 can be seen in Figure 7-12.
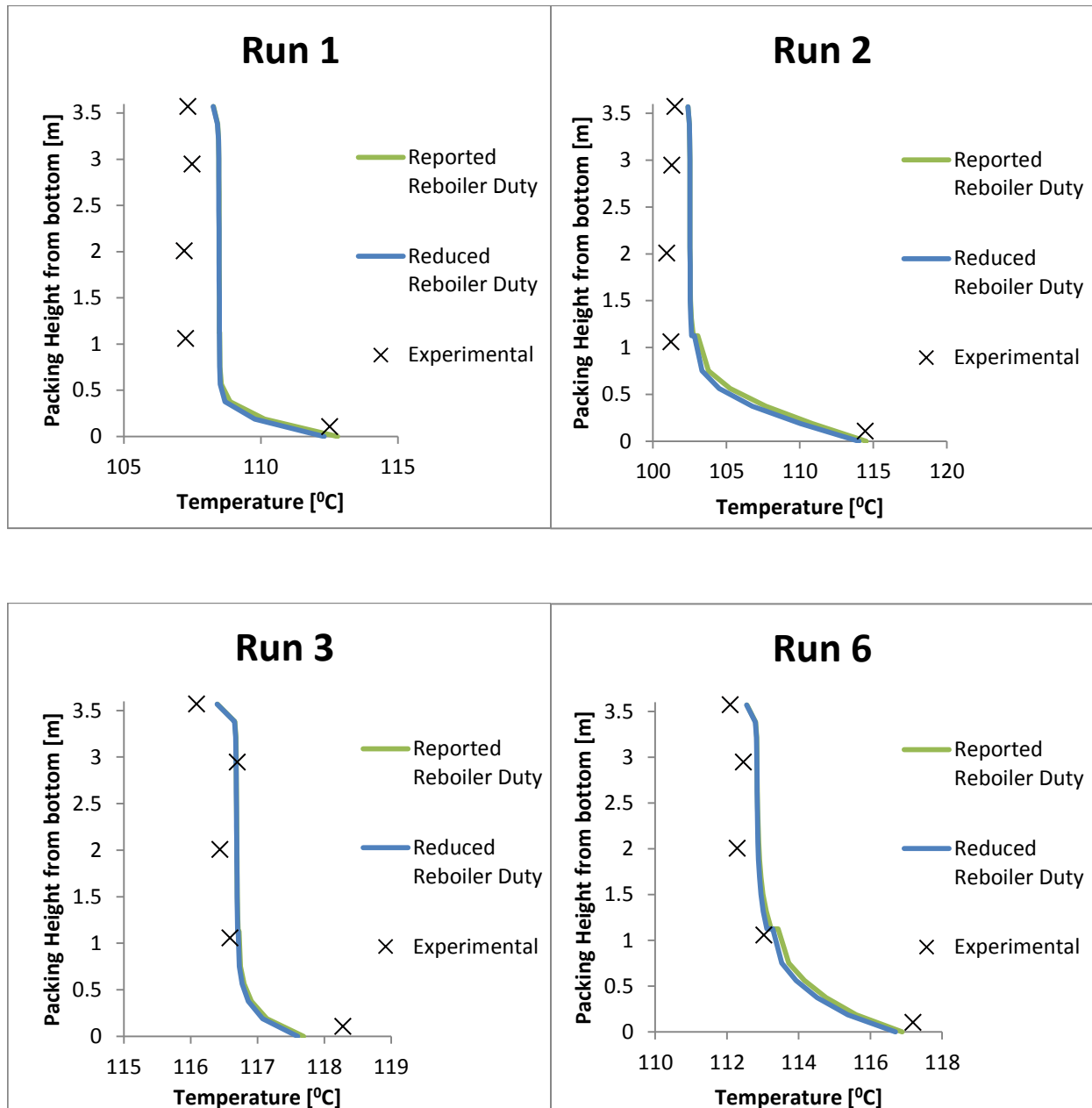
Figure 7-12 Temperature profiles for run 1, 2, 3 and 6 from the Pinto et al. campaign. The green line is the simulation with the given reboiler duty, the blue line is the simulation with reduced reboiler duty and the experimental measurements are marked with black.

As can be seen, the temperature profiles agree quite well with the experimental temperature measurements throughout the column. The deviation between the simulated and measured temperatures is between 0 °C and 1.5 °C for all runs.

8 Absorber Simulation Results Summarized

8.1 Table Overview

Table 8-1 Overview of the simulated campaigns in the absorber part, with experimental and reported data, as well as the calculated average deviation and absolute average deviation.

	Tobiesen et al.	Pinto et al.	Enaasen et al.	Sønderby et al.	Notz et al.
Experimental data used for	Simulation model fitting	Validation	Validation	Validation	Validation
Column Diameter [m]	0.150	0.150	0.150	0.100	0.125
Packing Height [m]	4.36	4.23	4.23	1.60-8.20	4.20
Packing Type	Sulzer Mellapak 250Y	Sulzer BX	Sulzer BX	Sulzer Mellapak 250Y	Sulzer Mellapak 250Y
Fluegas Flow rate [kg/h]	137.0-165.4	97.5-101.7	94.4-140.8	39.8-44.2	55.5-100.0
Lean solution Flow rate [kg/h]	187.9-579.1	198.6-206.6	142.1-240.9	130.5-565.6	75.0-350.3
L/G [mol/mol]	1.3-4.5	2.3-2.4	1.3-2.1	3.9-18.1	1.3-5.4
Lean solution loading [mol CO_2/mol MEA]	0.183-0.409	0.210-0.350	0.215-0.341	0.112-0.300	0.111-0.356
Rich solution loading [mol CO_2/mol MEA]	0.276-0.451	0.250-0.479	0.323-0.485	0.149-0.356	0.297-0,501
Vol% CO_2 Fluegas in (dry basis)	1.6-15.3	0.9-12.1	1.6-7.4	9.2-10.9	1.3-13.2
Vol% CO_2 Fluegas out (dry basis)	0.3-13.0	0.0-7.7	0.0-3.1	0.0-2.1	0.1-11.1*
Available CO_2 profile through absorber column	No	No	No	No	Yes
Temperature Fluegas [°C]	39-69	38-51	38-51	20-28	23-49

Temperature Lean solution [°C]	40-66	41-41	41-58	20-28	30-50
Available Temperature Profile through absorber column	Yes	Yes	Yes	Yes	Yes
Absorber pressure [kPa]	99-104	104-106	102-106	101-104	100
Error in mass balance between gas and liquid (reported)	**	< 21.6%	< 3.4%	< 11.1%	< 5%
Average Deviation between Experimental and Simulated absorbed CO_2 (AD)***	8.5	8.2	4.9	11.7	14.0
Absolute Average Deviaton between Experimental and Simulated absorbed CO_2 (AAD)***	7.4	9.3	4.9	11.6	7.1

Vol% CO_2 out for this campaign are calculated using the temperature measurement on the top of the packing and assuming that the mole fraction of N_2 and O_2 is constant from inlet. However, this was not possible for run 30-47 because the temperature measurement was missing.

*** Not given mass balance in Tobiesen et al., but given AAD=4.43% and AD=5.58%.*

****AD and AAD is computed using Equation (2) and (3) from Chapter 4.3.1, and compares experimental and simulated data.*

As can be seen from Table 8-1, the column specifications for the four campaigns are virtually equal regarding height and diameter, but the column used in the Sønderby et al. experiments has the smallest diameter, and is also of variable height from 1.60 m to 8.20 m. The flue gas flow rate is also lower in the Sønderby et al. experiments compared to the other campaigns. The lean solution flow rates are similar for the different campaigns, but the Tobiesen et al. and Sønderby et al. campaigns cover a larger range of flow rates than the other campaigns. Also the lean and rich loadings are similar, but the vol% of CO_2 in the gas out is lowest in the

Enaasen et al. and Sønderby et al. campaigns. The inlet temperatures of the streams cover a large range for the campaigns as a whole.

In general the simulation results could be considered satisfactory, with average deviations and absolute average deviations below 15% for all campaigns. Calculating the overall AD and AAD including all runs from the campaigns gives 11.4% and 9.7% respectively. However, as discussed in Chapter 6.4 giving the results from the absorber simulations of the Notz et al. campaign, there are three outliers which may be attributable to calibrating errors. Thus, if these three points are disregarded, AD and AAD are reduced to 9.8% and 8.5% respectively, which could be taken as a satisfactory outcome.

8.2 Discussion

As can be seen from Table 8-1, the average deviation and absolute average deviation vary from 5% to 14% for the five individual campaigns. Since it is usual to allow for a 5% error in experimental data, this can be considered as an acceptable simulation result. The Aspen Plus simulation model can therefore be considered as a reliable and efficient tool to predict CO_2 capture in 30wt% MEA over a wide range of operating conditions in the absorber. It is worth noting that none of the campaigns stands out, but that all campaigns gives good simulation results. This also indicates that the experimental data are valid and consistent with each other.

Regarding the campaign used to make the simulation model, the Tobiesen et al. campaign, AD is 8.5% and AAD is 7.4%. In the case of the two other campaigns with packing type Mellapak 250Y, the Notz et al. and the Sønderby et al. campaigns, AD and AAD are somewhat higher. However, as can be seen from the simulation results in Chapter 6.3 and 6.4, the high AD and AAD values for these campaigns were caused by the large spread of the points in the Sønderby et al. campaign, and a couple of outliers in the Notz et al. campaign. If one disregards the outliers in Notz et al., AD would be decreased to 10.6% and AAD to 3.4% for this campaign.

The simulations of the Pinto et al. and Enaasen et al. campaigns, which have a different packing type, also show quite good results. Especially the results from the Enaasen et al. campaign is satisfactory, but also the results from the Pinto et al. campaign is good except for one point when the liquid measurements are used for comparison. The discrepancies between the experimental and simulated CO_2 mass transfer rates are so small that the experimental data from these campaigns can be considered good and consistent with each other. It is also worth noting that the Enaasen et al campaign has the lowest error in the mass balance between gas and liquid measurements. This might also explain why the overall simulation result for this campaign is better than for the other campaigns.

Simulation results from all campaigns except the Notz et al. campaign both over-predict and under-predict the absorption rate of CO_2 compared to experimental measurements. When the simulation model both over-predict and under-predict the mass transfer, it is a clear indication that there is no systematic discrepancy between the model and the experimental campaigns as a whole. However, for the Notz et al. campaign, the simulation model over-predicts the CO_2 absorption in all 46 runs. In every run except four, the over-prediction is

between 6% and 18%. Nevertheless, plots with either rich or lean loadings, inlet temperatures and inlet flow rates as well as the L/G ratio on the x-axis, do not reveal a trend for the five campaigns as a whole. The plots can be seen in Appendix A, section A6.

Column type (e.g. structured packing or random packing, valve or sieve trays) and the size of the mass transfer region (i.e. height of packing, number of trays) are important design variables. However, it does not seem that the packing type has a significant impact on the performance of the simulation model for the five different campaigns simulated. But, as was mentioned under the result section for the Sønderby et al. campaign, the results found when the packing height was 4.9 m and 3.3 m seemed to be less reliable than the other results. Additionally, one run was performed with packing height 1.6 m. For this run, however, the simulation model performed better, with only 6% deviation from the experimental measurement of CO_2 absorption rate.

When comparing the absorber specifications, it can be seen that the column used by Sønderby et al. has the smallest diameter, 0.100 m, and a packing height varying from 1.60 m to 8.20 m. The three other columns have similar heights, varying from 4.20 to 4.36 m, and similar diameters, 0.150 m in the campaigns run at the NTNU pilot plant and 0.125 m in the column at the University of Kaiserslautern. The small diameter in the column used in the Sønderby et al. campaign can affect the results in that the streams may flow along the column wall rather than through the packing as desired. This will decrease the mass transfer because of the shorter residence time in the column. It is unknown whether this effect is taken into account in the Aspen Plus simulation model. This can generally be the case in pilot plants compared to full-scale plants with larger diameters. However, the simulation results from Sønderby et al. show both over-prediction and under-prediction of the CO_2 absorption, thus there is no clear indication that this is a problem.

An attempt was made to vary the number of stages in the absorber from 20 to 15 and 25. However, the number of stages in a rate-based Aspen Plus model only gives the number of calculation points through the column, which do not correspond to the number of actual stages. Therefore, varying the number of stages did not have any impact on the results.

Generally, it was shown that the modified Aboundheir simulation model accurately predicts the temperature profiles for the five pilot campaigns, except for the Pinto et al. campaign where it is assumed that the reported values could be wrong. As mentioned in Chapter 6.3, the temperature profiles from the Sønderby et al. campaign have the largest

disagreement in cases with lower packing heights and low L/G ratio. However, for all the other campaigns, the L/G ratio is in the lower range of the Sønderby et al. campaign or even lower, but the predictions of the temperature throughout the column are still deemed acceptable.

When the placement of the temperature bulge in the column are compared for the individual campaigns, it can be seen that only the Sønderby et al. campaign had a clear bulge at the bottom of the column. In the other three campaigns, disregarding the Pinto et al. campaign because of poor results, the temperature bulge tends to appear at the top of the column. In several of the runs from the Notz et al. campaign, however, the temperature bulge appears less clear. If one looks at the flue gas and solvent flow rates for the different campaigns in Table 8-1, it is clear that the flue gas flow rate is lower in the Sønderby et al. campaign. However, the solvent rate in this campaign is relatively high. This indicates that there may be excess solvent in this campaign, and therefore theory would predict that the temperature bulge should appear at the bottom of the column. In the other three campaigns, the higher flue gas rates may give insufficient solvent and a temperature bulge higher up in the column.

Nevertheless, temperature profiles are not only dependent on the CO_2 absorption rate, but are also strongly dependent on the amount of evaporation and condensation of water and amine in the packing. Estimates of water content in the inlet and outlet gas are therefore important factors. As mentioned earlier, the inlet concentration of water is estimated assuming that the gas is saturated with water. This could thus be a source of discrepancies between the simulation results and the experimental measurements.

9   Desorber Simulation Results Summarized

9.1 Table Overview

In the comparison of the desorber simulations, the results using the original Aspen Plus model with the reported reboiler duties (without heat losses for Enaasen et al. and Pinto et al.) are used. In addition, the simulation results are compared only with the gas measurements for each single run in all campaigns. Table 9-1 gives an overview of the desorber specifications, including experimental and reported data, as well as the calculated average deviation and absolute average deviation.

Table 9-1 Overview of the simulated campaigns in the desorber part, with experimental and reported data, as well as the calculated average deviation and absolute average deviation.

	Tobiesen et al.	Notz et al.	Enaasen et al.	Pinto et al.
Experimental data used for	Validation	Validation	Validation	Validation
Column Diameter [m]	0.100	0.125	0.100	0.100
Packing Height [m]	3.89	2.52	3.57	3.57
Packing Type	Sulzer Mellapak 250Y	Sulzer Mellapak 250Y	Sulzer BX	Sulzer BX
Rich solution Flow rate [kg/h]	183.5-569.7	79.8-359.0	157.0-246.1	203.4-201.2
Rich solution loading [mol CO_2/mol MEA]	0.264-0.457	0.297-0.501	0.323-0.485	0.250-0.479
CO_2 Desorption Rate [kg/h]	3.2-11.7	3.4-10.6	3.3-9.0	2.0-7.9
Available CO_2 profile through absorber column	No	Yes	No	No
Reboiler Duty [kW] *	3.9-13.8	5.2-16.7	6.1-10.4	4.2-8.4
Temperature Rich solution [°C]	103-118	106-117	100-110	102-112

Temperature Lean solution [°C] **	107-122	113-125	113-121	109-117
Available Temperature Profile through absorber column	No	Yes	Yes	Yes
Desorber pressure [kPa]	194-216	200-230	169-190	175-177
Error in mass balance between gas and liquid (reported)	***	< 14.6%	< 13.8%	< 35.3%
Average Deviation between Experimental and Simulated desorbed CO_2 (AD)****	5.3	22.8	7.4	12.0
Absolute Average Deviaton between Experimental and Simulated desorbed CO_2 (AAD)****	5.2	16.0	5.0	10.4

The reboiler duties listed in the table are the ones reported as experimental data without heat losses.

**The lean solution temperature is measured after the reboiler in the Tobiesen et al. and Notz et al. campaign, in the reboiler in the Enaasen et al. campaign, and before the reboiler in the Pinto et al. campaign.*

***Not given mass balance in Tobiesen et al., but given AAD=4.2% and AD=4.5%.*

****AD and AAD is computed using Equation (2) and (3) from Chapter 4.3.1, and compares experimental and simulated data.*

As can be seen from Table 9-1, the column specifications for the four campaigns are quite equal regarding height and diameter. The Tobiesen et al. and Notz et al. campaigns covers a large range of rich solution flow rates, while the Enaasen et al. and Pinto et al. campaigns are somewhere in the middle of the range for the Notz et al. campaign. Also the rich loadings, CO_2 desorption rate and reboiler duties for the four campaigns are similar. The desorber

pressure for the Enaasen et al. and Pinto et al. campaigns are slightly lower compared to those of the other two campaigns.

In general, the simulation results are quite good, especially for the Tobiesen et al., Enaasen et al. and Pinto et al. campaigns, with average deviation under 12.0% and absolute average deviation under 10.4% for all three campaigns. If the one outlier in the Pinto et al. campaign is disregarded, the average deviation will be less than 7.9% and the absolute average deviation will be under 7.6% for all three campaigns. The overall AD and AAD including the Notz et al. campaign, was found to be 16.1% and 14.5% respectively. It does not look like the performance of the simulation model is dependent on the packing material, since the simulation results of both the Tobiesen et al. and the Enaasen et al. and Pinto et al. campaigns are good.

9.2 Discussion

As previously mentioned, the performance of the simulation model for the desorber part was deemed satisfactory for three out of the four simulated campaigns. When all runs in the four campaigns are included, the overall AD and AAD is found to be 16.1% and 14.5%. As for the absorber simulations, both over-predictions and under-predictions of the CO_2 mass transfer rates compared to experimental measurements are seen. And, as mentioned under the absorber discussion, this indicates that there is no systematic discrepancy between the model and the experimental campaigns as a whole.

Three simulation models were tested during the desorber simulations, and the effect of different factors were studied. Since the reactions in the desorber occur rapidly, equilibrium simulations should give approximately the same results as kinetic simulations. This was shown to be the case when the performance of the original Aspen Plus model was compared to an equilibrium model in the Tobiesen et al. campaign in Chapter 7.1. In the Notz et al. simulations, the effect of the water wash section was studied as well as the heat loss in the desorber column. This heat loss can heavily influence the simulation results, and should be properly accounted for in the simulations. A 10% heat loss based on the reboiler duty was introduced in some of the runs with the largest over-predictions of the CO_2 desorption rate in the Notz et al. campaign (12% to 92% over-prediction). However, this did not improve the results more than 6% to 11%, so it is probably safe to assume that is was not the main reason for the large over-predictions.

It seems as if the deviation in the CO_2 mass transfer rates increases with increased vapor fraction for the Notz et al. campaigns, giving increasing over-prediction. However, this trend is not seen in the Tobiesen et al. or the Enaasen et al. campaigns. In these campaigns it does not appear that there is any correlation between the vapor fraction in the inlet stream and the performance of the simulation model. Similarly, in the case of the Pinto et al. campaign, increasing vapor fraction does not yield correspondingly higher deviations between the simulated and experimental CO_2 desorption rates. Both over-prediction of 6% and under-prediction down to 36% can be seen in runs with zero vapor fraction in the Pinto et al. campaign. A graphic illustration of the results can be seen in Figure 9-1.
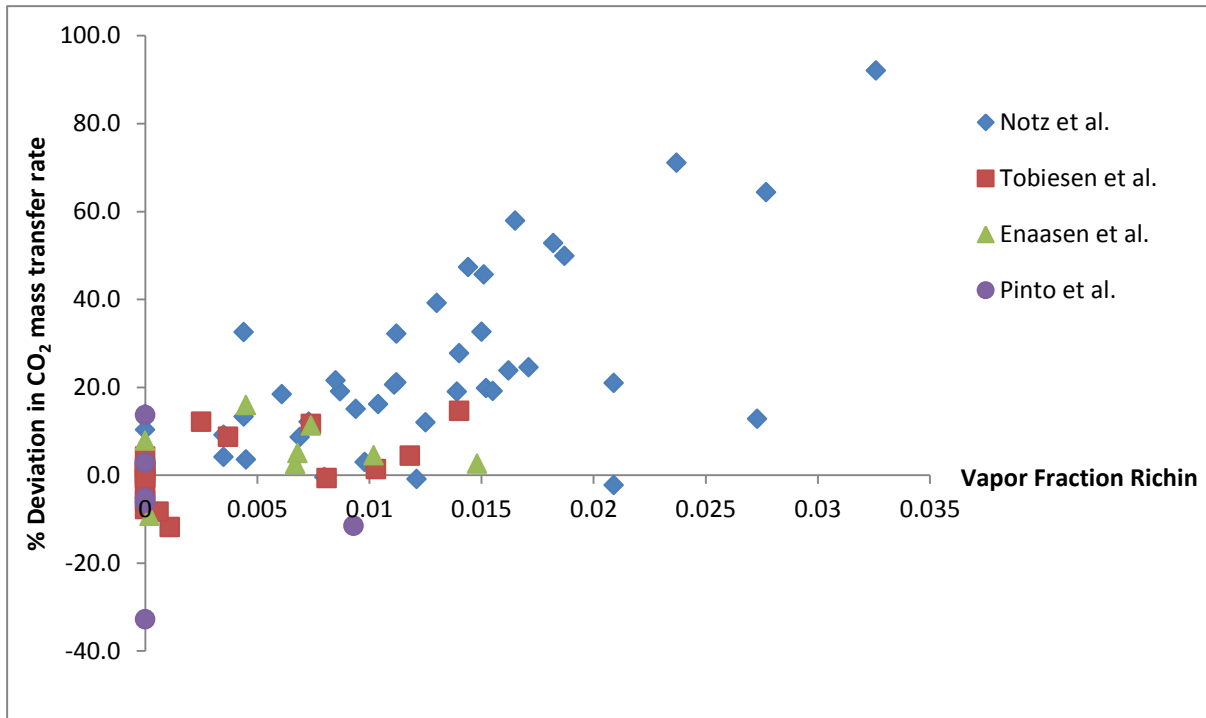
Figure 9-1 Plot showing the deviation in CO$_2$ mass transfer rate in the desorber as a function of the vapor fraction for all four campaigns simulated.

The CO$_2$ mass transfer has also been plotted against the inlet rich loading to determine whether there are any overall trends in the campaigns regarding rich loading. It can be seen that the trend for all campaigns is that the CO$_2$ mass transfer rate increases with increasing rich loading. However, it is apparent that four points from the Tobiesen et al. campaign deviate from the trend. These points are run 11, 13, 15 and 16, which have the lowest reboiler duties in this campaign. It can also be seen that the points from the Pinto et al campaign have a lower mass transfer rate than the points from the other campaigns. A plot of the CO$_2$ mass transfer rate as a function of the rich loading is shown in Figure 9-2.
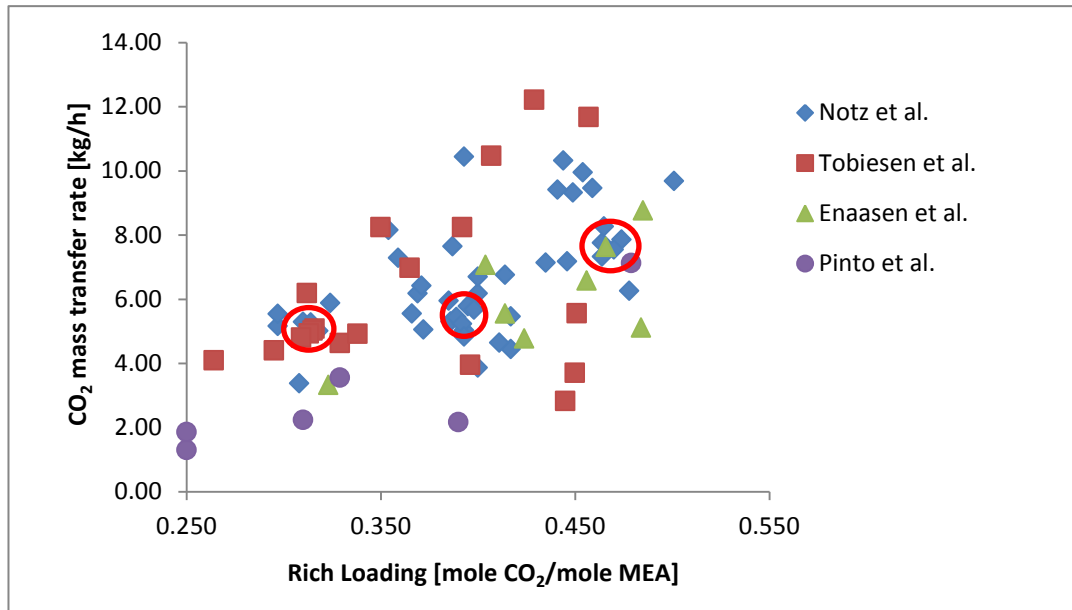
Figure 9-2 Plot showing the CO_2 mass transfer rate in the desorber as a function of rich solvent loading for all four campaigns simulated.

If one compares the reboiler duty for runs with equal CO_2 mass transfer rate and rich loading, indications of consistency between the campaigns can be found. It should be noted that since each of the pilots is designed for certain solvent flows, some of the compared runs here might be performed in nonoptimal liquid flow rates which influence the desorber performance. However, this approach of comparing runs with similar reboiler duties, similar CO_2 mass transfer rates and rich loading can give an indication of whether the runs are consistent with each other. Three areas, marked in red in the figure above, are examined. The areas are numbered from left to right and the results are listed and more closely examined in Appendix B, section B5. It could be seen that the reboiler duties for the individual points in the same areas are similar, thus indicating consistency in and between the campaigns.

In addition, a plot of the reboiler duty/stripped CO_2 (in MJ/kgCO_2) as a function of the rich loading was made. Also here it is shown that all the campaigns follow the same trend. The plot can be seen in Figure 9-3.

112
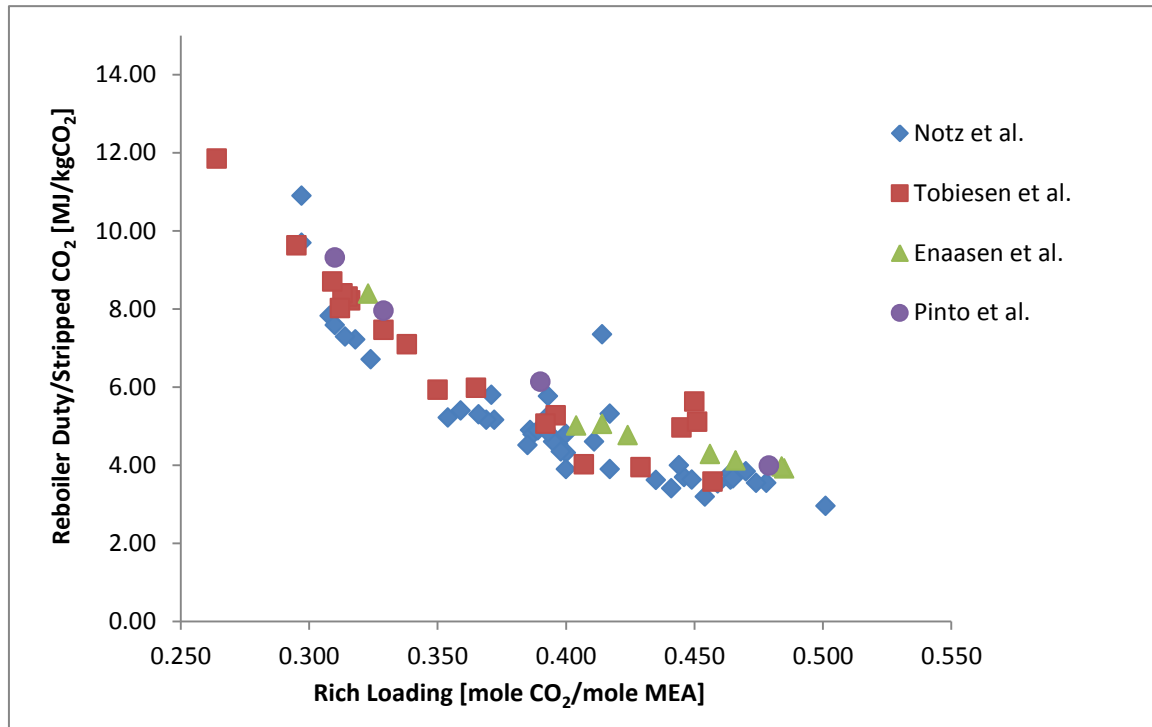
Figure 9-3 Plot showing the reboiler duty/stripped in the desorber as a function of the rich solvent loading for all four campaigns simulated.

As can be seen from the figure, one point from Notz et al. and three points from Tobiesen et al. deviate slightly from the trend. The three points from Tobiesen et al. are run 13, 15 and 16, which also deviated from the trend in the plot of CO_2 mass transfer rate as a function of the rich loading. The point from the Notz et al. campaign that deviates most from the trend is run 16. This point has good agreement between the simulated and experimental desorption rate, with 2.95% over-prediction in the simulation. Nothing can be found in this experimental run that might explain the deviation from the trend. Nevertheless, this plot also strengthens the assumption about consistency between the campaigns.

In an enlargement on the investigation into trends in the desorber simulations, the temperature of the rich flow was plotted against rich loading, and the temperature of the lean flow out of the column was plotted against the rich loading. However, these plots did not provide any additional information that could help to explain the poor results of the Notz et al. campaign compared to the three other campaigns. Thus they are not shown here, but can be found in Appendix B, section B6. The same applies to plots with the deviation in the CO_2 desorption rate between simulated and experimental values on the y-axis and lean loading or delta loading (the difference between the rich and the lean loading) on the x-axis. In addition, an attempt was made to find a correlation between the reboiler duty and the rich and lean

113

loading. In theory, cases with low rich loading require more steam and thus a higher reboiler duty to achieve the same CO_2 desorption rate. This seemed to be the case also during simulations. However, since this also depends on the temperature of the inlet stream, as well as the size of the stream, it is not easy to show this in a figure. As mentioned above, the simulation results can also be heavily influenced if the heat loss is not properly accounted for in the Aspen Plus simulations.

Nevertheless, it is somewhat strange that none of the correlations examined and discussed can explain or indicate why the simulation of the Notz et al. campaign stands out as being less reliable than the three other campaigns from the desorber simulations. Thus, this may be due to uncertainties or mistakes in the reported measurements. However, it is not possible to conclude on this matter.

10 Evaluation of the simulation model

In the course of work on this Master Thesis, an Aspen Plus simulation model was tested on five different absorber pilot campaigns and four different desorber pilot campaigns, all using 30wt% MEA for CO_2 capture. As a basis for the simulation model an Aspen Plus template, "ENRTL-RK_Rate_based_MEA_Model", was used without any changes in the physicochemical properties package.

In the absorber simulations, the Tobiesen et al. campaign (2007) was used to fit the simulation model. In the simulation of this campaign, experimental data from 20 runs were used. The best option was found using the modified kinetic model from Aboundheir et al. (2003) for the MEA carbamate reaction. The four other campaigns were used to validate this modified simulation model, and the simulation results were deemed satisfactory. This is despite the fact the experimental data are taken from three different pilot campaigns, and with two different packing materials. The validation included experimental data from 6 runs performed by Pinto et al., 8 runs performed by Enaasen et al., 23 runs performed by Sønderby et al., and 46 runs performed by Notz et al. (one of the runs did not converge). The overall average deviation and absolute average deviation, including all campaigns, was found to be 9.8% and 8.5% respectively. The simulation results were fairly good for all campaigns, indicating that the campaigns are consistent with each other. The performance of the simulation model was independent of the packing material, and it also predicted the temperature profiles and CO_2 profiles quite accurately, mostly within a 2 °C deviation for the temperature profiles. Furthermore, no dependency was found between the performance of the simulation model and the simulation conditions including temperatures, flow rates, solvent loading and CO_2 concentration.

With regard to the desorber simulations, the performance of the simulation model was satisfactory, especially for the Tobiesen et al., Enaasen et al. and Pinto et al. campaigns. In all 19 runs from Tobiesen et al., 45 runs from Notz et al. (2 runs did not converge), 8 runs from Enaasen et al., and 6 runs from Pinto et al. were simulated and compared with experimental data. Three different simulation models were tested, and it was found that the performance of the original Aspen Plus model was better than the modified model using kinetic parameters from Aboundheir et al. (2003). However, since the reactions in the desorber column occur

rapidly, it was found that an equilibrium model gave approximately the same results as the original Aspen Plus model, as shown for the Tobiesen et al. campaign. Nevertheless, the overall average deviation and absolute average deviation including all four campaigns was found to be 16.1% and 14.5% respectively using the original Aspen Plus model. No clear trends or explanations of the poor results obtained in the Notz et al. simulations could be found, even though several factors were examined. Additionally, the accurate predictions of the temperature profiles and CO_2 profiles were also true for the desorber simulations. Overall, the temperature profiles were mostly within a 2 °C deviation from experimental measurements.

Overall, Aspen Plus predicted the experimental data well, both for the absorber and desorber campaigns. However, it is possible to define different reactions set for the absorber and desorber in Aspen Plus, and thus different kinetic reactions and parameters. As a recommendation for future work, more studies of the desorber performance should be carried out, as well as finding the right kinetic parameters for the reaction set, or alternatively defining new or other reactions, or running the desorber without kinetic reactions at all. An attempt should also be made to connect the absorber and desorber to test the performance of the simulation model as a whole. Additionally, the robustness of the model can be tested using campaigns from different pilots with different packing materials, column diameters and packing heights.

11 References

1. Environmental Protection Agency, U.S. *Climate Students*. 25.04.2015].
2. Change, I.P.o.C., *Climate Change 2014 Sunthesis Report Summert for Policymakers*. 2014: www.ipcc.ch.
3. National Oceanic & Atmospheric Administration, N. *Collected data from the Mauna Loa Observatory, Hawaii*.
4. Administration, U.S.E.I. *Independent Statistics & Analysis*. 17.04.2015].
5. Institute, G.C. *Global CCS*. 19.04.2015].
6. Herzog, H., Meldon, J. , Hatton, A. *Advanced Post-Combustion CO_2 Capture*. 2009.
7. Organisation, Z.E.R. *Boundary Dam integrated CCS project* [cited 2015 15.05].
8. Government, T.N. *Norge som foregangsland for CO2 fangst*. 2006 18.04.2015].
9. Technology Sentre Mongstad, W.V.S. *Technology Centre Mongstad*.
10. Lie, Ø. *Aker Solustions: CO_2-fangsten hos Norcem har gått "over all forventning"*. 2014.
11. Rao, A.B.R., E. S., *A technical, economic, and environmental assessment of amine-based CO_2 capture technology for power plant greenhouse gas control.* Environmental Science and Technology, 2002. **20**: p. 4467-4475.
12. Tobiesen, F.A.S., H. F. and O. Juliussen, *Experimental validation of a rigorous desorber model for CO_2 post-combustion capture.* Chemical Engineering Science, 2008. **63**: p. 2641-2656.
13. van Nierop, E.A.H., S.; House, K. Z.; Aziz, M. J., *Effect of absorption enthalpy on temperature-swing CO_2 separation process performance.* Energy Procedia, 2011. **4**: p. 1783-1790.
14. Sanggie, F.W., *Process modeling and comparison study of acid gas removal unit by using different aqueous amines* in *Chemical Engineering*. 2011, Universiti Malaysia Pahang.
15. Kvamsdahl, H.M. and G.T. Rochelle, *Effects of the Temperature Bulge in CO_2 Absorption from Flue Gas by Aqueous Monoethanolamine.* Industrial & Engineering Chemistry Research, 2008. **47**: p. 867-875.
16. Alie, F.C., *CO_2 Capture With MEA: Integrating the Absorption Process and Steam Cycle of an Existing Coal-Fired Power Plant*, in *Chemcical Engineering*. 2004, University of Waterloo.
17. Soave, G.F., J. A., *Saving energy in distillation towers by feed splitting.* Applied Thermal Engineering, 2002. **22**: p. 889-896.
18. Stec, M.T., A.; Wieclaw-Solny, L.; Krótki, A.; Sciazko, M.; Tokarski, S., *Pilot plant results for advanced CO_2 capture process using amine scrubbing at the Jaworno II Power Plant in Poland.* Fuel, 2015. **151**: p. 50-56.
19. Tobiesen, F.A., H.F. Svendsen, and O. Juliussen, *Experimental validation of a rigorous absorber model for CO_2 postcombustion capture.* AlChE, 2007. **53**: p. 846-865.
20. Pinto, D.D.D., et al., *CO_2 post combustion capture with a phase change solvent. Pilot plant campaign.* International Journal of Greenhouse Gas Control, 2014. **31**: p. 153-164.
21. Sønderby, T.L.C., K. B.; Fosbøl, P. L.; Kiørboe, L. G.; von Solms, N. , *A new pilot absorber for CO_2 capture from flue gases: Measuring and modelling capture with MEA solution.* International Journal of Greenhouse Gas Control, 2013. **12**: p. 181-192.

22. Notz, R.M., H. P.; Hasse, H., *Post combustion CO_2 capture by reactive absorption: Pilot plant description and results of systematic studies with MEA.* International Journal of Greenhouse Gas Control, 2012. **6**: p. 84-112.
23. Razi, N.S., H. F.; Bolland, O., *Validation of mass transfer correlations for CO_2 absorption with MEA using pilot plant data.* International Journal of Greenhouse Gas Control, 2013. **19**: p. 478-491.
24. Liu, K.F., R. A.; Johnson, D.; Richburg, L.; Hogston, B.; Remias, J. E.; Neathery, J. K., *Comparison of solvent performance for CO_2 capture from coal-derived flue gas: A pilot scale study.* Chemical Engineering Research and Design, 2013. **91**: p. 963-969.
25. Shim, J.J., K. R.; Lee, I. Y.; Lee, J. H.; Kwak, N., *A study of CO_2 capture pilot plant by amine absorption.* Energy, 2012. **47**: p. 41-46.
26. Mejdell, T., et al., *Novel full height pilot plant for solvent development and model validation.* Energy Procedia, 2011. **4**: p. 1753-1760.
27. Tobiesen, F.A., *Modelling and Experimental study of Carbon Dioxide Absorption and Desoprtion*, in *Department of Chemical Engineering*. 2006, Norwegian University of Science and Technology.
28. Aspentech. *Rate-Based Distillation Column Modeling*. 1994-2015.
29. Chen, C. and Y. Song, *Symmetric Electrolyte Nonrandom Two-Liquid Activity Coefficient Model.* Industrial & Engineering Chemistry Research, 2009. **48**.
30. Adewumi, M. *Redlich-Kwong EOS (1949)*. 17.04.2015].
31. Zumdahl, S.a.S., *Chemistry*. Vol. Fifth edition. 2000: Boston, MA: Houghton Miffin Company.
32. Aspen Techonology, I., *Aspen Physical Property System, Physical Property Methods and Models 11.1*, Aspentech, Editor. 2001: www.aspentech.com.
33. Chen, C.T., D.; Bhat, C., *A Rate-Based Process Modeling Study of CO_2 Capture with Aqueous Amine Solutions unig aspenOne Process Engineering ^{TM}*, in *Clearwater Coal Conference*, aspentech, Editor. 2008: Clearwater Florida.
34. Jou, F.M., A. E.; Otto, F. D., *The solubility of CO_2 in a 30 mass percent monoethanolamine solution.* The CanadianJournal of Chemical Engineering, 1995. **73**: p. 140-147.
35. Aboundheir, A.T., P.; Chakma, A.; Idem, R., *Kinetics of the reactive absorption of carbon dioxide in high CO_2-loaded concentrated aqueous monoethalmine solutions.* Chemical Engineering Science, 2003. **58**: p. 5195-5210.

Appendix A: Absorber Simulation Results

In Appendix A, some simulation results, including loadings and absorption rates, from the five absorber campaigns are listed, as well as some trend plots including the runs from all campaigns. The results from the Tobiesen et al. campaign are given in section A1. The results from the Pinto et al. campaign are given in section A2. The results from the Enaasen et al. campaign are given in section A3. The results from the Sønderby et al. campaign are given in section A4. And the results from the Notz et al campaign are given in section A5. At last, some trend plots including the runs from all campaigns are given in section A6. Additional information for each campaign can be provided by request to hanna.knuutila@chemeng.ntnu.no.

A1: Tobiesen et al. Campaign (2007)

A1.1 Original Kinetic Model

Simulation results from the first simulation round using the original Aspen Plus model are shown in Table A.1 below. The original kinetic model defined in Aspen Plus for the MEA carbamate reaction was:

$$k = 3.02 \times 10^{14}$$

$$n = 0$$

$$E = 17.7404 \ MBtu/lbmol$$

$$[Ci]basis: Mole \ gamma$$

Table A.1 Overview of some simulation results from the Tobiesen et al. campaign. The solvent lean loading is listed as well as vol% CO_2 in the flue gas. Experimental and simulated values for rich loading and CO_2 absorption rate are also compared.

Run	Lean Loading Exp	Rich Loading Exp	Rich Loading Sim	Vol% CO_2 Fluegas (dry)	Exp [kg/h]	Sim [kg/h]	%dev Abs CO_2, x_i	N_{CO2abs},sim/ N_{co2abs},exp
1	0.218	0.284	0.276	1.65	3.27	3.02	-7.62	0.88
2	0.220	0.275	0.276	1.57	2.93	2.88	-1.75	1.01
3	0.215	0.272	0.270	1.56	2.98	2.88	-3.52	0.97
4	0.217	0.276	0.273	1.57	3.04	2.90	-4.64	0.95
5	0.216	0.274	0.291	2.04	3.24	3.84	18.44	1.28
6	0.183	0.267	0.276	2.41	4.43	4.79	8.17	1.10
7	0.284	0.345	0.351	3.03	4.66	5.20	11.67	1.16
8	0.241	0.296	0.298	2.41	4.22	4.45	5.45	1.08
9	0.233	0.299	0.312	3.19	5.01	6.09	21.65	1.24
10	0.217	0.333	0.351	2.81	4.66	5.17	10.91	1.13
11	0.219	0.309	0.323	2.16	3.64	4.01	10.14	1.14
12	0.307	0.401	0.418	2.96	3.79	4.31	13.67	1.16
13	0.297	0.390	0.421	6.65	7.43	9.52	28.19	1.28
14	0.370	0.433	0.465	4.34	3.02	3.69	22.15	1.26
15	0.357	0.435	0.462	12.12	9.25	12.15	31.32	1.28
16	0.402	0.447	0.474	9.44	3.88	5.72	47.51	1.52
17	0.409	0.451	0.475	15.33	4.94	7.57	53.20	1.49
18	0.346	0.429	0.456	12.50	10.70	12.60	17.77	1.25
19	0.347	0.400	0.433	8.35	7.05	9.87	39.97	1.52
20	0.292	0.339	0.357	4.54	5.75	7.44	29.32	1.28

A1.2 Changing the Activation Energy

During the first modification of the kinetic model, the activation energy was varied by a trial-and-error-approach. The best option was found when E=18.4 Mbtu/lbmol. Simulation results using this kinetic model can be found in Table A.2 below.

Table A.2 Overview of some simulation results from the Tobiesen et al. campaign. The solvent lean loading is listed as well as vol% CO_2 in the flue gas. Experimental and simulated values for rich loading and absorbed CO_2 are also compared.

Run	Lean Loading Exp	Rich Loading		Vol% CO_2 Fluegas (dry)	Absorbed CO_2		%dev Abs CO_2, x_i	N_{CO2abs},sim/ N_{co2abs},exp
		Exp	Sim		Exp [kg/h]	Sim [kg/h]		
1	0.218	0.284	0.268	1.65	3.27	2.59	-20.87	0.75
2	0.220	0.275	0.268	1.57	2.93	2.47	-15.77	0.86
3	0.215	0.272	0.262	1.56	2.98	2.46	-17.36	0.83
4	0.217	0.276	0.265	1.57	3.04	2.49	-18.21	0.81
5	0.216	0.274	0.281	2.04	3.24	3.37	4.04	1.12
6	0.183	0.267	0.266	2.41	4.43	4.28	-3.39	0.98
7	0.284	0.345	0.341	3.03	4.66	4.40	-5.62	0.98
8	0.241	0.296	0.291	2.41	4.22	3.86	-8.48	0.93
9	0.233	0.299	0.303	3.19	5.01	5.35	6.74	1.08
10	0.217	0.333	0.334	2.81	4.66	4.52	-2.98	0.99
11	0.219	0.309	0.309	2.16	3.64	3.50	-3.87	0.99
12	0.307	0.401	0.399	2.96	3.79	3.57	-5.91	0.96
13	0.297	0.390	0.401	6.65	7.43	8.00	7.73	1.07
14	0.370	0.433	0.449	4.34	3.02	3.07	1.82	1.05
15	0.357	0.435	0.447	12.12	9.25	10.41	12.59	1.10
16	0.402	0.447	0.462	9.44	3.88	4.76	22.59	1.26
17	0.409	0.451	0.464	15.33	4.94	6.37	28.95	1.25
18	0.346	0.429	0.440	12.50	10.70	10.84	1.34	1.07
19	0.347	0.400	0.417	8.35	7.05	8.01	13.56	1.23
20	0.292	0.339	0.346	4.54	5.75	6.26	8.83	1.07

A1.3 Using the Kinetic Constant from Aboundheir et al.

Since the modification of the original Aspen Plus model did not give satisfactory results, the kinetic constant for the MEA carbamate reaction from Aboundheir et al. was tested. The new kinetic model had the following parameters:

$$k = 4.61 \times 10^9$$

$$n = 0$$

$$E = \frac{4412 * 8.314}{1000} = 36.7 kJ/mole$$

$$[Ci]basis: Molarity$$

The simulation results are shown in Table A.3.

Table A.3 Overview of some simulation results from the Tobiesen et al. campaign. The solvent lean loading is listed as well as vol% CO_2 in the flue gas. Experimental and simulated values for rich loading and absorbed CO_2 are also compared.

| Run | Lean Loading Exp | Rich Loading | | Vol% CO_2 Fluegas (dry) | Absorbed CO_2 | | | |
		Exp	Sim		Exp [kg/h]	Sim [kg/h]	%dev Abs CO_2, x_i	N_{CO2abs},sim/ N_{co2abs},exp
1	0.218	0.284	0.265	1.65	3.27	2.46	-24.65	0.72
2	0.220	0.275	0.266	1.57	2.93	2.39	-18.41	0.84
3	0.215	0.272	0.260	1.56	2.98	2.98	-21.32	0.79
4	0.217	0.276	0.262	1.57	3.04	3.04	-22.39	0.77
5	0.216	0.274	0.274	2.04	3.24	3.24	-7.06	1.00
6	0.183	0.267	0.257	2.41	4.43	4.43	-13.19	0.88
7	0.284	0.345	0.335	3.03	4.66	4.66	-15.62	0.88
8	0.241	0.296	0.286	2.41	4.22	4.22	-17.11	0.85
9	0.233	0.299	0.292	3.19	5.01	5.01	-9.48	0.92
10	0.217	0.333	0.322	2.81	4.66	4.66	-12.72	0.89
11	0.219	0.309	0.300	2.16	3.64	3.64	-13.40	0.89
12	0.307	0.401	0.391	2.96	3.79	3.79	-14.00	0.88
13	0.297	0.390	0.381	6.65	7.43	7.43	-13.24	0.86
14	0.370	0.433	0.444	4.34	3.02	3.02	-4.36	0.99
15	0.357	0.435	0.435	12.12	9.25	9.25	-3.17	0.95
16	0.402	0.447	0.453	9.44	3.88	3.88	5.20	1.08
17	0.409	0.451	0.454	15.33	4.94	4.94	4.03	1.01
18	0.346	0.429	0.424	12.50	10.70	10.70	-16.29	0.88
19	0.347	0.400	0.402	8.35	7.05	7.05	-10.62	0.97
20	0.292	0.339	0.336	4.54	5.75	5.75	-12.45	0.86

A1.4 Changing the Activation Energy in the Aboundheir et al. Model

Also during the modification of the kinetic model from Aboundheir et al, the activation energy was varied by a trial-and-error-approach. The best option was found when E=36.0 kJ/mol. Simulation results using this kinetic model can be found in Table A.4 below.

Table A.4 Overview of some simulation results from the Tobiesen et al. campaign. The solvent lean loading is listed as well as vol% CO_2 in the flue gas. Experimental and simulated values for rich loading and absorbed CO_2 are also compared.

Run	Lean Loading Exp	Rich Loading Exp	Rich Loading Sim	Vol% CO_2 Fluegas (dry)	Absorbed CO_2 Exp [kg/h]	Absorbed CO_2 Sim [kg/h]	%dev Abs CO_2, x_i	N_{CO2abs},sim/ N_{co2abs},exp
1	0.218	0.284	0.269	1.65	3.27	2.66	-18.51	0.78
2	0.220	0.275	0.270	1.57	2.93	2.58	-11.93	0.90
3	0.215	0.272	0.264	1.56	2.98	2.54	-14.90	0.86
4	0.217	0.276	0.266	1.57	3.04	2.55	-16.07	0.83
5	0.216	0.274	0.279	2.04	3.24	3.25	0.28	1.08
6	0.183	0.267	0.263	2.41	4.43	4.11	-7.24	0.94
7	0.284	0.345	0.340	3.03	4.66	4.31	-7.43	0.96
8	0.241	0.296	0.290	2.41	4.22	3.79	-10.27	0.92
9	0.233	0.299	0.297	3.19	5.01	4.94	-1.46	1.00
10	0.217	0.333	0.330	2.81	4.66	4.38	-5.93	0.96
11	0.219	0.309	0.307	2.16	3.64	3.40	-6.49	0.97
12	0.307	0.401	0.400	2.96	3.79	3.60	-4.91	0.97
13	0.297	0.390	0.391	6.65	7.43	7.19	-3.22	0.97
14	0.370	0.433	0.453	4.34	3.02	3.20	6.07	1.09
15	0.357	0.435	0.442	12.12	9.25	9.84	6.39	1.04
16	0.402	0.447	0.460	9.44	3.88	4.62	18.96	1.23
17	0.409	0.451	0.460	15.33	4.94	5.83	17.93	1.15
18	0.346	0.429	0.432	12.50	10.70	9.90	-7.51	0.98
19	0.347	0.400	0.409	8.35	7.05	7.16	1.58	1.10
20	0.292	0.339	0.341	4.54	5.75	5.63	-2.06	0.97

A2: Pinto et al. Campaign (2014)

Some results from simulating the Pinto et al. campaign are shown in Table A.5 below.

Table A.5 Overview of some simulation results from the Pinto et al. campaign. The solvent lean loading is listed as well as vol% CO_2 in the flue gas. Experimental and simulated values for rich loading and absorbed CO_2 are also compared.

Run	Lean Loading Exp	Rich Loading Exp	Sim	Vol% CO_2 Fluegas (dry)	Absorbed CO_2 Exp [kg/h]	Sim [kg/h]	%dev Abs CO_2, x_i	N_{CO2abs},sim/ N_{co2abs},exp
1	0.350	0.390	0.398	1.66	2.12	1.98	-6.56	0.94
2	0.308	0.479	0.485	12.14	7.65	7.31	-4.41	0.95
3	0.230	0.250	0.256	0.85	1.02	1.27	25.50	1.26
4	0.210	0.250	0.256	1.24	1.95	1.87	-3.78	0.97
5	0.260	0.310	0.315	1.58	2.11	2.30	9.10	1.09
6	0.247	0.329	0.336	2.52	3.71	3.69	-0.33	1.00

A3: Enaasen et al. Campaign (2015)

Some results from simulating the Enaasen et al. campaign can be found in Table A.6.

Table A.6 Overview of some simulation results from the Enaasen et al. campaign. The solvent lean loading is listed as well as vol% CO_2 in the flue gas. Experimental and simulated values for rich loading and absorbed CO_2 are also compared.

Run	Lean Loading Exp	Rich Loading Exp	Rich Loading Sim	Vol% CO_2 Fluegas (dry)	Absorbed CO_2 Exp [kg/h]	Absorbed CO_2 Sim [kg/h]	%dev Abs CO_2, x_i	$N_{CO2abs},sim/N_{co2abs},exp$
1	0.290	0.424	0.425	3.52	4.57	4.57	-0.06	1.00
2	0.270	0.466	0.469	6.77	7.35	7.00	-4.80	0.95
3	0.210	0.485	0.474	7.41	8.78	8.30	-5.50	0.95
4	0.250	0.414	0.434	3.57	5.71	5.36	-6.08	0.94
5	0.270	0.404	0.406	3.90	6.68	6.68	0.01	1.00
6	0.340	0.484	0.485	5.41	4.68	5.20	11.10	1.11
7	0.320	0.456	0.457	4.57	6.28	6.44	2.56	1.05
8	0.260	0.323	0.316	1.55	3.01	2.73	-9.14	0.91

A4: Sønderby et al. Campaign (2013)

Some results from simulating the Sønderby et al. campaign can be found in Table A.7.

Table A.7 Overview of some simulation results from the Sønderby et al. campaign. The solvent lean loading is listed as well as vol% CO_2 in the flue gas. Experimental and simulated values for rich loading and absorbed CO_2 are also compared.

Run	Lean Loading Exp	Rich Loading Exp	Sim	Vol% CO_2 Fluegas (dry)	Exp [kg/h]	Sim [kg/h]	%dev Abs CO_2, x_i	N_{CO2abs},sim/ N_{co2abs},exp
1	0.112	0.356	0.318	9.30	6.72	5.66	-15.78	0.84
2	0.112	0.286	0.255	9.30	6.85	5.63	-17.77	0.82
3	0.112	0.214	0.214	9.50	5.61	5.62	0.23	1.00
4	0.112	0.190	0.184	9.50	6.14	5.63	-8.23	0.92
5	0.112	0.165	0.163	10.50	6.19	5.97	-3.55	0.96
6	0.112	0.325	0.334	9.50	5.87	6.12	4.40	1.04
7	0.112	0.275	0.266	9.40	6.41	6.06	-5.53	0.94
8	0.112	0.211	0.223	9.70	5.45	6.13	12.48	1.12
9	0.112	0.187	0.187	9.40	5.90	5.88	-0.39	1.00
10	0.112	0.187	0.189	9.80	5.90	6.02	2.07	1.02
11	0.112	0.325	0.331	9.50	5.87	6.02	2.61	1.03
12	0.112	0.288	0.270	9.40	6.92	6.24	-9.95	0.90
13	0.112	0.217	0.233	10.10	5.78	6.65	14.99	1.15
14	0.112	0.212	0.224	9.60	5.50	6.15	11.71	1.12
15	0.112	0.184	0.193	10.10	5.67	6.37	12.43	1.12
16	0.112	0.149	0.164	10.40	4.42	6.15	39.19	1.39
17	0.112	0.291	0.323	9.20	4.93	5.80	17.72	1.18
18	0.112	0.206	0.238	10.90	5.17	6.91	33.69	1.34
19	0.112	0.165	0.164	10.20	6.33	6.15	-2.84	0.97
20	0.112	0.165	0.162	9.70	6.33	5.94	-6.14	0.94
21	0.254	0.338	0.354	9.60	4.61	5.49	19.17	1.19
22	0.271	0.364	0.373	9.90	5.09	5.59	9.67	1.10
23	0.300	0.387	0.403	10.20	4.76	5.66	18.81	1.19

A5: Notz et al. Campaign (2012)

Some results from the simulation of the Notz et al. campaign are shown in Table A.8.

Table A.8 Overview of some simulation results from the Notz et al. campaign. The solvent lean loading is listed as well as vol% CO_2 in the flue gas. Experimental and simulated values for rich loading and absorbed CO_2 are also compared.

Run	Lean Loading Exp	Rich Loading		Vol% CO_2 Fluegas (dry)	Absorbed CO_2		%dev Abs CO_2, x_i	N_{CO2abs},sim/ N_{co2abs},exp
		Exp	Sim		Exp [kg/h]	Sim [kg/h]		
1	0.265	0.386	0.394	5.44	4.65	5.26	13.21	1.13
2	0.308	0.464	0.479	10.83	6.11	6.92	13.29	1.13
3	0.230	0.308	0.319	3.53	3.35	3.65	9.02	1.09
4	0.268	0.397	0.400	5.64	4.83	5.40	11.72	1.12
5	0.306	0.446	0.464	8.42	5.65	6.41	13.43	1.13
6	0.317	0.464	0.486	13.22	6.24	6.84	9.62	1.10
7	0.356	0.478	0.483	10.92	4.82	5.10	5.79	1.06
8	0.228	0.444	0.464	10.78	9.06	9.71	7.14	1.07
9	0.147	0.393	0.415	10.90	10.56	11.21	6.15	1.06
10	0.299	0.402	0.421	5.58	4.34	4.94	13.89	1.14
11	0.280	0.396	0.410	5.69	4.59	5.31	15.60	1.16
12	0.256	0.372	0.391	5.63	4.76	5.53	16.13	1.16
13	0.287	0.400	0.412	5.26	3.53	3.92	10.94	1.11
14	0.253	0.369	0.377	5.31	5.41	6.04	11.65	1.12
15	0.241	0.359	0.364	5.37	6.34	7.04	10.98	1.11
16	*Error*	*Error*	*Error*	*Error*	*Error*	*Error*	*Error*	*Error*
17	0.166	0.371	0.403	5.42	6.38	7.41	16.20	1.16
18	0.215	0.387	0.391	5.48	6.43	7.27	13.13	1.13
19	0.247	0.354	0.346	5.47	6.43	7.12	10.71	1.11
20	0.261	0.395	0.392	5.47	4.71	5.34	13.40	1.13
21	0.270	0.400	0.394	5.39	4.64	5.06	9.11	1.09
22	0.263	0.389	0.400	5.80	4.80	5.61	16.84	1.17
23	0.274	0.393	0.410	5.95	4.73	5.56	17.62	1.18
24	0.251	0.392	0.382	5.46	4.57	5.38	17.63	1.18
25	0.166	0.435	0.305	5.44	4.19	5.80	38.52	1.39
26	0.288	0.474	0.477	10.83	5.89	7.70	30.67	1.31
27	0.169	0.501	0.433	10.86	5.03	10.98	118.22	2.18
28	0.266	0.470	0.483	10.82	6.63	6.65	0.23	1.00
29	0.306	0.465	0.480	10.74	6.64	7.06	6.27	1.06

30	0.316	0.459	0.467	10.45	6.67	7.66	14.86	1.15
31	0.338	0.454	0.467	10.49	6.71	7.12	6.18	1.06
32	0.335	0.449	0.459	10.27	6.61	7.51	13.57	1.14
33	0.360	0.441	0.459	10.34	6.60	6.97	5.57	1.06
34	0.146	0.417	0.464	5.32	4.44	4.99	12.35	1.12
35	0.208	0.411	0.456	1.25	4.55	5.12	12.54	1.13
36	0.252	0.393	0.418	5.28	4.46	5.11	14.48	1.14
37	0.296	0.398	0.413	5.31	4.41	4.77	8.14	1.08
38	0.308	0.385	0.403	5.41	4.50	4.83	7.33	1.07
39	0.319	0.400	0.404	5.36	4.48	4.73	5.53	1.06
40	0.111	0.297	0.324	5.23	5.27	5.62	6.55	1.07
41	0.130	0.297	0.308	5.24	5.27	5.60	6.33	1.06
42	0.190	0.310	0.325	5.41	5.26	5.61	6.57	1.07
43	0.200	0.318	0.331	5.22	4.98	5.42	8.89	1.09
44	0.209	0.314	0.314	5.25	5.01	5.41	8.05	1.08
45	0.219	0.324	0.319	5.43	5.18	5.61	8.23	1.08
46	0.318	0.417	0.429	5.43	4.01	4.49	11.93	1.12
47	0.255	0.366	0.383	5.43	4.86	5.25	8.05	1.08

X

A6: Trend Plots

Several plots were made to investigate whether any overall trends could be found in the simulations of the five campaigns. In the first plots seen in Figure A.1, the ratio of the CO_2 absorption rates between simulated and experimental data is plotted against lean solvent loading, rich solvent loading and the delta loading (difference between rich and lean solvent loading).
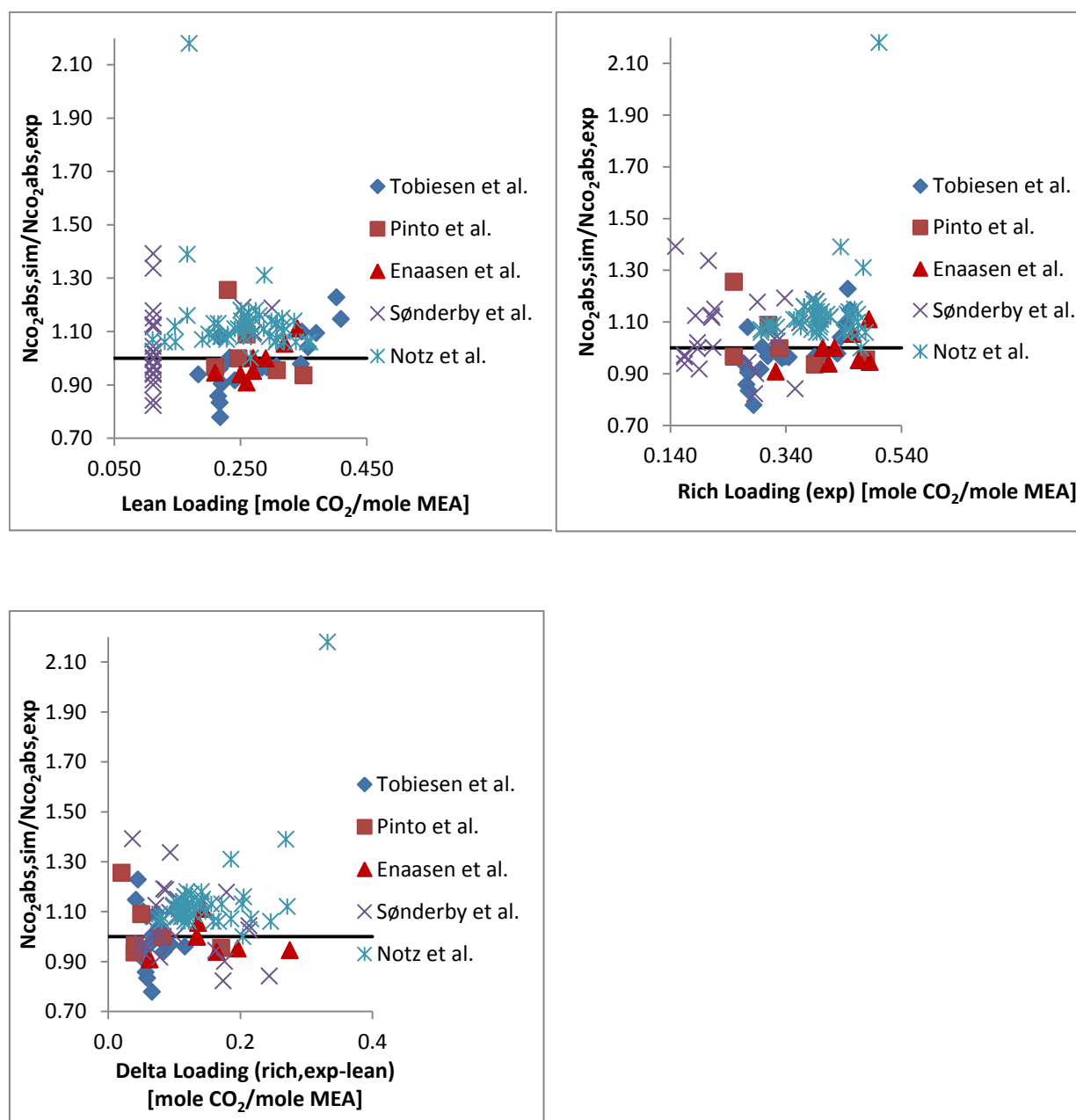
Figure A.1 The ratio of the CO_2 absorption rates between simulations and experimental data is plotted against lean solvent loading, rich solvent loading and the delta loading (difference between rich and lean solvent loading) for the five absorber campaigns simulated.

The ratio of the CO_2 absorption rates are also plotted against the inlet temperatures of the stream as well as the temperature of the gas stream leaving the column. These plots can be seen in Figure A.2.
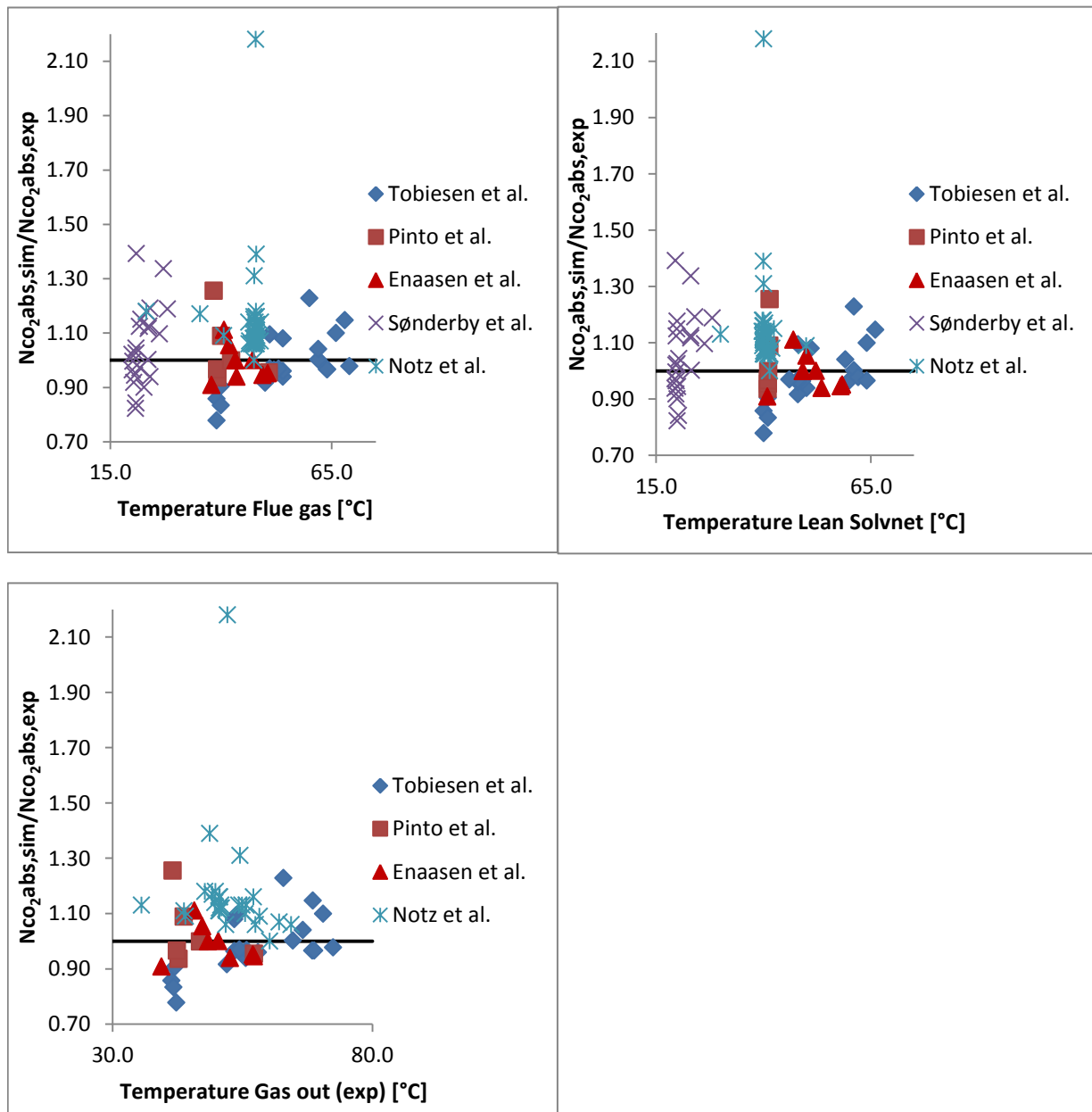
Figure A.2 The ratio of the CO_2 absorption rates between simulations and experimental data is plotted against the inlet temperature of the flue gas, lean solvent and the temperature of the gas leaving the column for the five absorber campaigns simulated.

Additionally the ratio of the CO_2 absorption rates is plotted against the flue gas flow rate and the lean solvent flow rate, as well as the liquid to gas ratio. These plots can be seen in Figure A.3.
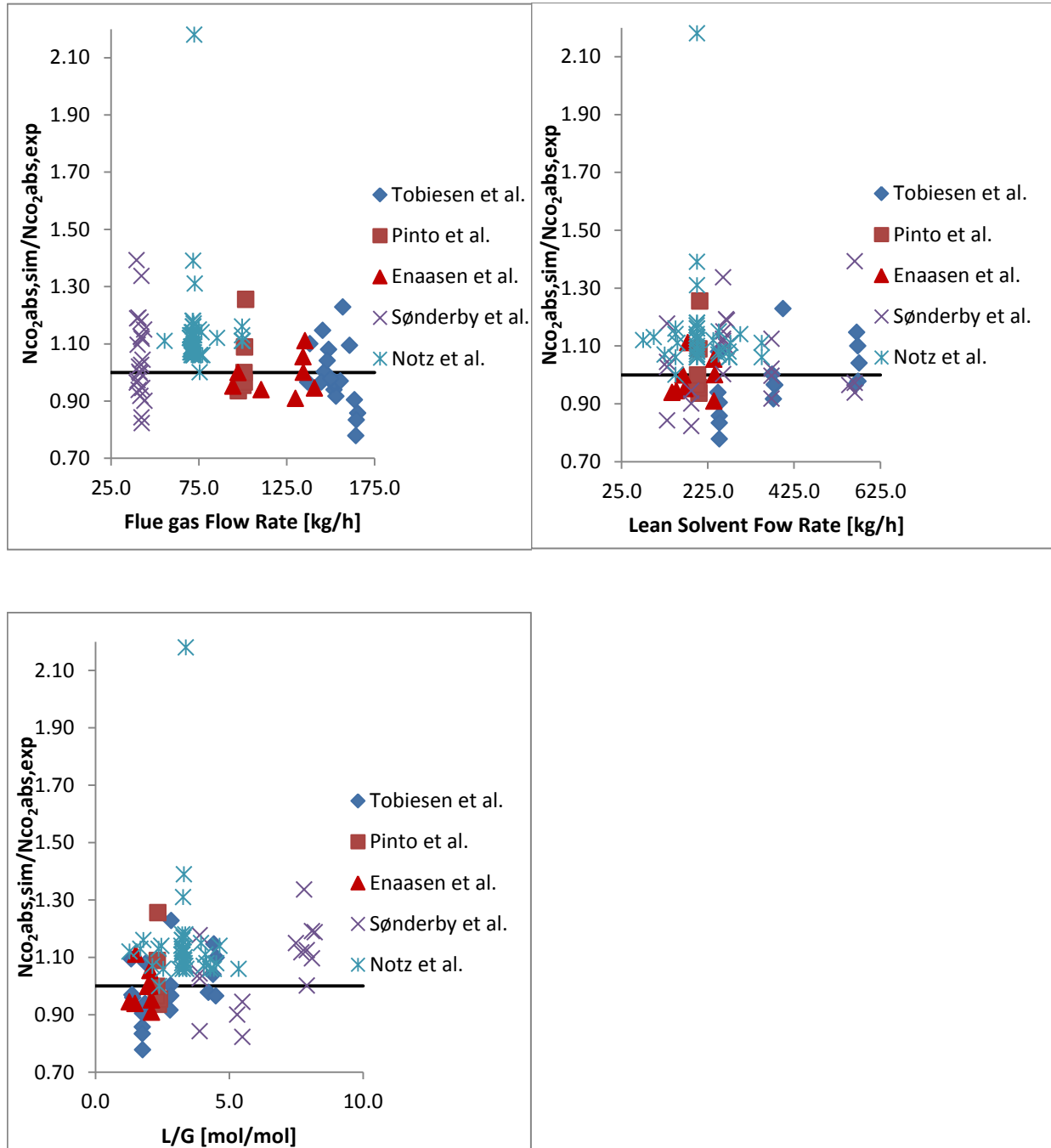
Figure A.3 The ratio of the CO$_2$ absorption rates between simulations and experimental data is plotted against flue gas flow rate, lean solvent flow rate and the liquid to gas ratio for the five absorber campaigns simulated.

At last, the ratio of the CO$_2$ absorption rates was plotted against the vol% of CO$_2$ in the flue gas entering the column. This plot can be seen in Figure A.4.
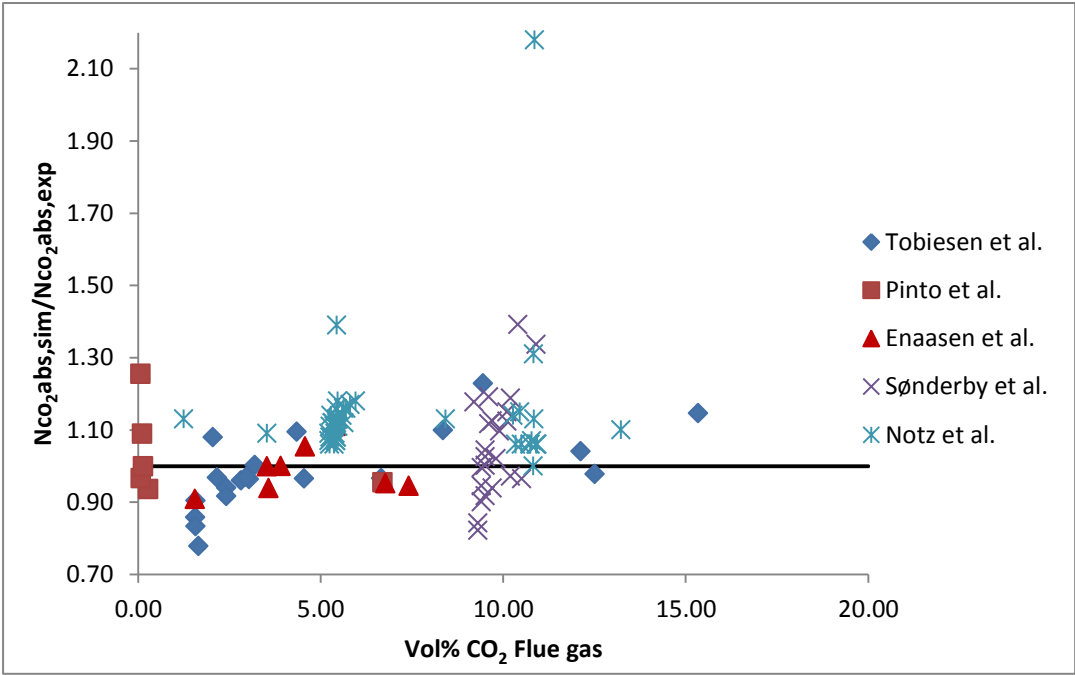
Figure A.4 The ratio of the CO_2 absorption rates between simulations and experimental data is plotted against vol% CO_2 in the flue gas entering the column ratio for the five absorber campaigns simulated.

As can be seen in Figure A.1, Figure A.2, Figure A.3 and Figure A.4, no clear trends are found regarding the performance of the simulation model with respect to loadings, flow rates, temperatures or CO_2 content in the flue gas. Both over-prediction and under-prediction of the CO_2 absorption rate can be seen in all cases, and there are no systematic discrepancies to be detected.

Appendix B: Desorber Simulations

In Appendix B, some simulation results, including loadings and desorption rates, from the four desorber campaigns are listed, as well as some trend plots including the runs from all campaigns. The results from the Tobiesen et al. campaign are given in section B1. The results from the Notz et al. campaign are given in section B2. The results from the Enaasen et al. campaign are given in section B3. And the results from the Pinto et al. campaign are given in section B4. At last, the investigation of the correlation between CO_2 mass transfer, rich solvent loading and reboiler duty are given in section B5, and some trend plots are given in section B6. Additional information for each campaign can be provided by request to hanna.knuutila@chemeng.ntnu.no

B1: Tobiesen et al. Campaign (2008)

B1.1 First Simulation Round

In the first simulation round for the Tobiesen et al. campaign, the original Aspen Plus model was used. The rich inlet stream is a "Vapor-Liquid" two-phase stream that is specified on a volume flow basis (l/min). The percentage deviation between the simulated and experimental desorption rates for the 19 runs are given in Table B.1. Note that the rich solvent vapor fraction are given by Aspen Plus and not specified by the user. As can be seen, the percentage deviation between simulated and experimental desorption rates tend to increase with increased vapor fraction in the rich solvent. The runs with the largest vapor fraction are marked in green in the table.

Table B.1 Table showing the rich solvent volume flow rate, the percentage deviation between simulated and experimental desorption rates and the vapor fraction of the rich solvent streams for the 19 runs.

Run	Volume Flow Rate, Rich Solvent [l/min]	%dev, Des CO_2, x_i	Vapor Fraction, Rich solvent
1	4.01	-0.46	0
2	4.01	1.18	0
3	4.01	1.71	0
4	4.01	1.12	0
5	4.01	-7.74	0
6	6.00	0.97	0.0025
7	6.00	-3.39	0
8	6.00	0.59	0
9	3.00	-0.84	0
10	3.00	4.19	0
11	3.00	-15.96	0.0037
12	6.00	`-55.97`	`0.0081`
13	3.00	`-10.21`	`0.0011`
14	9.01	`-51.68`	`0.0103`
15	6.00	-5.68	0
16	9.01	-7.74	0.0006
17	9.01	`-61.27`	`0.0118`
18	9.01	`-60.59`	`0.0140`
19	9.01	`-35.36`	`0.0074`

B1.2 Rich Solvent "Vapor-Liquid" Compared to "Liquid-Only"

It was attempted to define the rich solvent entering the desorber column as a one-phase "Liquid-Only" stream instead of a two-phase "Vapor-Liquid" stream based on the paper by Tobiesen et al., and because the deviations between the simulated and experimental desorption rates increased with increased vapor fraction in the rich solvent. The results from these simulations are given in Table B.2. In both cases the original Aspen Plus model is used.

Table B.2 Table showing the deviation in mass transfer between experimental measurements and simulated values for Vapor-Liquid and Liquid-Only rich inlet stream. The table also shows the condensate rate and the CO_2 desorption rate.

Run	%dev, Des CO_2, x_i		Condensate rate/CO_2 top flow [kg/h]	
	Vapor-Liquid	Liquid-Only	Vapor-Liquid	Liquid-Only
1	-0.46	-0.46	9.8/5.1	9.8/5.1
2	1.18	1.18	9.9/5.0	9.9/5.0
3	1.71	1.71	9.8/5.0	9.8/5.0
4	1.12	1.12	10.1/4.8	10.1/4.8
5	-7.74	-7.74	12.8/4.1	12.8/4.1
6	0.97	9.36	9.2/6.3	7.6/6.8
7	-3.39	-3.39	9.7/4.4	9.7/4.4
8	0.59	0.59	11.4/6.2	11.4/6.2
9	-0.84	-0.84	7.6/4.6	7.6/4.6
10	4.19	4.19	7.5/4.9	7.5/4.9
11	-15.96	4.32	4.7/3.1	3.3/3.8
12	-55.97	-8.10	12.5/3.7	7.1/7.7
13	-10.21	-14.30	1.5/2.9	1.4/2.8
14	-51.68	-15.56	10.5/5.6	4.9/9.8
15	-5.68	-5.68	1.7/3.7	1.7/3.7
16	-7.74	-10.75	2.7/5.6	2.6/5.4
17	-61.27	-11.40	14.5/4.6	6.9/10.5
18	-60.59	-6.60	13.0/3.6	7.1/8.6
19	-35.36	1.51	14.4/4.8	10.2/7.5

As can be seen from the table above, the overall deviation between experimental measurements and simulation results for the CO_2 desorption rate is far less when the rich inlet

stream is defined as "Liquid-Only" compared to "Vapor-Liquid". The five runs with the largest decrease are marked in yellow. It is worth noticing that the total outlet flow from the top of the stripper, including the condensate and CO_2 stream, was decreased when the rich inlet flow was defined as "Liquid-Only". This is as expected since it requires more reboiler duty to get the same vapor fraction in the desorber when the flow is only liquid compared to a combination of both vapor and liquid. Thus, a smaller vapor flow from the top of the stripper, including the CO_2 top flow and condensate rate, is expected in the "Liquid-Only" case.

It was tried to understand the results by comparing the rich stream in kg/h and the density of the stream, both of which was given from Aspen Plus for the two cases, "Vapor-Liquid" and "Liquid-Only". These numbers are listed in

Table B.3. As can be seen, several of the flow rates in kg/h and the densities in the "Vapor-Liquid" simulations have to be wrong. It was found that this was caused by how Aspen Plus trades "Vapor-Liquid" flows when they are defined as a volume flow (l/min) compared to a mass flow (kg/h). As a result of this, the simulations were performed one more time, where the rich inlet stream was defined as "Vapor-Liquid" and the mass flows were used as inputs instead of the volume flows.

Table B.3 Table showing the flow rates in kg/h and the density of the rich solvent flow when the stream is defined as "Vapor-Liquid" and "Liquid-Only".

Run	Rich Loading	Flow Richin	Flow Richin "Vapor-Liquid"	Density Richin "Vapor-Liquid"	Flow Richin "Liquid-Only"	Density Richin "Liquid-Only"
	[mole CO_2/ mole MEA]	[l/min]	[kg/h]	[kg/m^3]	[kg/h]	[kg/m^3]
1	0.316	4.01	244.6	1016.4	244.6	1016.6
2	0.315	4.01	244.5	1016.4	244.5	1016.4
3	0.313	4.01	244.5	1016.0	244.5	1016.0
4	0.309	4.01	244.3	1015.2	244.3	1015.2
5	0.264	4.01	241.9	1005.3	241.9	1005.3
6	0.365	6.00	145.4	403.8	369.6	1016.4
7	0.295	6.00	364.5	1012.4	364.5	1012.4
8	0.312	6.00	364.8	1013.2	364.8	1013.2
9	0.329	3.00	183.5	1019.3	183.5	1019.3
10	0.338	3.00	183.8	1021.1	183.8	1021.1
11	0.396	3.00	55.4	308.1	186.4	1035.5
12	0.392	6.00	59.2	164.5	372.2	1033.8
13	0.445	3.00	110.6	614.2	189.2	1050.9
14	0.457	9.01	77.1	142.6	568.0	1050.8
15	0.450	6.00	379.6	1054.5	379.6	1054.5
16	0.451	9.01	401.2	742.2	569.7	1053.9
17	0.429	9.01	65.3	120.7	564.0	1043.2
18	0.407	9.01	55.3	102.3	560.6	1036.9
19	0.350	9.01	96.0	177.6	552.8	1022.6

B1.3 Simulation Results Specifying the Rich Stream on a Mass Flow Basis

As a result of the investigations comparing the simulation results from the "Vapor-Liquid" case with the "Liquid-Only" case, a simulation round where the rich solvent was a two-phase "Vapor-Liquid" stream defined on a mass flow basis (kg/h) was performed. Some of the results from this simulation round can be seen in Table B.4.

Table B.4 Table showing the percentage deviation between the simulated and experimental desorption rates for the 19 runs. Also the rich solvent flow input are given.

Run	Volume Flow Rate Rich Solvent [kg/h]	%dev, Des CO_2, x_i
1	244.6	-0.46
2	244.5	1.18
3	244.5	1.71
4	244.3	1.12
5	241.9	-7.74
6	369.6	12.18
7	364.5	-3.39
8	364.8	0.59
9	183.5	-0.84
10	183.8	4.19
11	186.4	8.69
12	372.2	-0.66
13	189.2	-11.80
14	568.0	1.35
15	379.6	-5.68
16	569.7	-8.36
17	564.0	4.44
18	560.6	14.59
19	552.8	11.60

B1.4 Gas Measurements vs. Liquid Measurements

Tobiesen et al. reported that there was uncertainty whether the gas measurements or liquid measurements were most trustworthy. Therefore the gas and liquid measurements were compared to the simulation results found using the original Aspen Plus model. The results from these simulations can be found in Table B.5. As can be seen, it varies whether the gas or liquid measurements are closest to the simulated value for the desorption rate.

Table B.5 Table showing the deviation in mass transfer between experimental gas measurements and simulated values and between experimental liquid measurements and simulated values using the original Aspen Plus model. The vapor fraction calculated by Aspen Plus for the rich stream entering the desorber are also listed for the individual runs.

Run	%dev, Des CO_2, x_i Gas measurements	Liquid measurements	Best measurement/ Least deviation
1	-0.46	0.20	Liquid
2	1.18	2.45	Gas
3	1.71	0.20	Liquid
4	1.12	1.69	Gas
5	-7.74	-3.30	Liquid
6	12.18	7.72	Liquid
7	-3.39	15.45	Gas
8	0.59	-2.52	Gas
9	-0.84	2.43	Gas
10	4.19	3.58	Liquid
11	8.69	9.09	Gas
12	-0.66	1.98	Gas
13	-11.80	0.71	Liquid
14	1.35	5.51	Gas
15	-5.68	-4.38	Liquid
16	-8.36	2.58	Liquid
17	4.44	9.01	Gas
18	14.59	21.04	Gas
19	11.60	13.17	Gas

It can be seen that the difference between comparing the simulation with the gas or liquid measurements are small in most cases, from 0.5% to 4%. In a few cases, marked in green, the deviations are a bit larger. However, there is not found a correlation between which conditions (temperature, loading, flow rate) and which measurement that gave the best match. This can be seen in Figure B.1 below.
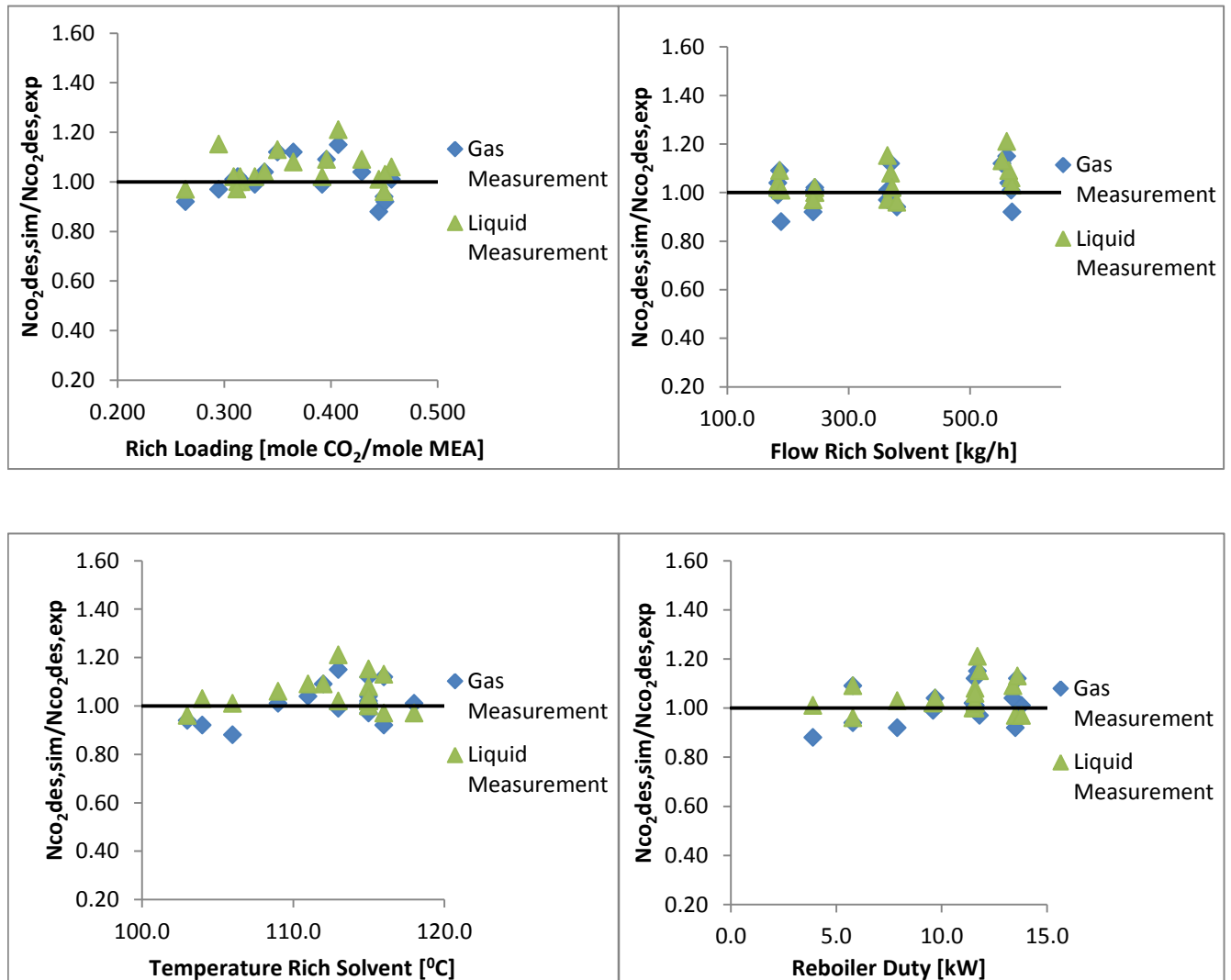
Figure B.1 Four figures showing the ratio between the simulated and experimental CO_2 desorption rates plotted against rich solvent loading, rich flow rate, the inlet temperature of the rich solvent and the reboiler duties for the 19 runs.

B1.5 The Original Aspen Plus Model Compared to an Equilibrium Model

The performance of the original Aspen Plus model, which is rate-based, was compared to an equilibrium stage model for the 19 runs in the Tobiesen et al. campaign. In both cases the desorber column consisted of 20 stages, and the rich solvent was a two-phase "Vapor-Liquid" stream specified on a mass flow basis (kg/h). The deviation in CO_2 desorption rates between experimental gas measurements and simulated values for the two cases can be found in Table B.6 below.

Table B.6 Table showing the deviation in desorption rate between experimental measurements and simulated values for the rate-based and equilibrium case.

Run	%dev, Des CO_2, x_i (gas measurements)	
	Original Aspen Plus model	Equilibrium Model
1	-0.46	1.53
2	1.18	3.16
3	1.71	3.87
4	1.12	3.17
5	-7.74	-3,81
6	12.18	13.08
7	-3.39	1.24
8	0.59	2.20
9	-0.84	1.15
10	4.19	5.84
11	8.69	9.54
12	-0.66	0.02
13	-11.80	-11.36
14	1.35	1.79
15	-5.68	-5.08
16	-8.36	-8.05
17	4.44	5.00
18	14.59	15.40
19	11.60	12.61

As can be seen, the results using rate-based simulations were approximately equal to the results found using the equilibrium model. This is as expected since the reactions in the desorber column occur rapidly, thus it is almost in equilibrium.

B1.6 The Original Aspen Plus Model Compared to the New Kinetic Model

The performance of the original Aspen Plus kinetic model was also compared to the performance of the new kinetic model, the modified Aboundheir et al. model, developed for the absorber part. The kinetic parameters in these models can be found in Chapter 5.2.2 Also here the desorber column consisted of 20 stages, and the rich solvent was a two-phase "Vapor-Liquid" stream specified on a mass flow basis (kg/h). The deviation in CO_2 desorption rates between experimental gas measurements and simulated values for the two cases can be found in Table B.7.

Table B.7 Table showing the deviation desorption rate between experimental measurements and simulated values for the original kinetic model and the new kinetic model.

| Run | %dev, Des CO_2, x_i (gas measurements) | | Rich loading |
	Original Aspen Plus model	New Kinetic model	[molCO2/molMEA]
1	-0.46	42.82	0.316
2	1.18	45.97	0.315
3	1.71	47.25	0.313
4	1.12	23.26	0.309
5	-7.74	57.97	0.264
6	0.97	33.75	0.365
7	-3.39	45.23	0.295
8	0.59	41.51	0.312
9	-0.84	36.16	0.329
10	4.19	40.00	0.338
11	-15.96	6.20	0.396
12	-55.97	-49.06	0.392
13	-10.21	-3.43	0.445
14	-51.68	-44.32	0.457
15	-5.68	-0.96	0.450
16	-7.74	-2.42	0.451
17	-61.27	-56.24	0.429
18	-60.60	-55.11	0.407
19	-35.36	-19.36	0.350

As can be seen from the table above, the overall performance of the new kinetic model is less reliable than the original Aspen Plus model. However, it looks like the new kinetic model predicts slightly better for runs with high rich loading. These runs are colored in yellow in the table.

B2: Notz et al. Campaign (2012)

B2.1 Original Aspen Plus Model vs. the New Kinetic Model

Also for the Notz et al. campaign, simulation results using the original kinetic model were compared to simulation results using the new kinetic model, the modified Aboundheir model. The results are listed in Table B.8.

Table B.8 Table showing the deviation in desorption rates between experimental measurements and simulated values for the original Aspen Plus and new kinetic model.

Run	%dev, Des CO_2, x_i Original Aspen Plus model	New Kinetic model	Rich loading [mole CO2/mole MEA]	Lean loading (exp) [mole CO2/mole MEA]	Rich solution flow rate [kg/h]
1	8.66	27.49	0.386	0.265	206.5
2	19.78	29.36	0.464	0.308	207.4
3	10.35	52.74	0,308	0.230	204.3
4	21.12	40.52	0.397	0.268	206.3
5	24.55	36.86	0.446	0.306	206.3
6	20.62	29.23	0.464	0.317	207.4
7	32.17	39.26	0.478	0.356	205.8
8	12.78	31.35	0.444	0.228	210.6
9	-2.25	22.16	0.393	0.147	213.6
10	Error	Error	Error	Error	Error
11	Error	Error	Error	Error	Error
12	9.13	27.96	0.372	0.256	205.8
13	13.32	28.92	0.400	0.287	158.6
14	19.10	44.50	0.369	0.253	244.2
15	15.03	42.97	0.359	0.241	285.2
16	2.95	20.67	0.414	0.096	107.1
17	3.52	32.26	0.371	0.166	157.0
18	20.93	48.34	0.387	0.215	207.4
19	18.97	48.78	0.354	0.247	358.7
20	16.18	35.49	0.395	0.261	208.1

21	23.79	43.92	0.400	0.270	205.4
22	18.43	37.80	0.389	0.263	205.3
23	13.92	30.03	0.393	0.274	205.9
24	32.53	53.08	0.392	0.251	206.0
25	71.06	92.08	0.435	0.166	205.5
26	32.63	41.94	0.474	0.288	207.3
27	92.03	106.95	0.501	0.169	206.5
28	11.97	21.14	0.470	0.266	157.7
29	19.13	28.85	0.465	0.306	207.7
30	49.87	63.62	0.459	0.316	256.9
31	64.37	80.78	0.454	0.338	281.6
32	47.34	60.15	0.449	0.335	307.8
33	57.86	71.97	0.441	0.360	359.0
34	-0.47	22.96	0.417	0.146	79.8
35	-0.91	16.93	0.411	0.208	106.8
36	12.15	31.15	0.393	0.252	155.4
37	27.76	48.34	0.398	0.296	208.3
38	39.15	64.17	0.385	0.308	256.8
39	52.78	75.68	0.400	0.319	281.8
40	-5.13	22.13	0.297	0.111	129.7
41	2.13	37.84	0.297	0.130	155.0
42	2.11	44.84	0.310	0.190	205.6
43	-1.63	36.93	0.318	0.200	207.2
44	2.76	43.21	0.314	0.209	255.9
45	4.11	40.58	0.324	0.219	280.1
46	45.67	63.61	0.417	0.318	204.4
47	21.52	49.44	0.366	0.255	205.4

As can be seen from the table above, run 25, 26 and 27 have large deviations between the simulated and experimental desorption rate of CO_2. These runs are marked in blue in the table. Also in the absorber simulation of the Notz et al. campaign, large deviations were found for these three runs regarding the CO_2 absorption rate. In addition it looks like the deviation

between experimental measurements and simulation results increase with high flow rates and increasing rich loading. Some of these runs are marked in yellow in the table.

B2.2 Water Wash Section Compared to No Water Wash Section

The desorber column at the University of Kaiserslautern has a water wash section over the packing at the top of the desorber column. It was tried to remove the water wash section in order to understand why there were so large deviations between simulated and experimental data in the simulations with the water wash section. The results found when the water wash section was removed was slightly better regarding the CO_2 desorption rate. This can be seen in the plots in Figure B.2. However, the difference between the two simulations are not significant, and therefore not the reason for the large deviations.
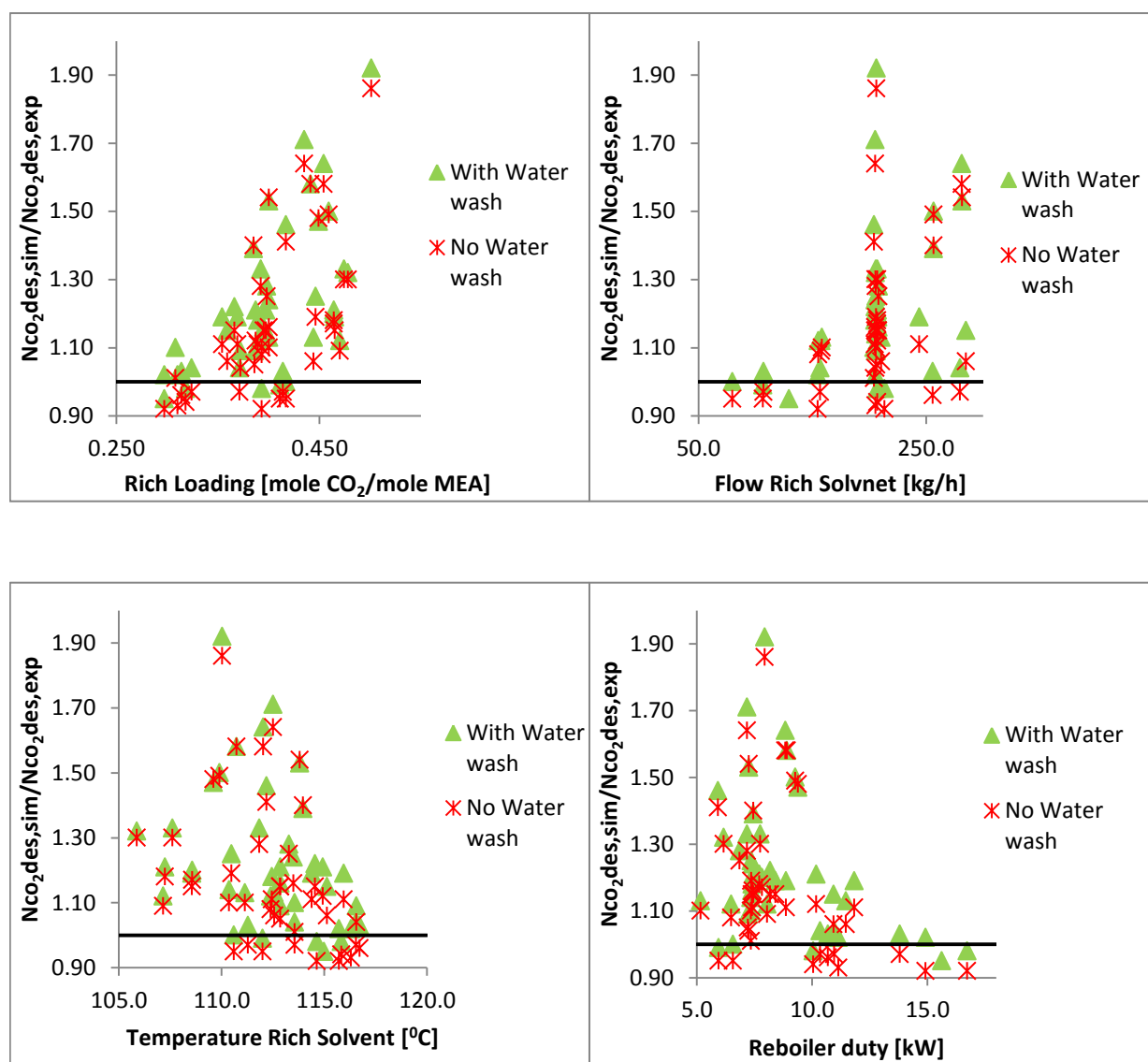

Figure B.2 Four figures showing the ratio between the simulated and experimental CO_2 desorption rates plotted against rich solvent loading, rich flow rate, the inlet temperature of the rich solvent for the 45 runs.

XXXI

B2.3 Check if Back-Absorption Occurred in the Water Wash

Experimental measurements of the CO_2 mass fraction throughout the desorber column were used to create CO_2 profiles. It was seen that run 12-20 stood out as worse than the other runs, having the largest deviations between experimental measurements and simulation results. It was thought that this may be a result of back-absorption of CO_2 in the water wash section. The CO_2 amount in the recycled stream in the simulations with a water wash section was therefore compared to the CO_2 amount in the recycled stream in the simulations without a water wash section. The results from the simulation with a water wash section can be seen in Table B.9, and the results from the simulation without a water wash section can be seen in

Table B.10. It is shown that there is no significant difference in the CO_2 amount in the recycled stream for the two cases. Therefore it is assumed that there is no back-absorption in the water wash section.

Table B.9 Overview of the CO_2 content in the recycled stream and the size of the condensate and recycled rate for run 12-20 and 1, 6 and 40 for the simulations with a water wash section.

| Run	Condensate rate [kg/h] / Recycled rate [kg/h]		CO_2 amount in recycled (sim)	% CO_2 in recycled (sim)
	Exp	Sim	[kg/h]	
12	1.28 / 2.07	1.81 / 2.93	0.01219	0.42
13	1.14 / 1.08	1.68 / 1.59	0.00520	0.33
14	1.10 / 3.79	1.63 / 5.61	0.01942	0.35
15	1.02 / 5.58	1.45 / 7.91	0.02382	0.30
16	1.16 / 10.24	1.31 / 11.50	0.03977	0.35
17	1.07 / 5.47	1.29 / 6.59	0.02342	0.36
18	1.05 / 5.08	1.65 / 8.02	0.02927	0.36
19	2.78 / 5.04	4.31 / 7.82	0.02706	0.35
20	3.41 / 0.60	5.30 / 0.94	0.00332	0.35
		Comparison with three other runs		
1	2.04 / 1.6	3.03 / 2.41	0.00856	0.36
6	1.40 / 0.98	2.54 / 1.78	0.00632	0.36
40	0.95 / 13.98	1.01 / 14.81	0.05082	0.34

Table B.10 Overview of the CO$_2$ content in the recycled stream and the size of the condensate and recycled rate for run 12-20 and 1, 6 and 40 for the simulations without a water wash section.

| Run	Condensate rate [kg/h] / Recycled rate [kg/h]		CO$_2$ amount in recycled (sim) [kg/h]	% CO$_2$ in recycled (sim)
	Exp	Sim		
12	1.28 / 2.07	1.91 / 3.09	0.01277	0.41
13	1.14 / 1.08	1.74 / 1.65	0.00537	0.33
14	1.10 / 3.79	1.74 / 5.98	0.02051	0.34
15	1.02 / 5.58	1.55 / 8.45	0.03019	0.36
16	1.16 / 10.24	1.35 / 11.85	0.04056	0.34
17	1.07 / 5.47	1.36 / 6.94	0.02444	0.35
18	1.05 / 5.08	1.76 / 8.55	0.03094	0.36
19	2.78 / 5.04	4.53 / 8.23	0.02820	0.34
20	3.41 / 0.60	5.35 / 0.94	0.00333	0.35
	Comparison with three other runs			
1	2.04 / 1.6	3.14 / 2.50	0.00882	0.35
6	1.40 / 0.98	2.63 / 1.85	0.00653	0.35
40	0.95 / 13.98	1.05 / 15.35	0.05199	0.34

B2.4 Heat Loss in the Desorber Column

Since the reboiler duty and the heat loss can heavily influence the desorber calculations, these parameters were looked closer into for the Notz et al. campaign. It was found that the reported heat loss varied from almost 0% to 14% when calculations were performed with respect to the reported reboiler duty. Run 10 and 11 are not included because of convergence problems in Aspen Plus. A graphic illustration of the heat loss in the desorber based on the reported reboiler duty can be seen in Figure B.3.
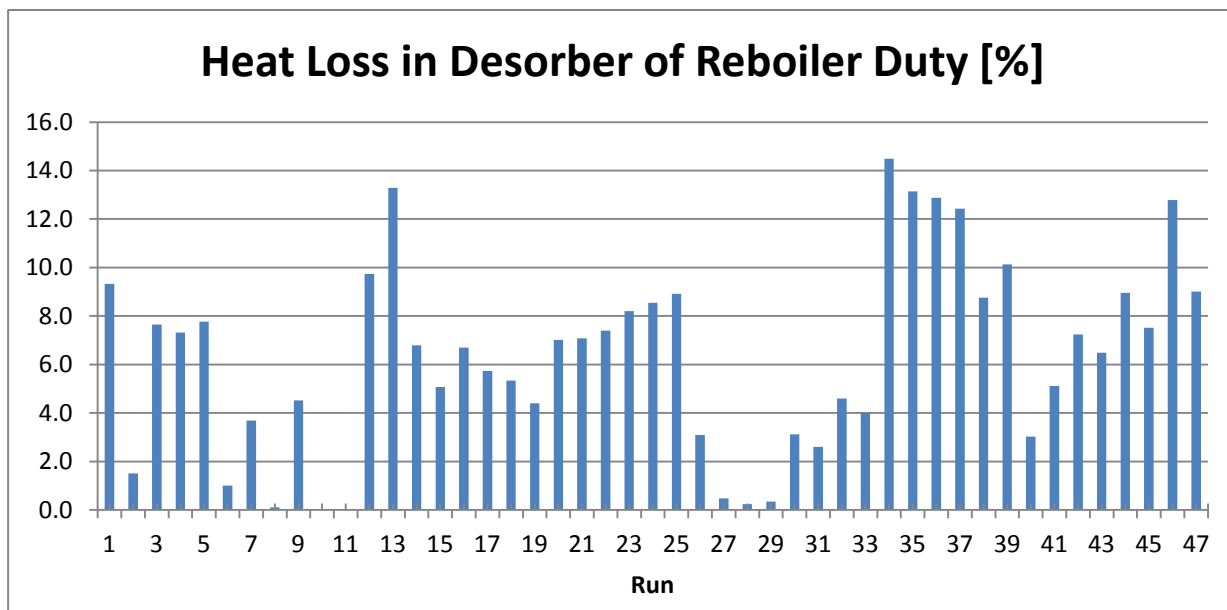
Figure B.3 Graphic illustration of the percentage heat loss in the desorber calculated based on the reported reboiler duty. Run 10 and 11 are not included because of convergence problems.

There was also reported a number called "Evaporator power required to compensate heat losses". The percentage of this number with respect to the reboiler duty was also calculated to see if the same trend was shown. In this case the percentage varied from 5% to 25%, and a graphic illustration can be seen in Figure B.4.

Evaporator power required to compensate heat losses of reboiler duty [%]
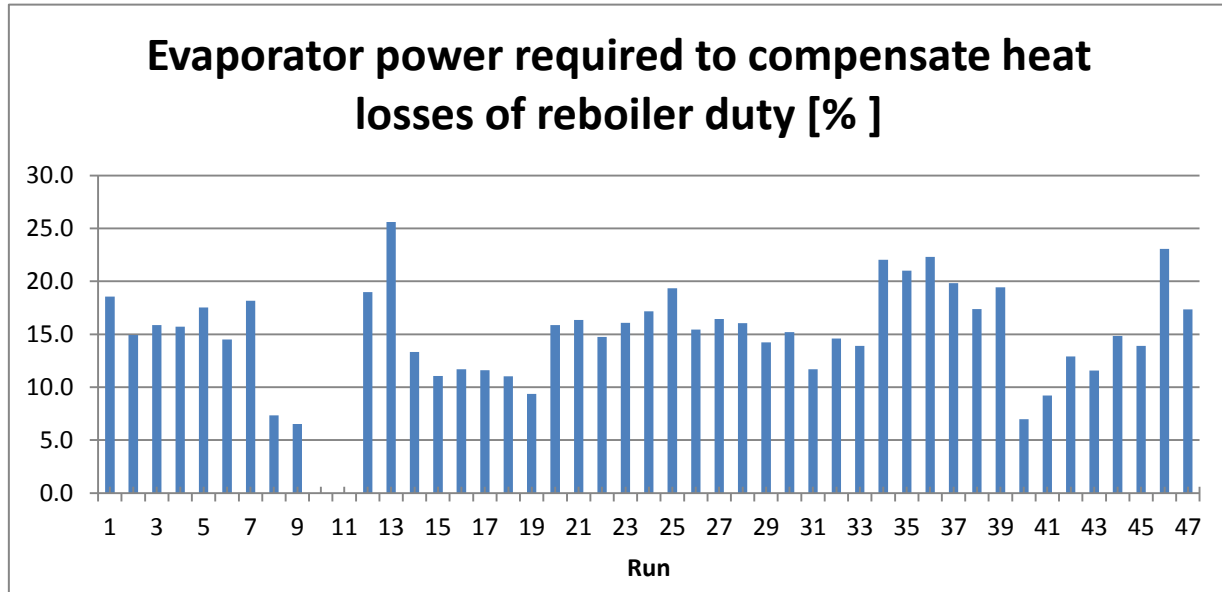
Figure B.4 Graphic illustration of the percentage "evaporation power required to compensate for heat losses" in the desorber calculated based on the reported reboiler duty. Run 10 and 11 are not included because of convergence problems.

To evaluate whether the varying heat losses in the reported data was the cause for the large deviation in the CO_2 desorption rates, a heat loss of 10% was introduced in run 2, 8, 26, 27, 28, 29, 30, 31 and 32. The results are listed in Table B.11, and it can be seen that the simulations gives better result with 10% heat loss.

Table B.11 Table giving the percentage deviation between experimental and simulated CO_2 desorption rate with the reported heat loss and with 10 % heat loss for run 2, 8, 26, 27, 28, 29, 30, 31 and 32.

Run	%dev, Des CO_2, x_i, originally	%dev, Des CO_2, x_i, with 10% heat loss
2	20	12
8	13	6
26	33	25
27	92	81
28	12	2
29	19	10
30	50	42
31	64	57
32	47	41

B3: Enaasen et al. Campaign (2015)

In the experimental data from Enaasen et al. (2015), there was not provided any information about heat loss in the column. Based on the publication by Tobiesen et al. (2008), it was decided to introduce a heat loss of 0.5 kW in all runs. As can be seen in Table B.12, the simulations with reduced reboiler duty have a lower overall deviation from experimental data than the simulations using the reported reboiler duty. The experimental mass balance is also included in the table.

Table B.12 Simulation results from the Enaasen et al. campaign with the reported reboiler duty and reduced reboiler duty. The experimental mass balance is also included.

Run	%dev, Des CO_2, x_i		Experimental mass balance, gas and liquid measurements [%]*
	Reported Reboiler Duty	Reduced Reboiler Duty	
1	15.95	7.61	5.38
2	4.48	-0.86	-0.63
3	2.59	-1.95	-0.69
4	-9.28	-15.27	-13.80
5	2.54	-2.14	-3.94
6	11.30	3.13	-4.48
7	4.97	-0.81	-3.17
8	7.81	0.66	-9.97

Calculated using $deviation[\%] = \frac{v_{gas} - v_{liq}}{average(v_{gas}, v_{liq})} \cdot 100$, where v_{gas} and v_{liq} are amount of CO_2 in kg/h.

B4: Pinto et al. Campaign (2014)

Neither in the experimental data from Pinto et al. (2014), there was provided any information about heat loss in the column. Based on the publication by Tobiesen et al. (2008), it was decided to introduce a heat loss of 0.5 kW in all runs also for this campaign. As can be seen in Table B.13, the simulations with reduced reboiler duty have a higher overall deviation from experimental data than the simulations using the reported reboiler duty. The experimental mass balance is also included in the table.

Table B.13 Simulation results from the Pinto et al. campaign with the reported reboiler duty and reduced reboiler duty. The experimental mass balance is also included.

| | %dev, Des CO_2, x_i | | Experimental mass balance, gas and liquid measurements [%]* |
Run	Given Reboiler Duty	Reduced Reboiler Duty	
1	2.79	-10.41	12.96
2	-11,54	-16.29	6.67
3	-32.80	-39.21	35.25
4	-6.26	-12.57	0.16
5	13.64	3.50	-8.48
6	-5.25	-11.45	3.88

*Calculated using $deviation[\%] = \frac{v_{liq} - v_{gas}}{v_{gas}} \cdot 100$, where v_{gas} and v_{liq} are amount of CO_2 in kg/h.

B5: Correlation CO$_2$ Mass Transfer, Reboiler Duty and Rich Loading

Several plots were made to investigate whether any overall trends could be found in the simulations of the five campaigns. Some of these plots are given in Chapter 9.2 in the main part of the thesis, but additional information to Figure 9-2 are given here, as well as showing the figure once more.

In the plot in Figure B.5, the CO$_2$ desorption rate/mass transfer rate are given as a function of the rich solvent loading. This is done in order to find indications of consistency between the campaigns. It should be noted that since each of the pilots is designed for certain solvent flows, some of the compared runs here might be performed in nonoptimal liquid flow rates which influence the desorber performance. However this approach to compare runs with similar reboiler duties, similar CO$_2$ mass transfer rates and rich loading can give an indication if the runs are consistent with each other.
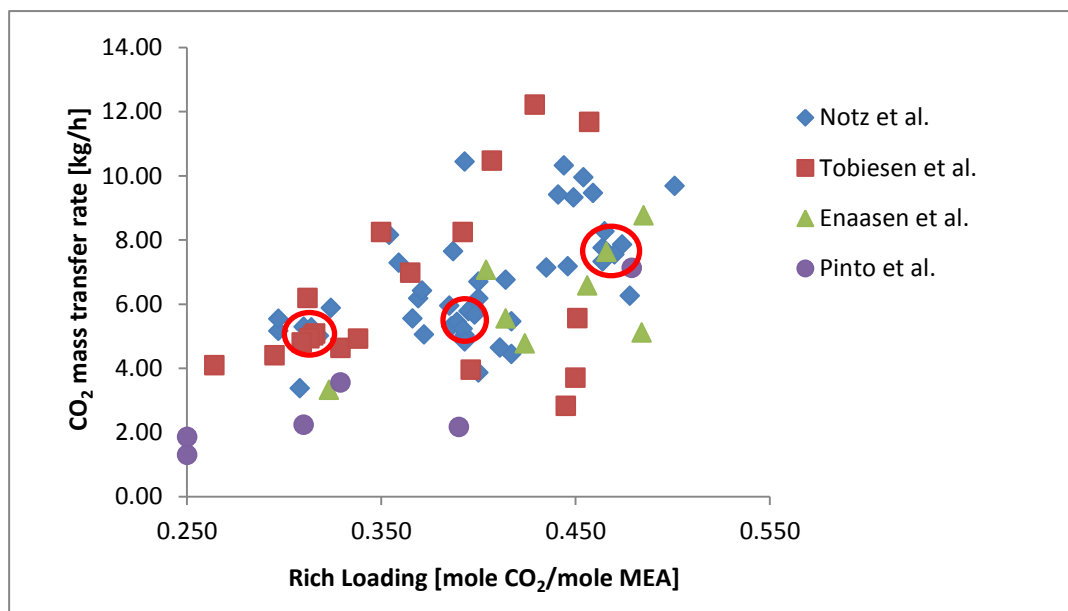
Figure B.5 Plot showing the CO$_2$ mass transfer in the desorber as a function of the rich solvent loading for all four campaigns simulated.

Three areas, marked in red in the figure above, are examined closer regarding CO$_2$ mass transfer rate, solvent loading and reboiler duty. The areas are numbered from left to right, and the results are listed in Table B.14.

Table B.14 The rich loading, CO_2 mass transfer and reboiler duty are listed for the points from each campaigns that are included in Area 1, 2 and 3.

Area	Campaign, point (loading , mass transfer)	Reboiler duty [kW]
1	Tobiesen et al. (0.309 , 4.80)	11.6
	Tobiesen et al. (0.313 , 4.93)	11.5
	Tobiesen et al. (0.315 , 5.02)	11.6
	Tobiesen et al. (0.316 , 5.08)	11.6
	Notz et al. (0.310 , 5.29)	11.1
	Notz et al. (0.314 , 5.27)	10.7
	Notz et al. (0.318 , 5.01)	10.0
2	Notz et al. (0.385 , 5.95)	7.5
	Notz et al. (0.386 , 5.30)	7.2
	Notz et al. (0.389 , 5.44)	7.4
	Notz et al. (0.392 , 5.23)	7.2
	Notz et al. (0.393 , 5.03)	7.3
	Notz et al. (0.395 , 5.78)	7.4
	Notz et al. (0.397 , 5.91)	7.5
	Notz et al. (0.398 , 5.67)	6.9
3	Notz et al. (0.464 , 7.76)	7.8
	Notz et al. (0.464 , 7.33)	7.7
	Notz et al. (0.465 , 8.27)	8.4
	Notz et al. (0.470 , 7.55)	8.1
	Notz et al. (0.474 , 7.86)	7.8
	Enaasen et al. (0.466 , 7.63)	8.7
	Pinto et al. (0.479 , 7.13)	7.9

In area 1 it can be seen that the Notz et al. points have a bit higher reboiler duty than the Tobiesen et al. points. It can also be seen that the reboiler duties follows a logical trend with respect to solvent loading and mass transfer rates for the individual campaigns. Higher solvent loading requires a lower reboiler duty to give the same mass transfer as lower solvent loading. This is because the driving forces are stronger when the difference in the CO_2 concentration between the gas and liquid phase are larger.

In area 2, the reboiler duty varies 0.6 kW between the eight points. This indicates consistency in the Notz et al. campaign, and also here it can be seen that the reboiler duties are logical with respect to loading and CO_2 mass transfer rate. In the third area, it also looks like the same trend applies. However, it can be seen that the reboiler duty required for the Enaasen et al. point are about 1 kW higher than the two points from Notz et al. with similar solvent loading (0.464). The reported reboiler duties are used for comparison, and therefore this can explain the high reboiler duty from the Enaasen et al. campaign, since this is given without any heat loss.

An even closer look was taken on area 2, comparing the rich and lean solvent loadings, CO_2 mass transfer rate, rich solvent flow rates and reboiler duties. The results can be seen in Table B.15.

Table B.15 Overview of the rich and lean solvent loadings, CO_2 mass transfer rates, rich solvent flow rate, reboiler duty and percentage deviation between simulated and experimental desorption rates for the points in Area 2. All the points are from the Notz et al. campaign.

Area	Run	Rich Loading	Lean Loading	Delta Loading (Rich-Lean)	Mass Transfer rate [kgCO2/h]	Rich Stream [kg/h]	Reboiler Duty [kW]	%dev
	1	0.386	0.265	0.121	5.30	206.5	7.2	8.66
	4	0.397	0.268	0.129	5.91	206.3	7.5	21.12
	20	0.395	0.261	0.134	5.78	208.1	7.4	16.18
2	22	0.389	0.263	0.126	5.44	205.3	7.4	18.43
	23	0.393	0.274	0.119	5.03	205.9	7.3	13.92
	24	0.392	0.251	0.141	5.23	206.0	7.2	32.53
	37	0.398	0.296	0.102	5.67	208.3	6.9	27.76
	38	0.385	0.308	0.077	5.95	256.8	7.5	39.15

Run 38 have the highest deviation in mass transfer rate between simulated and experimental data, and it can be seen that the delta loading is small even though the reboiler duty is high compared to the other runs in the table. This can indicate suboptimal stripping in this case. Run 24, which have the second largest deviation in the mass transfer rate, have the lowest lean loading out and the highest deviation between rich and lean loading. However, it does not have the highest reported reboiler duty of the runs in the table.

B6: Trend Plots

Several plots were made to investigate whether any overall trends could be found in the simulations of the four campaigns. In Figure B.6, the temperature of the rich solvent is plotted against the rich solvent loading, and the temperature of the lean solvent loading is plotted against the rich solvent loading. Note that the temperature of lean solvent is measured in different places in the column. In the Tobiesen et al. and Notz et al. campaigns, the lean solvent temperature is measured after the reboiler. In the Enaasen et al campaign, it is measured in the reboiler, and in the Pinto et al. campaign it is measured before the reboiler.
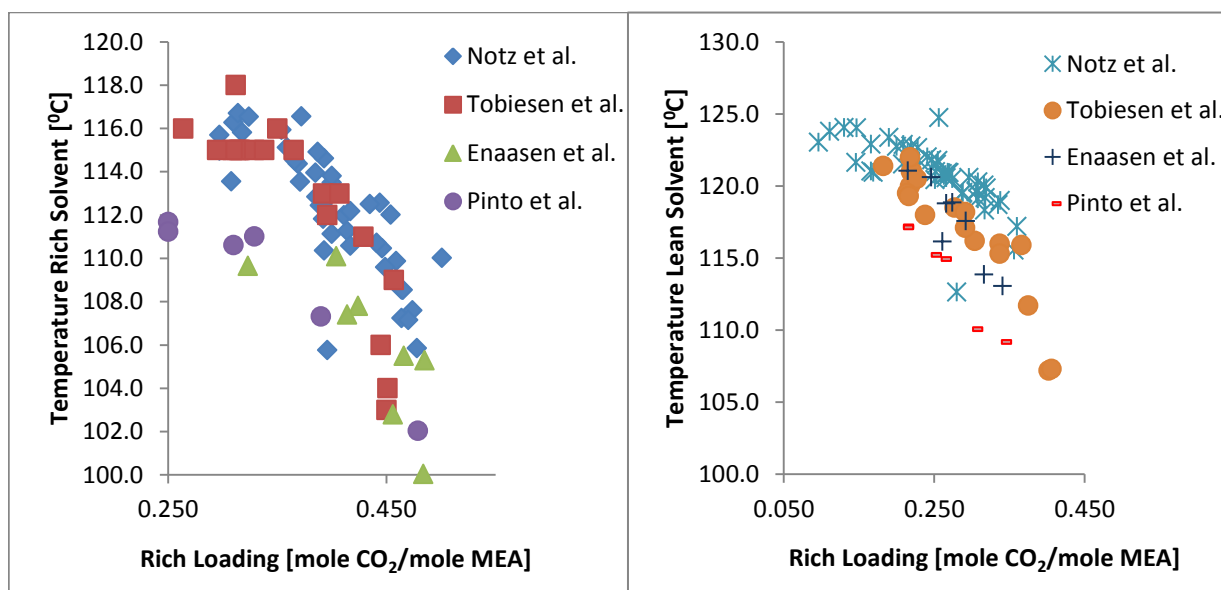
Figure B.6 Plot of the rich solvent temperature as a function of the rich solvent loading, and of the lean solvent temperature as a function of the rich solvent loading.

From these plots it looks like all the campaigns follows the same trends. Thus, they do not reveal the poor performance of the Notz et al. campaign compared to the other campaigns.

Also plots of the deviation between the CO_2 desorption rates in the simulations and experiments as a function of the lean solvent loading and delta loading (the difference between the rich and lean loading) were made. These can be seen in Figure B.7.
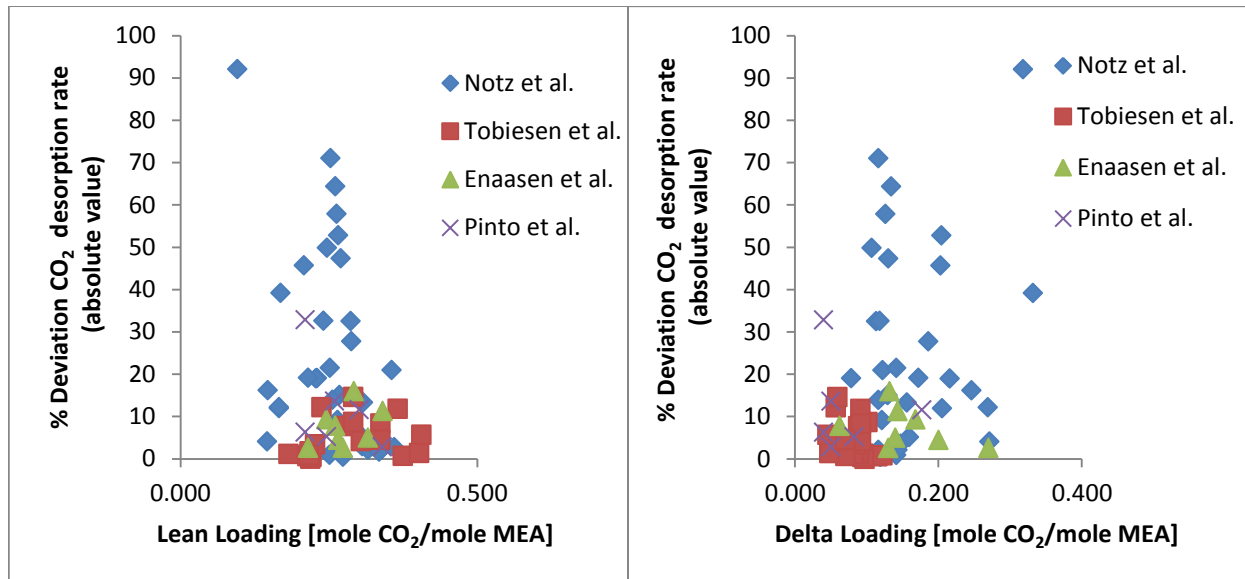
Figure B.7 Plot of the percentage deviation in the desorption rate between simulated and experimental values as a function of the lean solvent loading and the delta loading

Neither these plots reveal trends that can explain the poor performance of the simulation model on the Notz et al. campaign.